



universität
wien

DISSERTATION

Titel der Dissertation

„Transgenic mouse models enabling photolabeling of
individual neurons *in vivo*“

Verfasser

Mag.rer.nat Manuel Peter

angestrebter akademischer Grad

Doktor der Naturwissenschaften (Dr.rer.nat.)

Wien, 2012

Studienkennzahl lt. Studienblatt:	A 091490
Dissertationsgebiet lt. Studienblatt:	Molekulare Biologie UniStG
Betreuerin / Betreuer:	Dr. Simon Rumpel

Table of Contents

Table of Contents

1. Abstract	3
2. Kurzfassung	5
3. Introduction	7
3.1 Cortical circuits.....	10
3.1.1 Plasticity in primary cortical areas	11
3.1.2 Neuronal activity in the auditory cortex.....	12
3.1.3 Neuronal coding and the cell assembly	13
3.1.4 Auditory cued fear conditioning	14
3.1.5 Molecular mechanisms of cortical plasticity.....	15
3.2 Immediate early genes	17
3.2.1 Cellular functions of IEGs	17
3.2.2 IEGs as marker for neuronal activity.....	19
3.3 Photoactivatable fluorescence proteins.....	21
4. Aim of this work	23
5. Manuscript I: Induction of immediate early genes in the mouse auditory cortex after auditory cued fear conditioning to complex sounds.....	25
6. Manuscript II: Correlation of neuronal activity <i>in vivo</i> with gene expression levels in a transgenic mouse model allowing single cell resolution photolabeling.....	38
6.1 Abstract.....	39
6.2 Introduction	40
6.3 Results	41
6.3.1 Selection of a photactivatable fluorescent protein for <i>in vivo</i> expression... 41	
6.3.2 Generation of genetically modified reporter mice expressing PA-GFP..... 45	

Table of Contents

6.3.3	Functional characterization of mice expressing PA-GFP::NLS.....	50
6.3.4	Single cell correlation of <i>in vivo</i> activity and endogenous Fos expression.	57
6.4	Discussion.....	62
6.5	Experimental Procedures.....	64
6.5.1	Cell culture.....	64
6.5.2	In vitro Imaging.....	64
6.5.3	Histology.....	65
6.5.4	Generation of genetically modified mice.....	66
6.5.5	Slice preparation.....	67
6.5.6	Electrophysiology.....	68
6.5.7	<i>In vivo</i> imaging.....	69
6.6	Acknowledgements.....	72
7.	General discussion.....	73
7.1.1	The auditory cortex is necessary for auditory cued fear conditioning to complex sounds.....	73
7.1.2	Immediate early genes show strong upregulation after AFC.....	75
7.1.3	Neuronal activity under basal conditions does not correlate with <i>c-fos</i> expression.....	76
7.1.4	Applications of the PA-GFP::NLS mice.....	78
8.	References.....	82
9.	Acknowledgements.....	92
10.	Curriculum vitae.....	93

Abstract

1. Abstract

It is believed, that activity patterns in the cortex are correlates of higher brain functions such as perception or decision making. However the mechanisms how and why these activity patterns emerge are not known. One major experimental obstacle to understand the function of brain circuits is the lack of tools to determine both the precise function of a neuron and its position in the connectivity diagram of the circuit. Therefore, it would be necessary to tag neurons *in vivo* at single cell resolution, based on functional criteria, and to re-identify these neurons *in vitro*. This would allow us to obtain more information about the connectivity, the gene expression or the morphology of these neurons and thus to gain information that goes beyond its *in vivo* activity pattern. This information is crucial to gain a mechanistic understanding of the neurons function.

We conceived two strategies to label neurons in the auditory cortex *in vivo*. First we tested if immediate early genes can be reliable markers to tag active neurons in the auditory cortex during associative learning. We established an auditory cued fear conditioning protocol that depends on the auditory cortex and tested the expression of *c-fos* and *Arc* using quantitative PCR following the acquisition of this fear memory. We also compared paired conditioning to several control paradigms to disassociate gene expression that arises from the learning event from gene expression that arises from other factors unrelated to associative learning. We found that *c-fos* and *Arc* show strong induction after paired fear conditioning but also in all other paradigms that involved shocks indicating that other unspecific factors or cross-modal inputs can activate immediate early gene expression in the auditory cortex. We further used a near genome wide mRNA microarray analysis to screen for genes other than *c-fos* and *Arc* that could be specifically upregulated during learning. We again observed upregulation of known immediate early genes but could not detect genes specifically induced by associative learning to sound.

The second strategy is based on photoactivatable fluorescence proteins. We explored the ability of photoactivatable fluorescence proteins to serve as conditional markers in the living brain. We tested six PA-FPs and generated mouse lines

Abstract

expressing PA-GFP::NLS either under the Thy1.2 promoter or conditionally as a knock in construct from the Rosa26 locus. Using two-photon excitation we were able to conditionally label neurons at single cell resolution *in vivo* for many hours. Labeling greatly facilitated re-identification of these neurons *in vitro* in acute brain slices and in fixed samples and can therefore be combined with targeted patch clamp recordings and histology. Furthermore, photolabeling can also be combined with functional *in vivo* calcium imaging which allows us to link *in vivo* neuronal activity with a further analysis of these neurons. We demonstrate this by correlating spontaneous activity levels in the auditory cortex with a histological analysis of *c-fos* expression. We observed that particularly active neurons can have highly variable *c-fos* expression levels and we could not find a direct correlation between neuronal activity and *c-fos* expression. Furthermore, the results from both studies highlight that IEG expression is also controlled by other factors than neuronal activity. This again emphasizes the value of a method to label neurons independent of IEG expression. In this study we achieved this by generating PA-GFP expressing mice to photolabel neurons. This photolabeling approach can also be applied to other cell types and fields of biology.

2. Kurzfassung

Viele grundlegende Prinzipien der Funktion neuronaler Netzwerke sind noch immer unbekannt. Eine Theorie besagt, dass die gleichzeitige, geordnete Aktivität vieler Nervenzellen im Cortex das grundlegende Substrat höherer Gedächtnisfunktionen ist. Allerdings ist der Mechanismus wie und warum diese Aktivitätsmuster entstehen unbekannt. Ein grundlegendes Problem dies genauer zu untersuchen ist, dass die experimentellen Werkzeuge dazu noch immer fehlen. Darum ist es nicht möglich die spezifische Funktion einer Nervenzelle in einem neuronalen Netzwerk festzustellen. Deshalb wäre es ein großer Fortschritt Nervenzellen anhand ihrer Aktivität im Netzwerk zu markieren. Dies würde uns erlauben diese Zelle wieder zu identifizieren und weiteren Analysen zu unterziehen. Dadurch wäre es uns möglich mehr über die Verbindungen zu anderen Nervenzellen, die Proteinexpression oder die Morphologie dieser Zelle zu erfahren.

In dieser Arbeit testeten wir zwei verschiedene Strategien um Nervenzellen zu markieren. Zuerst untersuchten wir die Spezifität der Genexpression früher Gene im auditorischen Cortex. Wir verwendeten ein vom auditorischen Cortex abhängiges Lernprotokoll und testeten die Genexpression der zwei Gene *c-fos* und *Arc*. Weiters testeten wir auch andere Verhaltensprotokolle um lerninduzierte Genexpression von unspezifisch induzierter Genexpression zu unterscheiden. Wir fanden einen starken Anstieg beider Gene bei allen Protokollen die einen Schock beinhalteten. Dies ist ein Hinweis darauf, dass auch andere unspezifische Faktoren die Expression von *c-fos* und *Arc* aktivieren können. Weiters verwendeten wir eine mRNA Mikroarray Analyse um weitere lernspezifisch aktivierte Genen zu finden. Auch in diesem Experiment fanden wir einen starken Anstieg bekannter früher Gene konnten aber keinen neuen Genen die spezifisch während des Lernens aktiviert werden finden.

Die zweite Strategie beruht auf photoaktivierbaren fluoreszierenden Proteinen. Wir testeten ob es mit diesen Proteinen möglich ist Zellen im lebenden Gehirn konditional zu markieren. Dafür testeten wir sechs verschiedenen photoaktivierbare Proteine und generierten drei Mäuselinien die photoaktivierbares GFP exprimieren. Mit diesen

Kurzfassung

Mäusen ist es möglich einzelne Zellen *in vivo* für viele Stunden zu markieren. Durch die Markierung können diese Zellen auch in Hirnschnitten wiedergefunden und dadurch weiter charakterisiert werden. Weiteres kann Photolabeling auch mit funktionellem Calicum Imaging kombiniert werden. Dadurch ermöglichen es diese Mäuse eine direkte Verbindung zwischen der Aktivität einzelner Zellen in einem Netzwerk mit einer weiteren Charakterisierung dieser Zellen herzustellen. Wir testeten diese Mäuse und korrelierten die spontane *in vivo* Aktivität einzelner Zellen mit der Genexpression des frühen Genes *c-fos*. Wir fanden, dass die *c-fos* Genexpression sehr variable in stark aktive Nervenzellen war und konnten keine Korrelation zwischen hoher spontaner Aktivität und hoher *c-fos* Genexpression finden. Unsere Ergebnisse deuten darauf hin, dass auch andere, unspezifische Faktoren die *c-fos* Genexpression beeinflussen können. Diese Ergebnisse zeigen wie wichtig es ist Neuronen unabhängig von frühen Genen markieren zu können. Wir erreichten das durch die PA-GFP exprimierenden Mäuselinien. Weiters kann die photolabeling Methode auch auf andere Zelltypen angewandt werden.

3. Introduction

One of the major challenges in neuroscience is to understand the link between neuronal activity and behavior. It is believed that activity patterns in neuronal networks are the biological correlates of neurobiological processes like memory formation, thoughts or decision making. In the past, techniques like electrophysiological recordings or *in vivo* calcium imaging yielded much information about firing patterns of populations of neurons in response to various stimuli or during a specific behavior task. Generally, this network activity is generated as a result of interactions between different groups of neurons. It can occur spontaneously, but can also be triggered by perception, information processing or memory formation and retrieval. However the mechanisms by which functional activity patterns emerge in brain networks remains elusive because one major problem is to link the function of a neuron with the structure of the network. In order to understand how activity patterns emerge it would therefore be desirable to gain additional information about neurons that are active during a specific task.

In an ideal experiment one would be able to label neurons based on their *in vivo* activity. This label should greatly facilitate the unambiguous re-identification of these neurons either *in vitro* or *in vivo* which would further allow a histological or electrophysiological characterization. Therefore it would be possible to gain more information like the connectivity in the circuit, the cell type or the expression profile of a previously functionally characterized neuron.

Currently different methods are used to combine *in vivo* recordings and a further analysis of the same neuron. Classically, the electrophysiological properties can be used to classify the neuronal class (Bean, 2007). Further, *in vivo* recorded neurons can be filled through a recording electrode with biocytine. Biocytine can be visualized immunohistochemically and the dendritic and axonal morphology of the neuron becomes visible. This method has been successfully used to combine *in vivo* electrophysiological recordings with a subsequent morphological reconstruction of a given neuron afterwards (Pinault, 1996; Klausberger et al., 2005).

Introduction

It is also possible to use genetic approaches to label particular cell types. One widely used strategy is to mimic the endogenous expression pattern of a gene by using regulatory elements like enhancers and promoters to drive the expression of a reporter gene, (reviewed in: Luo et al., 2008). Different mouse models have been developed using either short promoter elements (Caroni, 1997; Feng et al., 2000) bacterial artificial chromosomes (Gong et al., 2003; Haubensak et al., 2010; Zhao et al., 2011) or knock-in strategies (Tamamaki et al., 2003; Madisen et al., 2010; Portales-Casamar et al., 2010) to label particular neurons. With these mice it is possible to identify and record from neurons belonging to the same cell type *in vivo* (Kerlin et al., 2010; Runyan et al., 2010). Furthermore, cell type specific expression of Channelrhodopsin, (Boyden et al., 2005) a light-gated cation-selective channel, allows selective light-induced firing of a specific neuron, thus providing information about the recorded cell (Lima et al., 2009). Most of the genetic strategies used to restrict gene expression to certain cell types depend on the bacteriophage recombinase Cre which mediates the recombination between two loxP sites (Sauer, 1987; Orban et al., 1992, reviewed in: Branda and Dymecki, 2004). Spatially and temporally restricted transgene expression can be achieved by an intersectional genetic strategy. Mice expressing Cre under the control of a cell type specific promoter can be infected with viral vectors expressing a floxed transgene (Kuhlman and Huang, 2008) or these mice can be crossed with reporter mice (Madisen et al., 2010). Indeed, many Cre driver lines have been generated and are currently generated in a concerted effort from the GENSAT project (www.gensat.org) (Gong et al., 2007) and others (Madisen et al., 2010). However, it is not known how many distinct cell types really exist in the brain and it is further not clear if it will be possible to generate mice expressing Cre specifically in all these different cell types.

In most cases the connectivity of a neuron *in vivo* is not known and it is further unclear which specific inputs a particular neuron receives. Therefore, several techniques were developed to better understand the connectivity of a circuit *in vivo*. Serial electron microscopy can be used for an anatomical reconstruction of neuronal circuits and can be combined with *in vivo* functional imaging of neuronal populations which allows to link the function of a given neuron with the structure of the circuit. This method allows to obtain a very detailed view on the connectivity of a neuronal circuit,

Introduction

however great effort is necessary to reconstruct even a very small tissue sample (Bock et al., 2011). Large scale *in vivo* calcium imaging of the visual cortex of the mouse has been combined with random paired patch clamp recordings *in vitro*. Images of *in vitro* patched neurons can be realigned with images obtained during calcium imaging. This approach allows to combine a functional *in vivo* characterization and a subsequent electrophysiological characterization of the same neurons which revealed that functionally similar tuned neurons form connections at a much higher rate compared to neurons with uncorrelated responses (Ko et al., 2011). Single-cell electroporation allows to precisely target neurons *in vivo* and *in vitro*. By combining single cell electroporation with replication deficient monosynaptic retrograde spreading rabies viruses it is possible to determine the inputs of a single neuron *in vivo* and therefore to label a neuronal microcircuit (Marshel et al., 2010). This method is not limited to the expression of fluorescence proteins but could also be used to genetically manipulate (eg. Channelrhodopsin, Halorhodopsin) (Boyden et al., 2005; Zhang et al., 2007) or record from (eg. GCamp3) (Tian et al., 2009; Zhao et al., 2011) not only the electroporated but also all its input neurons.

All these methods and strategies are good efforts to combine *in vivo* recordings with a further analysis of the recorded neuron. However, they are difficult to implement, in particular, if the neurons are sparse, if they have to be maintained alive for further analysis or if they have to be labeled based on their function. A full genetic approach would most likely not be suitable to label functionally similar neurons. Functionally the neocortex is a very heterogeneous structure however different areas like the auditory cortex or the visual cortex consist of the same underlying building blocks. Genetically it is most likely not possible to label only neurons from the auditory cortex or only from the visual cortex. Furthermore, neurons from the same cell type can have different functions and can therefore form separate sub-circuits (Yoshimura and Callaway, 2005; Yassin et al., 2010). These functionally different, but most likely genetically similar neurons can therefore only be separated by a strategy that labels neurons based on their function. Therefore, we wanted to find strategies that would allow us to conditionally label neurons based on their *in vivo* activity. Labeling and re-identification should allow us to further analyze these neurons and could therefore help to understand

Introduction

how and why particular activity patterns emerge in the brain. This could ultimately help us to understand how the brain processes external stimuli and how the brain is able to form memories.

3.1 Cortical circuits

It is believed that the neocortex plays a critical role in higher brain functions like memory formation, conscious thoughts and speech (Marr, 1970). It forms around 80% of the human brain and consists of a complex neuronal network of tightly interconnected cells. Around 70% - 80% of all neurons in the neocortex are excitatory pyramidal cells and the remaining 20% - 30% are interneurons (Markram et al., 2004). The neocortex is a six layered structure and depending on the species has a thickness of approximately 1.4 – 4mm. The mini-column is the basic building unit of the neocortex (Mountcastle, 1997; Silberberg et al., 2002). It has few neurons, but still contains all major cortical cell types, that span vertically over Layer II to Layer VI. These mini-columns are connected to each other by horizontal connections and form cortical columns, the building blocks of the neocortex. Interestingly, the thickness of the neocortex only scales very weakly with the size of the animal. Therefore it is believed that the expansion of the neocortex during evolution was not achieved by a change in thickness of the cortex but rather by expansion of the cortical surface. This expansion could be generated by an increase in the number of cortical column and not the column size (Mountcastle, 1997). Neurons of the same cortical column share similar response properties and it has been shown in the cat that neighboring columns also tend to have neighboring receptive field. Therefore cortical columns can give rise to functionally organized cortical maps.

Neocortical circuits in a cortical column consist of a large number of excitatory and inhibitory neurons which form dense connections within the same and across neocortical layers. Usually sensory information reaches the cortex from the thalamus via thalamocortical fibers that terminate primarily into Layer IV. Neurons from Layer IV project to Layer III, which are strongly interconnected with neurons from Layer II. Layer II/III neurons also form lateral connections between each other and neighboring columns. They provide output to the brain regions relevant to the stimulus or project to

Introduction

Layer V which in turn project to subcortical regions or to Layer VI neurons. Layer VI neurons either connect to other neocortical regions or to the thalamus as part of a positive feedback loop between cortical columns and the thalamus (Silberberg et al., 2005). This tells us how outside stimuli reach their target regions in the brain however it does not tell us how information is processed and stored in cortical circuits because the cortex is a highly plastic structure which can change with sensory experience.

3.1.1 Plasticity in primary cortical areas

In primary cortical areas like the primary visual cortex (V1), the primary motor cortex (M1) or the primary auditory cortex (A1) neurons have specific receptive fields or tuning properties which are topologically organized. Many different studies have shown that this organization can be changed under certain conditions. Neurons in the V1 region have a direction and orientation selectivity (Hubel and Wiesel, 1968) and this direction and orientation selectivity has been shown to be dependent on sensory experience (White et al., 2001). In the auditory cortex (ACx), A1 neurons have specific receptive fields and are tuned to a specific frequency (best frequency) which is the frequency where one particular neuron shows its strongest response to the tone. Neurons in A1 of the rat are organized from low to high frequencies along the cortex (Kilgard and Merzenich, 1998). It has been shown that this frequency tuning can be altered by sensory experience like auditory cued fear conditioning (AFC). After AFC responses to the conditioned stimulus are increased while responses to other frequencies like to the pre-conditioned best frequency are reduced. Therefore it is possible for a neuron to change its best frequency (Bakin and Weinberger, 1990). It has also been shown that the response properties of neurons can be modulated by attention. Experiment in ferrets, that were required to pay attention to a series of tones and detect the right target tone, showed that if the target tone was in the receptive field of a neuron it could reshape the responses of this neuron (Fritz et al., 2003). These results suggest that not only auditory stimuli but also other multimodal inputs can reshape neuronal responses in the auditory cortex. Taken together primary cortical

Introduction

areas can be highly plastic and neuronal activity due to outside stimuli can reshape cortical circuits.

3.1.2 Neuronal activity in the auditory cortex

In primary cortical areas both evoked and spontaneous activity is observed (Sakata and Harris, 2009). In the ACx single neurons can show a strong and sustained firing when driven by their best frequency (Wang et al., 2005) and can respond very precisely to a stimulus because often the first spike can be recorded within the range of a few milliseconds (Heil, 2004). It has been shown that different neurons in the ACx of awake rats can have very heterogeneous response patterns when stimulated with the same tone. The same tone is either able to increase, decrease, elicit, suppress or have no effect on the firing pattern of different neurons. Further, responses are often brief and sparse because only a very small fraction of neurons (<5%) shows high activity during tone presentation (Hromadka et al., 2008). In contrast to neurons in the visual cortex neighboring ACx neurons can have heterogeneous response patterns. Similar results have also been found in ACx neurons of the mouse. *In vivo* 2-photon calcium imaging in A1 in deeply anesthetized mice showed that responses to sounds are heterogeneous and sparse. Furthermore, tonotopicity could not be found at local scale because response properties varied significantly between neighboring neurons. Interestingly, tonotopicity could be found on the larger scale indicating that there is some order also in the ACx. Still it was possible to find high activity correlations between nearby neurons which was not found when neurons were farther away. This would argue that these neurons form small highly interconnected networks and these networks can also partially overlap in space (Rothschild et al., 2010). Unpublished data from our lab indicates that sound evoked activity patterns in the ACx are restricted to few distinct response modes. Sounds that are associated in a specific response mode vary across local populations and multiple local populations can form a sound representation. Given the fact that these neuronal populations also overlap in space could be a direct experimental verification of the theory that neurons in the ACx form small subnetworks (Brice Bathellier, unpublished data). Therefore, the activity of neuronal populations

Introduction

which are also highly interconnected could be the underlying basis of stimulus processing, learning and memory storage.

3.1.3 Neuronal coding and the cell assembly

Since activity patterns of neuronal populations can be observed during outside stimulation the fundamental question arises how the brain uses these patterns to encode and to store information. One widely discussed hypothesis how the brain uses these patterns is the cell assembly theory by Donald Hebb. It is based on the idea that synaptic connections between pre and postsynaptic neurons become strengthened when they are active at the same time. Hebb hypothesized that a particular, highly interconnected group of neurons, which he called the cell assembly, represents a distinct cognitive unit. Further, that the activity of such assemblies can not only be activated by outside sensory stimuli but also by internal factors like other cell assemblies. Combining or chaining of cell assemblies would allow the brain to generate complex learned behavior. Therefore these units and the combination of cell assemblies could provide the basis for complex cognitive processes like memory formation, memory recall, thoughts or decision making (Hebb, 1949).

Indeed, there is experimental evidence for this. First, long term potentiation has been observed at many synapses (Bliss and Lomo, 1973). Furthermore, neurons fire together in the gamma rhythm and can therefore produce downstream effects that cannot be achieved by single neurons (Fries et al., 2007). Assemblies of neurons can be activated by outside as well as by inside stimuli because it has been shown that the hippocampus is able to generate sequential activity patterns by either using environmental cues or also by self organized internal mechanisms (Pastalkova et al., 2008). However, the main fundamental processes how cell assemblies emerge is still poorly understood.

Introduction

3.1.4 Auditory cued fear conditioning

Pavlovian fear conditioning is a widely used behavior paradigm for associative learning and memory formation. During auditory cued fear conditioning (AFC) an animal learns that a neutral stimulus like a tone (conditioned stimulus, CS) predicts an aversive stimulus like a footshock (unconditioned stimulus, US). When confronted again with the CS mice respond with a conditioned response like freezing (Weinberger, 2004). The advantages of AFC are that it is a rapid learning paradigm, because one training session is enough for the animal to make the association, and that the US can be very well controlled by the experimenter. Also the brain regions involved in the acquisition and expression of this fear memory have been mapped out previously. One structure critically involved in the acquisition of this fear memory is the lateral amygdala (LA), the place where both stimuli converge. The CS (tone) reaches the LA via the auditory thalamus and the auditory cortex (ACx) and the US (pain from the footshock) reaches the LA via the somatosensory thalamus and the somatosensory cortex. After AFC LA neurons show increased responses to the CS (Rogan et al., 1997). Damage to the LA before AFC abolishes the fear response (LeDoux et al., 1990). The LA sends direct and indirect projections to the central nucleus of the amygdala which projects to the brainstem and thalamic regions which control the expression of fear responses like freezing and also other reactions associated with the expression of fear (LeDoux, 2007).

Auditory information can reach the LA via a direct (thalamo-amygdala) and an indirect (thalamo-cortical-amygdala) pathway. It has been shown that both pathways can support learning of simple pure tones because lesions of either one of these pathways does not interfere with the acquisition of fear memories (Romanski and LeDoux, 1992). Single cell recordings in the rat after AFC showed that plasticity in ACx neurons develops later than in the LA and also that these neurons are more resistant to extinction. Therefore, it was suggested that the direct pathway is involved in a rapid, less reliable learning and that the indirect pathway is used for discrimination of more complex sound stimuli (Quirk et al., 1995; Quirk et al., 1997; LeDoux, 2000). Indeed, it has been shown that pretraining lesions of the ACx in the Mongolian gerbil does affect the learning of a discrimination task that involves frequency modulated tones (complex tones) but not pure tones. Further posttraining lesions also impaired the retention or

Introduction

retrieval of the complex tones (Ohi et al., 1999). There is also evidence that the indirect pathway via the auditory cortex (ACx) is the principal pathway used in the intact brain (Boatman and Kim, 2006). Lesioning the ACx after fear conditioning completely attenuates the fear response indicating that fear memory storage is dependent of the ACx. Recently it has also been shown that the acquisition of a task which is based on the discrimination of two sounds relies on both the direct and the indirect pathway because lesioned mice failed to discriminate two sounds after repeated training, however only the direct pathway is required for the recall (Antunes and Moita, 2010). Given the fact that the ACx is important for the acquisition and expression of fear responses AFC serves as a well defined model to gain more insights in the role of memory formation in cortical circuits.

3.1.5 Molecular mechanisms of cortical plasticity

In a classical experiment by Bliss and Lomo it has been shown that repeated stimulation of the perforant path fibers that project to the dentate area of the hippocampus, a brain region essential for learning and memory, leads to a long lasting potentiation at these synapse due to the increase in synaptic transmission and also due to an increase in the excitability of the cell population in the dentate area (Bliss and Lomo, 1973). This long lasting synaptic potentiation (LTP) is believed to be the cellular and molecular mechanism by which memories are formed and stored. Induction of LTP depends on the activation of postsynaptic *N*-methyl-D-aspartate (NMDA) receptors. During normal synaptic transmission the excitatory neurotransmitter glutamate is released from the presynaptic bouton and acts on both the NMDA and the α -amino-3-hydroxy-5-methyl-4-isoxazolepropionic (AMPA) receptors. AMPA receptors are permeable for Na^+ and K^+ and mediate most synaptic transmissions under basal conditions. NMDA receptors act as coincident detectors and are blocked by Mg^{2+} at rest. Upon AMPA receptor mediated depolarization of the postsynaptic membrane the Mg^{2+} block is removed and glutamate can act on the NMDA receptors which open and allow the influx of Ca^{2+} and Na^{2+} into the spine. The increase of Ca^{2+} in the postsynaptic spine is the critical trigger for LTP induction (Malenka and Nicoll, 1999). It has been

Introduction

shown that blocking of the NMDA receptors by the antagonist APV completely abolishes the induction of LTP (Coan and Collingridge, 1987) whereas the increase of Ca^{2+} in the spine by glutamate uncaging can induce LTP (Malenka et al., 1988). These findings could also be repeated in the mouse model where it has been shown that knocking out NMDA receptors in the CA1 region of the hippocampus lead to deficits in spatial learning tasks and the induction of LTP (Tsien et al., 1996a). Conversely, over-expression of NMDA receptors in the cortex and the hippocampus lead to increased performance in various memory tasks. Further, these mice also showed increased LTP induction (Tang et al., 1999). Ionotropic ion channels are not the only channels which can mediate LTP because also metabotropic glutamate receptors (mGluR) play a role in triggering LTP (Anwyl, 2009).

The increase of Ca^{2+} is crucial for the induction of LTP and acts as a second messenger in the postsynaptic neuron. Ca^{2+} increase is not only mediated by NMDA receptors or voltage gated calcium channels but is also released from internal Ca^{2+} stores. An increased Ca^{2+} level in the neuron leads to the formation of calcium/calmoduline complexes and the activation of a CamKII (Calcium/calmoduline dependent kinase II). CamKII can phosphorylate the GluR1 subunit of AMPA receptors making them more conductive and also triggers the insertion of new AMPA receptors into the postsynaptic density (Malenka and Nicoll, 1999; Lynch, 2004; Rumpel et al., 2005). Further, increased Ca^{2+} levels lead to cAMP dependent induction of protein kinase A (PKA) and activation of the mitogen-activated protein kinase (MAPK/ERK) via Ras-GTP and the phosphorylation of the ERK kinase. ERK activation leads to an increased conductance of K^{+} channels in the post synaptic density. ERK further phosphorylates the cAMP response element binding protein (CREB). CREB can bind to the CREB response element (CRE) which is present at many promoter regions and activates the transcription of downstream genes responsible for synaptic remodelling. One of the target genes of CREB is the immediate early gene and transcription factor *c-fos* which is also involved in the induction and maintenance of LTP (Peng et al., 2011). However, the exact mechanism how this is mediated is still unclear.

Introduction

3.2 Immediate early genes

Immediate early genes (IEGs) are genes that have low basal expression levels however, show a strong and transient increase of expression after stimulation. Over the last decade different IEGs like *c-fos*, *Arc/larg3.1* or *zif-268* have been found and characterized. Most of them belong to the class of transcription factors (e.g. *c-fos*, *zif-268*) but they can have multiple roles like postsynaptic effector proteins (*Arc*), secretion factors, membrane proteins or intracellular signaling (Okuno, 2011). Since they are rapidly induced in the brain after neuronal activity IEGs were suggested to play a crucial role in memory formation. Indeed it has been shown that *c-fos* (Dragunow et al., 1989), *Arc* (Link et al., 1995; Lyford et al., 1995) and *zif-268* (Abraham et al., 1993) can not only be induced by LTP (long term potentiation) but also by various learning paradigms like fear conditioning (Milanovic et al., 1998; Radulovic et al., 1998), operant conditioning (Bertaina and Destrade, 1995) or spatial learning (Guzowski et al., 2001).

3.2.1 Cellular functions of IEGs

The proto-oncogene *c-fos* is one of the best characterized IEGs and was the first IEG isolated from mouse brains after drug induced seizures (Morgan et al., 1987). Fos is part of a larger transcription factor family which consists of FOSB and the fos related antigens FRA1 and FRA2. Together with c-Jun, Fos forms the heterodimeric AP-1 complex (transcription factor activator protein-1) which binds to the AP-1 transcription sites on the promoter regions of various genes (Karin et al., 1997). Fos expression is induced upon membrane depolarization and activation of the MAPK/ERK pathway (Sheng et al., 1990; Wang et al., 2006). The activation of *c-fos* has been mapped out in detail however the downstream targets of Fos are still poorly understood. Different *c-fos* knock out models have been developed to study its role in the brain. Conventional *c-fos* null mutants show severe developmental phenotypes including smaller body weights, decreased viability at birth and osteoporosis however some of the mice are still able to survive which indicates that Fos is dispensable for the growth of most cell types (Johnson et al., 1992). Because of these severe phenotypes *c-fos* null mutants could not be tested for their behavioural phenotypes. Therefore, CNS specific *c-fos* knock-out

Introduction

mice have been developed to study the behavioural and synaptic role of *c-Fos* in the brain. It was found that hippocampal *c-fos* knock-out mice show normal brain development however have more severe seizures, a higher neuronal excitability and neuronal cell death after kainate injection. Furthermore, decreased *c-fos* expression also leads to changes in the AP-1 composition complex which could change the expression of downstream target genes. Indeed it has been shown that the *c-fos* knock-out mice have increased GluR6 levels in the hippocampus which could mediate the increased neuronal excitability (Zhang et al., 2002). Another mouse line with a CNS specific *c-fos* knock-out showed normal locomotion, motor skills and anxiety behaviour however was impaired in hippocampus dependant learning paradigms like the Morris water maze, a test for spatial learning and context dependent fear conditioning, a test for associative learning. Further, electrophysiological experiments showed that NR2A containing NMDA receptor dependant LTP induction was impaired however could be restored by repeated tetanic stimulation arguing that LTP induction is not blocked per se but inhibited by a CNS specific *c-fos* knock out (Fleischmann et al., 2003).

Another well characterized brain specific IEG is *Arc/arg3.1* (activity-regulated cytoskeleton-associated protein/activity-regulated gene 3.1). Unlike Fos, Arc is not a transcription factor but an effector protein which regulates other proteins. Similar to *c-fos* *Arc* induction depends on voltage gated calcium channels or metabotropic glutamate receptors. It has been shown that PKA (protein kinase A) and the MAPK pathway are involved in the induction of *Arc* expression however, the exact signaling cascades are poorly understood. The binding of at least three transcription factors (SRF, MEF2, CREB) to the synaptic activity responsive element of the *Arc* promoter is needed for the transcriptional activation of *Arc* (Kawashima et al., 2009). There is evidence that *Arc* mRNA further travels to synaptically activated dendrites and is locally translated (Steward et al., 1998). At the synapse Arc effects the AMPA receptor cycling because overexpression of *Arc* leads to a decrease of AMPA receptors in the postsynaptic density and *Arc* knock-out neurons show an increase of AMPA receptors. Therefore Arc was implicated to play a role in homeostatic synaptic scaling (Rial Verde et al., 2006; Shepherd et al., 2006). Unlike *c-fos* null mutants *Arc* null mutants develop normally, have a normal brain morphology and normal dendritic arborization. However

Introduction

they have impairments in re-learning and processing of spatial information, cued and contextual fear conditioning and conditioned taste aversion memory. *Arc* null mutants also have problems forming long term memories but not short term memories implicating an involvement of *Arc* also during memory consolidation. Electrophysiologically *Arc* null mutants have normal synaptic baseline transmission however fail to consolidate LTP and LTD (Plath et al., 2006). Complementary, infusion of *Arc* mRNA antisense oligodeoxynucleotides into the hippocampus of rats impairs LTP and LTM consolidation (Guzowski et al., 2000). *Arc* knock-out mice further show reduced tuning orientation specificity in the visual cortex (Wang et al., 2006).

Other IEGs like *zif-268* or *homer1* also play crucial roles in memory formation and memory expression. *Zif-268* knock-out mice have problems in maintaining late phase LTP. Short term memory formation is intact in these mice however they also have impairments in forming LTM assayed by a spatial, novel recognition and food preference task (Jones et al., 2001). Likewise, *ves1-IS/homer1a* knock-out mice show impairments in long term memory formation but not in the acquisition of a memory (Inoue et al., 2009).

3.2.2 IEGs as marker for neuronal activity

Since IEGs show a strong induction after behavioral manipulation they have been extensively used to mark active neurons either post hoc using immunohistochemistry, *in-situ* hybridization and quantitative PCR or *in vivo* using several mouse models. IEG protein and mRNA induction has been observed in different brain regions after contextual fear conditioning and retrieval (Milanovic et al., 1998; Huff et al., 2006; Mamiya et al., 2009), cued fear conditioning (Radulovic et al., 1998; Hall et al., 2001), spatial memory tasks (Guzowski et al., 2001; Shires and Aggleton, 2008), inhibiting avoidance learning (Zhang et al., 2011) and also different operant conditioning tasks (Bertaina and Destrade, 1995; Carpenter-Hyland et al., 2010; Rapanelli et al., 2010). Taking advantage of that *Arc* mRNA translocates from the nucleus to the dendrites within 5 minutes after neuronal activity *Arc in-situ* hybridization can be used to

Introduction

assay the activity of a neuron at two different time points (catFISH) (Guzowski et al., 1999). This method has also been recently adapted to *c-fos* (Lin et al., 2011).

Alternatively, genetically modified rodent models have been developed that express reporter genes like fluorescence proteins (Fleischmann et al., 2003; Barth et al., 2004; Wang et al., 2006; Man et al., 2007; Eguchi and Yamaguchi, 2009; Grinevich et al., 2009) or beta-galactosidase (Smeyne et al., 1992; Reijmers et al., 2007) under the control of different IEG promoters allowing the visualization of neuronal populations that were activated *in vivo*. Arc-GFP transgenic mice have been used for *in vivo* 2-photon imaging of neuronal populations in the visual cortex. It was shown that visual stimulation lead to increased Arc-GFP expression and the same neuronal assemblies could be reactivated by consecutive rounds of stimulation. Interestingly, repetitive stimulation reduced the amount of reactivated cells and the initial neuronal assembly became smaller but reactivation became more reliable arguing for an experience dependant mechanism of cortical adaptation (Wang et al., 2006). TetTag transgenic mice have been used to test if learning and memory retrieval activates the same set of neurons. TetTag mice combine the tetracycline transactivator (tTA) expressed under the control of the *c-fos* promoter and lacZ expressed under the TetO operator. As long as these mice are fed with doxycyline neuronal activity does not lead to lacZ expression. Only in the time window when no doxycyline is present neuronal activity leads to a long lasting lacZ expression and tagging of active neurons. Combining this system with immunohistochemistry for Zif-268 allowed the authors to test if the same neurons are activated during memory formation and memory retrieval. Indeed the authors found a significant amount of neurons in the lateral and basolateral amygdala that were activated during auditory cued fear conditioning and retrieval of the fear memory. Further the amount of reactivated neurons also correlated with the strength of the memory retrieval (Reijmers et al., 2007). Interestingly, the amount of Fos positive neurons was much lower than what is usually found after AFC in the amygdala (Radulovic et al., 1998). In another study Fos-GFP transgenic mice were used to correlate *c-fos* expression with spontaneous neuronal activity under basal conditions in the somatosensory cortex of mice. Fos-GFP positive neurons showed higher firing rates *in vivo* and *in vitro*. Paired cell recordings revealed that Fos-GFP positive neurons also

Introduction

had a higher likelihood of being connected to each. This result could indicate that higher active neurons (neurons which have high Fos levels shown by GFP expression) form subnetworks in the cortex (Yassin et al., 2010).

Using IEGs as markers of neuronal activity can have limitations because it is well known that *c-fos* expression can be activated by many different cellular pathways (Eferl and Wagner, 2003; Zenz et al., 2008). Further, most of the studies were done post hoc and therefore it is difficult to disassociate IEG expression which comes from neuronal activity and IEG expression which was induced by stress (Cullinan et al., 1995) or other factors which accompany behavioral training and testing. Therefore, carefully chosen controls are essential to separate unspecific induction from neuronal specific induction and complementary methods to IEGs would be desirable.

3.3 Photoactivatable fluorescence proteins

Since the discovery that the green fluorescence protein (GFP) from the jellyfish *Aequorea Victoria* is encoded by a single gene, that its fluorescence does not require any cofactors and that GFP can be genetically expressed in the living animal, fluorescence proteins became valuable tools for many researchers. Several mutant forms of wtGFP and the discovery of red fluorescence proteins resulted in a palette of FPs spanning the whole spectral range of visible light.

Photoactivatable fluorescence proteins (PA-FPs) are a special class of fluorescence proteins that change their spectral properties after a brief pulse of light at a specific wavelength. PA-FPs can be divided into two different groups. Members of the first group like PA-GFP (Patterson and Lippincott-Schwartz, 2002) and PamCherry (Subach et al., 2010) or Kaede (Ando et al., 2002) and KikGR (Tsutsui et al., 2005) show an irreversible switch from a nonfluorescent to a fluorescent stage (PA-FP) or a switch from one color to another color respectively (PS-FP). Members from the second group like Dronpa (Habuchi et al., 2005) exhibit a reversible switch from the non-fluorescent to the fluorescent state and allow an on and off switch of the fluorescence. PA-FPs share the same structure as conventional fluorescence proteins consisting of a beta-barrel tightly

Introduction

formed by 11 beta strands on the outside and a alpha helix running diagonal through the barrel. The chromophore is attached to the alpha helix in the centre of the barrel and is therefore protected from the outside environment (Stiel et al., 2007). In wtGFP the absorption spectrum consist of two peaks one major at 397nm and one minor at 475nm which correspond to the neutral, protonated and the anionic, deprotonated chromophore respectively. Irradiation at ~400nm shifts the chromophore population ratio to the anionic form. It has been shown that this switch is mediated by a light induced oxidative decarboxylation of Glu222 that leads to a change in the hydrogen bonding network and chromophore deprotonation (van Thor et al., 2002). In PA-GFP the mutation of threonine at the position 203 to isoleucine (T203H) produces the most neutral chromophore form without an absorption peak at 475nm. Illumination at ~400nm leads to an irreversible photoconversion from the neutral to the anionic form with an absorption maximum at 504nm and emission maximum at 517nm respectively resulting in a 100fold increase of the green fluorescence (Patterson and Lippincott-Schwartz, 2002; Henderson et al., 2009). Over the past year many different PA-FPs have been described and characterized (reviewed in: Lippincott-Schwartz and Patterson, 2009). The ability to selectively switch on the fluorescent makes PA-FPs ideal tool to precisely label and track subpopulations of proteins (Luo et al., 2006), organelles (Molina and Shirihai, 2009) or cells (Sato et al., 2006) in the living tissue. Further transgenic mice have been reported that express Kaede (Tomura et al., 2008) or KiKGR (Nowotschin and Hadjantonakis, 2009) and have been successfully used to monitor the cellular migration and cell fate *in vivo*. Therefore PA-FP could be ideal tools to conditionally label cells in the living brain with single cell resolution.

Aim of this work

4. Aim of this work

A mechanistic understanding how specific activity patterns emerge in neuronal circuits is lacking in most systems. Most approaches to functionally analyze neuronal populations are limited to the description of their activity. This constitutes a major limitation. Therefore, it is essential to gain additional information about neuronal populations which goes beyond the description of their activity.

The aim of my thesis was to devise novel strategies that allow the tagging of neurons *in vivo* with single cell resolution based on functional criteria. Furthermore, tagged neurons should be readily identifiable *in vitro* again. Combining *in vivo* calcium imaging with conditional labeling of neurons allows us to gain additional information about neurons that are active and can define the identity and connectivity of neurons forming an assembly.

In the first part we tested the specificity of immediate early gene expression in the auditory cortex after auditory fear conditioning because IEG driven expression of a reporter could be a strategy to fulfill the aim of the thesis. We tested the expression of *c-fos* and *Arc* in the ACx and also included several control groups to test for factors which could lead to unspecific expression of IEGs. We further used mRNA microarrays to find other genes that could be used as activity markers. We concluded that IEGs would not be a specific solution to label active neurons in the auditory cortex.

In the second part we tested the suitability of photoactivatable proteins to label neurons *in vivo*. We generated mice that express PA-GFP, allowing photolabeling of individual neurons. We could combine photolabeling with calcium imaging *in vivo*. With this novel method we generated a system that allows conditional labeling of neurons even across cell types.

5. Manuscript I: Induction of immediate early genes in the mouse auditory cortex after auditory cued fear conditioning to complex sounds.

Manuel Peter¹, Harald Scheuch¹, Thomas. R. Burkard¹, Juliane Tinter¹, Tanja Wernle² and Simon Rumpel¹

1) Institute of Molecular Pathology (IMP), Dr. Bohr-Gasse 7, 1030 Vienna, Austria

2) Present address: Kavli Institute for Systems Neuroscience/Centre for Biology of Memory, Norwegian University of Science and Technology, Trondheim, Norway

Author contributions:

Manuel Peter: designed experiments, performed the behavior experiments, the quantitative PCR, the microarray analysis and prepared the manuscript

Harald Scheuch: performed the microarray analysis

Thomas. R. Burkard: analyzed the microarray data

Juliane Tinter: performed lesion studies

Tanja Wernle: performed lesion studies

Simon Rumpel: designed experiments and prepared the manuscript

Description of the manuscript

In this study tested the specificity of immediate early gene expression in the auditory cortex after auditory fear conditioning. This provides insights how the two widely used IEGs *c-fos* and *Arc* are expressed after fear conditioning. We included several control groups to test for factors that could lead to unspecific expression of IEGs. We further used mRNA microarrays to find other genes that could be used as learning specific markers. This manuscript has been published in *Genes, Brain and Behavior*.

Induction of immediate early genes in the mouse auditory cortex after auditory cued fear conditioning to complex sounds

M. Peter, H. Scheuch, T. R. Burkard, J. Tinter, T. Wernle[†] and S. Rumpel*

Research Institute of Molecular Pathology, Vienna, Austria, and
[†]Present address: Kavli Institute for Systems Neuroscience/Centre for Biology of Memory, Norwegian University of Science and Technology, Trondheim, Norway
*Corresponding author: S. Rumpel, Research Institute of Molecular Pathology, Dr. Bohr-Gasse 7, 1030 Vienna, Austria.
E-mail: simon.rumpel@imp.ac.at

Immediate early genes (IEGs) are widely used as markers to delineate neuronal circuits because they show fast and transient expression induced by various behavioral paradigms. In this study, we investigated the expression of the IEGs *c-fos* and *Arc* in the auditory cortex of the mouse after auditory cued fear conditioning using quantitative polymerase chain reaction and microarray analysis. To test for the specificity of the IEG induction, we included several control groups that allowed us to test for factors other than associative learning to sounds that could lead to an induction of IEGs. We found that both *c-fos* and *Arc* showed strong and robust induction after auditory fear conditioning. However, we also observed increased expression of both genes in any control paradigm that involved shocks, even when no sounds were presented. Using mRNA microarrays and comparing the effect of the various behavioral paradigms on mRNA expression levels, we did not find genes being selectively upregulated in the auditory fear conditioned group. In summary, our results indicate that the use of IEGs to identify neuronal circuits involved specifically in processing of sound cues in the fear conditioning paradigm can be limited by the effects of the aversive unconditional stimulus and that activity levels in a particular primary sensory cortical area can be strongly influenced by stimuli mediated by other modalities.

Keywords: *Arc*, *c-fos*, memory, microarray, qPCR

Received 1 September 2011, revised 16 November 2011 and 15 December 2011, accepted for publication 19 December 2011

Auditory cued fear conditioning is a widely used behavioral paradigm to investigate associative learning and memory formation (Fanselow & Poulos 2005; Maren 2001). During conditioning, an animal learns that a particular auditory

stimulus predicts an aversive stimulus. When confronted with this auditory conditional stimulus (CS), rodents respond with a cessation of movement (freezing). An advantage of this behavioral model is that a large number of brain areas mediating this behavior have been mapped out previously. The auditory cortex (ACx) has been suggested to play a role in the formation of fear memories. This is based on conditioning-induced changes in the firing of auditory neurons and lesion studies (Antunes & Moita 2010; Boatman & Kim 2006; Quirk *et al.* 1997; Romanski & Ledoux 1992; Weinberger 2004). Beyond the specific function in fear conditioning, storage of memories has been proposed to be one of the major functions of the neocortex in general (Marr 1970). Therefore, auditory fear conditioning could potentially serve as a well-defined behavioral model to gain a better understanding of the role of cortical circuits in memory formation.

Whereas in the last decades much of memory research was devoted to elucidate molecular mechanisms of synaptic plasticity as a cellular substrate of memory, increasing efforts have been made to investigate memory formation also at the level of neuronal circuits. A critical step is to identify elements in a circuit that are specifically involved in memory formation. A small number of genes (e.g. *c-fos*, *Arc/arg3.1*, *Egr1/Zif238*) have been discovered that show strong, fast and transient induction of expression upon neuronal activity (Abraham *et al.* 1993; Dragunow *et al.* 1989; Link *et al.* 1995; Lyford *et al.* 1995; Morgan *et al.* 1987) and behavioral manipulations (Bertaina & Destrade 1995; Guzowski *et al.* 1999, 2001; Montag-Sallaz *et al.* 1999). Therefore, immediate early genes (IEGs) have been used as cellular markers to identify neurons that are activated during a specific behavior. Expression of IEGs in the brain has been detected on mRNA (Carpenter-Hyland *et al.* 2010; Guzowski *et al.* 1999; Han *et al.* 2009; Lin *et al.* 2011) as well as on protein level (Frankland *et al.* 2006; Hall *et al.* 2001; Mamiya *et al.* 2009; Milanovic *et al.* 1998; Radulovic *et al.* 1998; Zhang *et al.* 2011). Furthermore, rodent models that rely on the activity of IEG promoters have been developed to report neuronal activation by expression of a reporter gene or activating other genes (Barth *et al.* 2004; Fleischmann *et al.* 2003; Grinevich *et al.* 2009; Man *et al.* 2007; Reijmers *et al.* 2007; Wang *et al.* 2006).

However, it is known that genes like *c-fos*, which was identified as a proto-oncogene, can be induced by a large number of different cellular pathways (Eferl & Wagner 2003; Zenz *et al.* 2008). It has also been shown that many factors can lead to the induction of IEGs in the brain (Cullinan *et al.* 1995; Guzowski *et al.* 1999; Sharp *et al.* 1991). Therefore, carefully chosen controls are essential to dissociate other factors that can lead to the induction of IEGs in a non-specific manner.

Here, we analyze the effects of auditory fear conditioning on the induction of IEGs in the ACx in a number of different paradigms using quantitative polymerase chain reaction (qPCR) and microarray experiments.

Materials and methods

Animals

Male CB57BL/6J mice (Charles River Laboratories, Wilmington, MA, USA) in the age of 3–4 month were used for all experiments. Mice were housed in groups of two to five animals with a 12-h light/dark cycle, and experiments were conducted during the light-phase cycle. All experiments were performed in accordance with the Austrian laboratory animal law guidelines for animal research and had been approved by the Viennese Magistratsabteilung 58 (Approval number: M58/02179/2007/11).

ACx lesions

Mice were deeply anesthetized for about 2–4 h (2.5 mg ketamine HCl and 0.02 mg medetomidine HCl/25 g mouse weight) and i.m. injected with 0.04 ml of dexamethasone. They were held in a modified stereotaxic apparatus (David Kopf Instruments, Tujunga, CA, USA) and kept on a heat pad at 37°C. The skin was disinfected and lidocaine/noradrenaline was injected subcutaneously before unilateral incision. Connective tissue was removed from the skull, and the musculus masseter dissected at its rostral end. A small piece of bone (~3–4 mm²) was cut out of the skull with a scalpel and put aside. The ACx was lesioned by cauterization. The procedure was repeated for the second hemisphere. Finally, the fragment of the skull was put back into place, fixed with bone wax and the skin was closed with tissue adhesive. After surgery, mice were left on a heat pad until gaining consciousness and subsequently put back in their home cage (HC) for at least 2–3 days before continuing behavioral training. As a control, sham surgery was performed in a subset of littermates. The procedure involved anesthesia, removal of the musculus masseter and reclosure of the skin; the ACx was left intact. Generally, mice recovered quickly from the surgery, and no gross behavioral differences were detectable between lesioned and sham-operated animals. The person performing behavioral training and testing was blinded to the surgery condition of the individual animals. Position and size of the lesions were documented and verified at the end of the experiment (Fig. S1).

Auditory cued fear conditioning

The behavioral setup was controlled by a personal computer with WINDOWS XP Professional, Version 2002, SP2 (Microsoft, Redmond, WA, USA) operating system running custom Matlab R2007a software (MathWorks, Natick, MA, USA). All behavioral experiments were performed in an isolation cubicle (H10-24, Coulbourn Instruments, Whitehall, PA, USA) which was equipped with white LEDs as house light, a microphone and a CCD KB-R3138 camera with infrared LEDs (LG Electronics Austria, Vienna, Austria) which was connected to a Cronos framegrabber (Matrox, Dorval, Quebec, Canada). The conditioning chamber (25 × 25 × 42 cm, model H10-11M-TC, modified, Coulbourn Instruments) was combined either with a stainless steel shock floor or a grid floor. A custom-made cartridge (round or quadrangular) was inserted to form different local environmental contexts. Foot shocks were delivered via an external shocker (Precision Animal shocker, Coulbourn Instruments). Sounds were played from a L-22 soundcard with a maximal sampling frequency of 192 kHz (Lynx Studio Technology, Costa Mesa, CA, USA) and delivered via an amplifier (Model SLA-1, Applied Research and Technology, TEAC Europe GmbH, TASCAM Division, Wiesbaden, Germany), a modified equalizer (Model #351, Applied Research and Technology, TEAC Europe GmbH, TASCAM Division, Wiesbaden, Germany) and a custom-made speaker for free field delivery of sounds. 'Complex sound' stimuli of 2-second duration used in the experiments shown in Fig. 1a,b were generated of pieces of

music that were delivered with a sampling rate of 192 kHz, i.e. approximately four times faster than real time. The pure tone sound stimulus used for reconditioning consisted of a sine wave with a frequency of 4 kHz. On- and offsets of stimuli were smoothed with a 10-millisecond long half-period cosine function. Sound levels for all stimuli used were normalized to a mean power of 78 dB sound pressure level (SPL). Peak sound levels ranged from 83 to 89 dB SPL.

Habituation

Mice were habituated for 3 days. They were handled (i.e. repeatedly picked up from cage and held in the hand for a few seconds) and placed in all test environments for 5 min. No sound was presented during habituation.

Conditioning

In the conditioning environment, lights were turned on (~20–30 lux), the roundish cartridge was inserted. A mild residual odor was present from previous cleaning of the chamber with ethanol. Mice were placed in the chamber directly before the start of each session. After at least 1 min, baseline (60–90 seconds) five sound-shock pairings (0.75 mA, 1 second, immediately following the sound) were given with a randomized interstimulus interval ranging from 50 to 75 seconds (paired). For unpaired conditioning, five foot shocks and five sounds were presented in a random order, separated by at least 1 min (unpaired). A third group of mice received only the five foot shocks without sound presentation. The foot shocks were delivered with a randomized interstimulus interval ranging from 50 to 75 seconds (shock). For the fourth group, only the sound was presented during the conditioning session (sound). To the fifth group, no sounds or shocks were presented (naïve).

Memory testing

One day after auditory fear conditioning, mice were tested for freezing responses (quadrangular cartridge, lights off, HC embedding underneath the metal grid). After at least 1 min of baseline (60–90 seconds), the CS and two unconditioned sounds were presented in two blocks of five presentations with an interstimulus interval of 2 seconds. Blocks were given in a random order and were separated by a randomized interval (22–37 seconds).

Quantitative analysis of behavior

During conditioning and memory testing, movies were recorded at a frame rate of 2.8 (frames per seconds). Movies were analyzed offline based on a similar approach as described by Kopec *et al.* (2007), which provides a rapid and unbiased analysis of animal behavior. In short, the number of 'significant motion pixels' (SMPs), i.e. pixels which varied by more than 20 gray values, was calculated for all pairs of consecutive frames using a custom Matlab R2007a script (Mathworks). For each movie, the size of the mouse was estimated by the median SMP value of the 25% highest SMPs calculated from pairs of frames at least 2 min apart, thus capturing the mouse likely at different positions in the chamber. The threshold for freezing was defined as fewer SMPs than corresponding to 0.3% of the mouse size, which separates SMP values during freezing and movement periods. Baseline freezing was assessed during silence between 30 and 60 seconds of each protocol run.

Quantitative PCR

Mice were habituated as described above and kept overnight in the behavior chamber to ensure low basal IEG expression levels. On the next day, animals were subjected to a conditioning, unpaired conditioning, shock-only or tone-only session. Mice which were directly taken from the HC or which were kept in the behavior chamber overnight without any shock or tone presentation served as HC and context controls, respectively. Thirty minutes after the session was over, animals were sacrificed, the brain was immediately removed and ACx tissue was isolated bilaterally. Total RNA was isolated using Trizol reagent (Life Technologies, Grand Island,

NY, USA), and 1 μ g total RNA was used as a template to generate cDNA using oligo(dT) primers with the Ready-To-Go You-Prime First-Strand Beads (GE Healthcare, Waukesha, WI, USA). Quantitative PCR was performed on a DNA Engine Opticon 2 system (Bio-Rad Laboratories, Hercules, CA, USA), and amplification was monitored using SYBRGreen reagent (Life Technologies, Grand Island, NY, USA). Quantitative PCR primers were as follows: *c-fos*: 5'-CGAAGGGAACGGAATAAG-3' and 5'-CTCTGGGAAGCCAAGGTC-3', *Arc*: 5'-GGAGGGAGGTCTTCTACCGTC-3' and 5'-CCCCACACCTACAGAGACA-3' and α -*tubulin* (*Tuba1a*): 5'-CCTGCTGGGAGCTCTACT-3' and 5'-GGGTTCCAGGTCTACGAA-3'. These primers were chosen because they show specific binding only to the mRNA of the target gene. mRNA copy numbers were calculated for each sample using the cycle threshold (Ct) value. The mRNA of the housekeeping gene α -*tubulin* was amplified in parallel and used for normalization. We used the $\Delta\Delta$ Ct method to assay changes in the gene expression of the target genes. Therefore, the number of amplification steps which were required to reach an arbitrary Ct value was computed and the relative gene expression was represented by $\log_2-\Delta\Delta$ Ct. The $\Delta\Delta$ Ct value was calculated as Δ Ct_{Target} - Δ Ct_{Tubulin} (Livak & Schmittgen 2001).

Microarrays

Custom-made cDNA arrays were generated using the Riken Fantom III library. The chip contained 20661 validated genes. For hybridization, total RNA was used to synthesize aRNA using the MessageAmp II aRNA Amplification kit (Life Technologies, Grand Island, NY, USA) following the manufacturer's protocol. Next, 4 μ g aRNA was used for the amino-allyl cDNA synthesis using Superscript II RT (Life Technologies, Grand Island, NY, USA) and aminoallyl-dUTP (Sigma-Aldrich, St.Louis, MO, USA). The amino-allyl cDNA was labeled with Alexa Fluor 555 and Alexa Fluor 647 (Life Technologies, Grand Island, NY, USA). For the common reference, the labeled cDNA

samples were mixed to equal amounts. Samples were hybridized at 45°C for 12 h using a Tecan HS4800 Hybridization Station (Tecan Group Ltd., Männedorf, Zuerich, Switzerland). After drying, the slides were scanned with a GenePix4000B Microarray Scanner (Molecular Devices, Sunnyvale, CA, USA) and analyzed using the GENEXPRO 6.0 software package (Molecular Devices, Sunnyvale, CA, USA). The Raw values were calculated with a custom-written script using R 2.13 as programming language (Institute for Statistics and Mathematics, WU Wien) using the LIMMA 2.18.2 package (Smyth 2004). The data were further analyzed with SPOTFIRE 2.2 (TIBCO Spotfire, Somerville, MA, USA). The primary data have been submitted to the publicly accessible database 'ArrayExpress' in compliance with the MIAME guidelines (Accession number: E-MTAB-661).

Data analysis and statistics

Results are presented as mean \pm SEM or mean \pm SD, as indicated in the corresponding figure legends. For statistical analyses, the Matlab R2007a 'statistics toolbox' package was used (Mathworks). To test for differences in median freezing levels in lesioned or sham-operated mice (Fig. 1) or differences in freezing during silence and sound presentation (Fig. 2), we used a two-sided Wilcoxon rank-sum test. To test if gene expression levels were altered across multiple behavioral treatments, a one-way analysis of variance (ANOVA) was performed.

Results

Fear conditioning to 'complex sounds'

The requirement of cortical pathways in auditory cued fear conditioning in rodents is a matter of active research. Despite

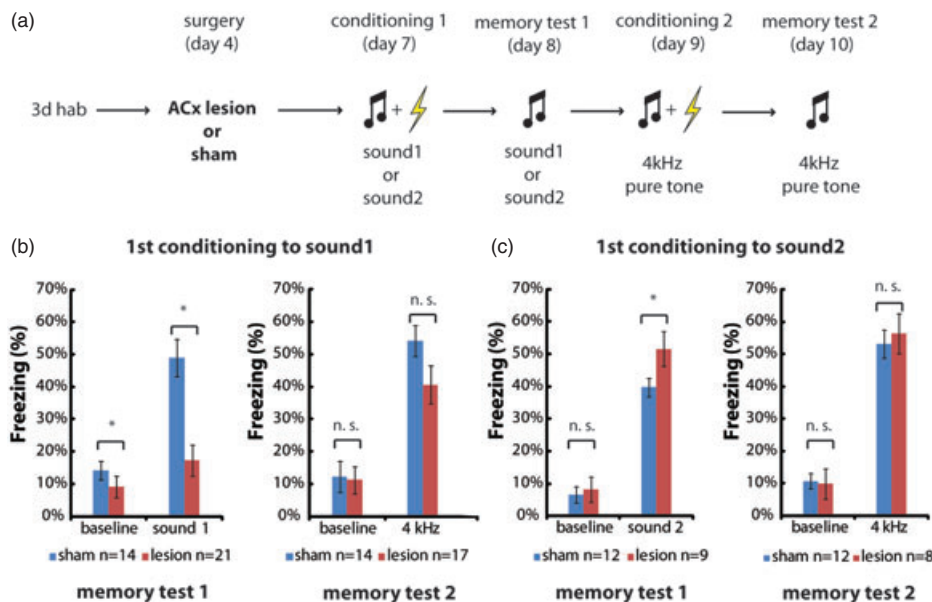


Figure 1: The ACx is required for conditioning to a subset of 'complex sounds'. (a) Schematic of the experimental design. (b) Behavioral data from lesioned (red) and sham-operated (blue) groups of mice that had been conditioned to the 'complex sound 1' as CS. Average freezing levels in a memory test session during silence and presentation of the CS 24 h after the first conditioning session (left panel) and in a memory test session 24 h after a second conditioning session to a 4-kHz pure tone (right panel). (c) Data from a similar experiment, except that a different CS ('complex sound 2') was used for conditioning. Note that ACx function was required for successful memory formation when sound 1 was used, whereas conditioning to sound 2 was not dependent on the ACx. Lesioned mice could be subsequently conditioned to a 4-kHz pure tone. Error bars represent SEM. Asterisk indicates significant difference, *P* value shown above bars.

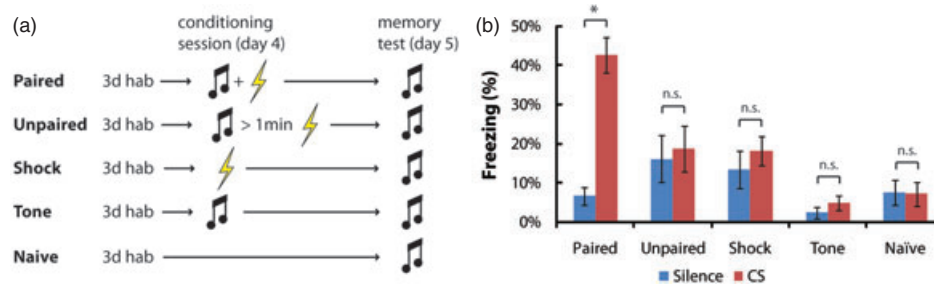


Figure 2: Freezing behavior in memory test sessions after various conditioning paradigms. (a) Behavior protocols used for auditory cued fear conditioning. (b) Mean freezing during silence and CS presentation 24 h after the paradigms described in (a). Error bars represent SEM. Asterisk indicates significant difference, P value shown above bars.

the observation of plastic changes in tone-evoked responses in ACx neurons following auditory fear conditioning (Quirk *et al.* 1997; Weinberger 2004), it has been shown that conditioning to pure tones leads to successful learning even without the contribution of cortical pathways (Romanski & Ledoux 1992; Song *et al.* 2010). However, recent studies indicated that cortical pathways nevertheless play a role under certain conditioning conditions. In particular, memory deficits were observed when lesions are performed after conditioning (Boatman & Kim 2006), discriminative conditioning paradigms are used (Antunes & Moita 2010) or, interestingly, conspecific communication sounds are used as CS (Kholodar-Smith *et al.* 2008a,b). To investigate the induction of IEGs in the ACx in the context of learning and memory, we first tested the requirement of the ACx for conditioning to a number non-conspecific of ‘complex sounds’. These arbitrary stimuli had been selected to have a broad frequency content and strong temporal and frequency modulation. ‘Complex sounds’ resemble much better the statistics of naturally occurring sounds (frequency and amplitude modulation, power in many frequencies in parallel) and so may better mimic the processes of fear memory formation occurring in the natural habitat of mice. Furthermore, broad-band ‘complex sounds’ lead to a more widespread and even activation of the auditory fields given the fact that several fields of the mouse ACx are organized in a tonotopic fashion (Stiebler *et al.* 1997). We reasoned that this will likely lower the variance in the induction of IEGs.

We conditioned a large number of groups of mice to various ‘complex sounds’ and tested freezing behavior in memory test sessions when the mice were exposed again to the CS alone as readout for successful memory formation. For each given CS, a group of mice received bilateral lesions of the ACx before conditioning and were analyzed in parallel with a group of sham-operated mice (Figs 1a and S1). We tested a total of 10 ‘complex sounds’ as CS for conditioning and observed in about half of the experimental series a strong reduction of freezing in the memory test session, indicating a cortex-dependent deficit in memory. In Fig. 1b (left panel), an example is shown from an experimental series using a ‘complex sound’ in which conditioning required ACx function. In the first memory test session following conditioning to the ‘complex sound’, we observed during silence generally very low freezing levels in both groups, mildly lower in the

lesioned group, but a marked reduction in freezing levels in the lesioned group when the CS was presented (sham: silence: 14% ± 3%, CS: 49% ± 6%, mean ± SEM, $n = 14$, lesion: silence: 9% ± 3%, CS: 17% ± 5%, mean ± SEM, $n = 21$; Wilcoxon rank-sum test sham vs. lesion during silence: $P < 0.019$, Wilcoxon rank-sum test sham vs. lesion during CS: $P < 0.001$). In Fig. 1c (left panel), an example is shown from an experimental series using a ‘complex sound’ in which conditioning was not dependent on ACx function. In the first memory test session following conditioning to the ‘complex sound’, we again observed during silence generally very low freezing levels in both groups but high and comparable freezing levels in both groups, that were even slightly higher in the lesioned group when the CS was presented (sham: silence: 7% ± 3%, CS: 40% ± 3%, mean ± SEM, $n = 12$, lesion: silence: 8% ± 4%, CS: 52% ± 5%, mean ± SEM, $n = 9$; Wilcoxon rank-sum test sham vs. lesion during silence: $P > 0.803$, Wilcoxon rank-sum test sham vs. lesion during CS: $P < 0.039$). Consistent with previous reports (Romanski & Ledoux 1992; Song *et al.* 2010), the lesioned mice could be effectively conditioned to a 4-kHz pure tone in a second conditioning session, and under all conditions, no significant differences between lesioned and sham-operated mice could be detected [Fig. 1b (right panel) sham: silence: 12% ± 5%, CS: 54% ± 5%, mean ± SEM, $n = 14$, lesion: silence: 11% ± 4%, CS: 41% ± 6%, mean ± SEM, $n = 17$; Wilcoxon rank-sum test sham vs. lesion during silence: $P > 0.720$, Wilcoxon rank-sum test sham vs. lesion during CS: $P > 0.147$; Fig. 1c (right panel) sham: silence: 11% ± 5%, CS: 53% ± 4%, mean ± SEM, $n = 12$, lesion: silence: 10% ± 5%, CS: 56% ± 6%, mean ± SEM, $n = 8$; Wilcoxon rank-sum test sham vs. lesion during silence: $P > 0.335$, Wilcoxon rank-sum test sham vs. lesion during CS: $P > 0.463$]. This indicates that the deficit in memory formation depends on the properties of the sound. With the limited set of tested sounds, we were not able to identify an obvious spectro-temporal feature of the complex sounds that would identify a given ‘complex sound’ dependent on cortex function during conditioning.

Freezing behavior is selectively induced by paired conditioning

We next characterized a number of behavioral fear conditioning paradigms in detail using the ‘complex sound’ #1 (Fig. 1b)

as CS. We used groups of mice that underwent auditory fear conditioning and also other procedures that allowed us to control for non-associative learning (e.g. sensitization) or general arousing conditions (Fig. 2a). Specifically, we used a first group of mice (paired) that underwent classical auditory fear conditioning in which five presentations of a 2-second auditory stimulus were paired with a 1-second electrical foot shock. One day after conditioning, the mice were placed in a different environment, and we automatically scored freezing behavior during silence and during presentation of the sound. As expected, mice showed a strong increase in freezing behavior (paired: silence: $7\% \pm 2\%$, CS: $43\% \pm 5\%$, mean \pm SEM, $n = 5$, Wilcoxon rank-sum test: $P < 0.008$; Fig. 2b), indicating successful association of sound and shock. A second group of mice (unpaired) underwent unpaired fear conditioning, in which the animals receive the same number of shocks and sound presentations as during classical conditioning. However, these two stimuli were separated in time by more than a minute. Mice cannot form an association between tones and shocks under these conditions (Lavond & Steinmetz 2003). We observed slightly increased freezing levels during baseline compared to the paired condition that did not change during tone presentation (unpaired: silence: $16\% \pm 6\%$, CS: $19\% \pm 6\%$, mean \pm SEM, $n = 8$, Wilcoxon rank-sum test: $P > 0.644$; Fig. 2b). A third group of mice (shock) received only foot shocks without presentation of auditory stimuli. This form of conditioning is referred to as contextual conditioning, as mice typically form an association to the environmental context in general. Again, a day later, the mice were placed in a different environment to selectively assess freezing behavior upon sound presentation without the contextual component. Freezing behavior was scored during silence and sound presentation. As expected, we observed slightly increased freezing levels in general but no significant increase in freezing behavior upon sound presentation (shock: silence: $13\% \pm 5\%$, CS: $18\% \pm 4\%$, mean \pm SEM, $n = 7$, Wilcoxon rank-sum test: $P > 0.335$; Fig. 2b). A fourth group (tone) was presented to the sound alone without shocks in a pseudo-conditioning session. We again measured freezing when the mice were re-exposed to the auditory stimulus on the next day. We observed low freezing levels during both silence and sound presentation (tone: silence: $2\% \pm 2\%$, CS: $5\% \pm 2\%$, mean \pm SEM, $n = 5$, Wilcoxon rank-sum test: $P > 0.294$; Fig. 2b). We used a fifth group (naïve) where the sound was presented for the first time only during the memory test. Here, we observed only minimal freezing during silence and sound presentation (naïve: silence: $8\% \pm 3\%$, CS: $7\% \pm 3\%$, mean \pm SEM, $n = 4$, Wilcoxon rank-sum test: $P > 1.0$; Fig. 2b). The last two groups control for sounds that would intrinsically induce freezing behavior, which has been reported for particularly loud sounds (Kamprath & Wotjak 2004). In summary, we observed sound-specific freezing behavior only after paired auditory cued conditioning indicating successful association of sound and shock.

Several behavioral paradigms induce expression of *c-fos* and *Arc* in the ACx

Next, we were interested in testing how far the protocols described above would induce the expression of the IEGs

c-fos and *Arc* in the ACx. As it is known that IEGs can be induced by various factors, ranging from novelty, stress and water deprivation (Cullinan *et al.* 1995; Guzowski *et al.* 1999; Sharp *et al.* 1991), we included additional cohorts of mice in which an induction would not be expected: one group of mice was taken directly from the HC and another group of mice was exposed to the familiar conditioning context, but no sounds or shocks were applied. To measure the expression levels of *c-fos* and *Arc*, we isolated tissue from the ACx 30 min after the behavioral paradigm, a time point in which the transient expression of IEGs reaches its maximum after induction (Zangenehpour & Chaudhuri 2002) (Fig. 3a,b). We isolated the total RNA, reverse transcribed the mRNA and performed a qPCR experiment in which we measured the relative expression levels of *c-fos* and *Arc* mRNA relative to α -*tubulin* mRNA, which is often used as reference due to its robust and constant expression (Vanguilder *et al.* 2008). We found that conditioning can induce significant changes in *c-fos* mRNA levels in the ACx (one-way ANOVA $P < 0.001$; Fig. 3c). Specifically, we observed relatively low expression levels for mice taken directly from the HC (HC: 0.0061 ± 0.0021 , mean \pm SD, $n = 3$), mice being exposed only to the context (context: 0.0047 ± 0.0004 , mean \pm SD, $n = 3$) and mice being exposed to the context and the auditory stimulus (tone: 0.0046 ± 0.001 , mean \pm SD, $n = 3$). In contrast, the mice that had previously undergone auditory cued fear conditioning (paired: 0.0190 ± 0.0078 , mean \pm SD, $n = 3$), unpaired auditory fear conditioning (unpaired: 0.0278 ± 0.0118 , mean \pm SD, $n = 3$) or contextual conditioning (shock: 0.0185 ± 0.0031 , mean \pm SD, $n = 3$) showed about threefold to fourfold increased expression levels. When quantifying the mRNA levels of the IEG *Arc*, we found that expression levels were also significantly altered after behavioral manipulation (one-way ANOVA $P < 0.0001$; Fig. 3d). Furthermore, the pattern looked remarkably similar to *c-fos*: the expression levels for mice taken directly from the HC (HC: 0.0148 ± 0.0091 , mean \pm SD, $n = 3$), mice being exposed only to the context (context: 0.0091 ± 0.0014 , mean \pm SD, $n = 3$) and mice being exposed to the context and the auditory stimulus (tone: 0.0136 ± 0.0023 , mean \pm SD, $n = 3$) were relatively low. Mice that had previously undergone auditory cued fear conditioning (paired: 0.0606 ± 0.0197 , mean \pm SD, $n = 3$), unpaired auditory fear conditioning (unpaired: 0.0384 ± 0.0153 , mean \pm SD, $n = 3$) or contextual conditioning (shock: 0.0594 ± 0.0164 , mean \pm SD, $n = 3$) showed about threefold to fourfold increased expression levels as well. To better quantify the apparent similarity in expression, we plotted the mean expression levels of *c-fos* against *Arc* for the various experimental conditions (Fig. 3e). Indeed, we found a strong correlation. Taken together, we found increased expression levels for both *c-fos* and *Arc*, after all behavioral paradigms that would involve foot shocks, whereas we observed increased freezing behavior only after paired conditioning. Thus, expression levels of these genes in the ACx do not faithfully report associative learning to sounds.

Microarray analysis of global gene expression levels

A hypothetical reporter gene that would signal sound-induced associative plasticity should show strong, reliable

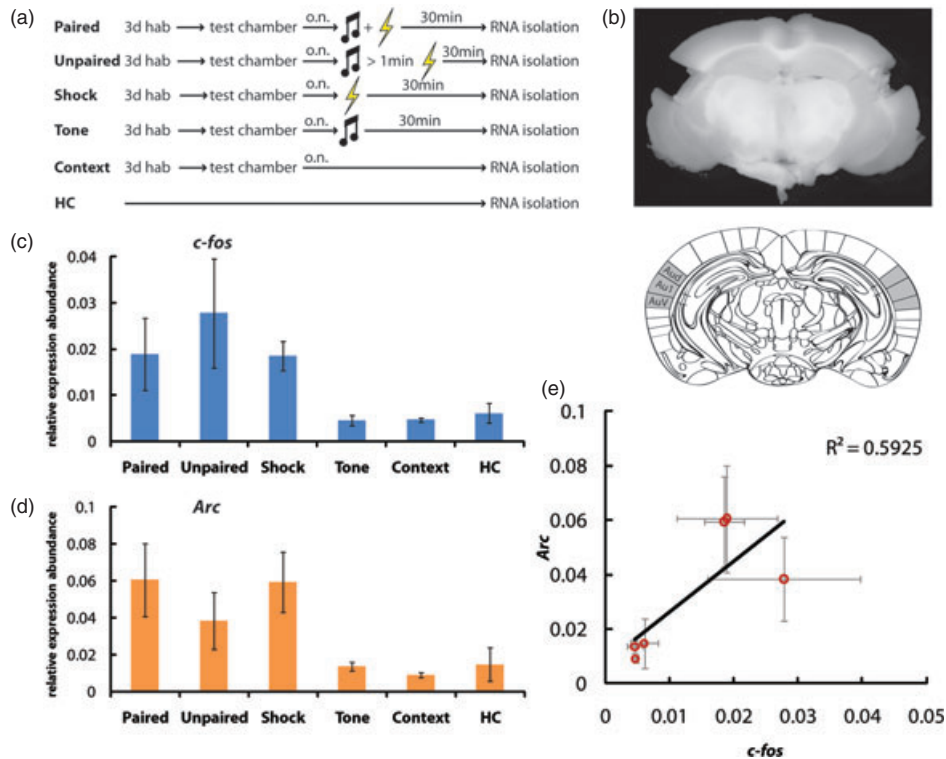


Figure 3: Expression of IEGs *c-fos* and *Arc* estimated by qPCR. (a) Schematic of the experimental design. (b) Coronal section of a mouse brain after bilateral removal of tissue from the ACx for sample preparation (top). Corresponding section from anatomical mouse brain atlas, AuD, secondary ACx, dorsal area; Au1, primary ACx; AuV, secondary ACx; ventral area (bottom; reproduced with permission from Paxinos and Franklin 2001). (c) Relative mean expression levels of the IEG *c-fos* after various experimental treatments, $n = 3$ mice per condition. (d) Relative mean expression levels of the IEG *Arc* after various experimental treatments, $n = 3$ mice per condition. (e) Correlation of mean *c-fos* and *Arc* expression levels across the various conditions. Error bars in all panels represent SD.

and specific expression only in mice previously exposed to paired conditioning. In particular, it should allow discriminating samples from mice undergoing paired and unpaired conditioning. To test if such a gene is expressed in the mouse ACx, we performed a microarray analysis of the previously isolated total RNA samples taken from the mice undergoing the various behavioral paradigms (see *Materials and methods*). We used custom-made microarrays that allow analysis of relative expression levels of 20661 genes simultaneously, which corresponds to about 94% of the predicted genes of the mouse (Waterston *et al.* 2002). The expression levels for each condition were measured with three biological replicates ($n = 3$ mice per condition) in relation to a common reference. The common reference was generated by mixing all samples to equal amounts. For each gene, we measured the mean log2 fold change relative to this reference. In our initial analysis, we performed a ‘significance analysis of microarrays (one class)’ on the primary data (Tibshirani 2006). We considered those genes that showed regulation larger than twofold in at least one of the six conditions significant (adjusted P value < 0.05). The mean log2 fold changes of those 283 differentially expressed genes are grouped by similarity using a hierarchical clustering algorithm (Fig. 4).

We found that the global expression patterns of the various conditions are clustered in the following way: paired → shock → unpaired → tone → context → HC. The behavioral treatments are characterized by a combination of parameters as change of context, display of sounds and delivery of shocks. Considering a treatment with a larger number of parameters as more intense, the clustering of columns almost perfectly correlates with the intensity of treatment (except shock/unpaired).

We next were interested to see how the expression patterns of the IEGs *c-fos* and *Arc* were captured by the microarray analysis. We found a cluster of reads for *c-fos* (two reads), *Arc* and the gene ‘early growth response gene 2’ (*Egr2*) that showed tight coregulation (Fig. 4, single asterisk). These genes showed upregulation upon any treatment involving shocks (paired, shock and unpaired), whereas the levels were low for the remaining conditions: tone, context and HC. This observation is consistent with our previous qPCR experiments.

Interestingly, we also found few genes that displayed high expression levels selectively in the paired condition (Fig. 4, double asterisks). To better quantify this, we displayed the data in a way that not only shows the average fold change but also at the same time the adjusted P value as

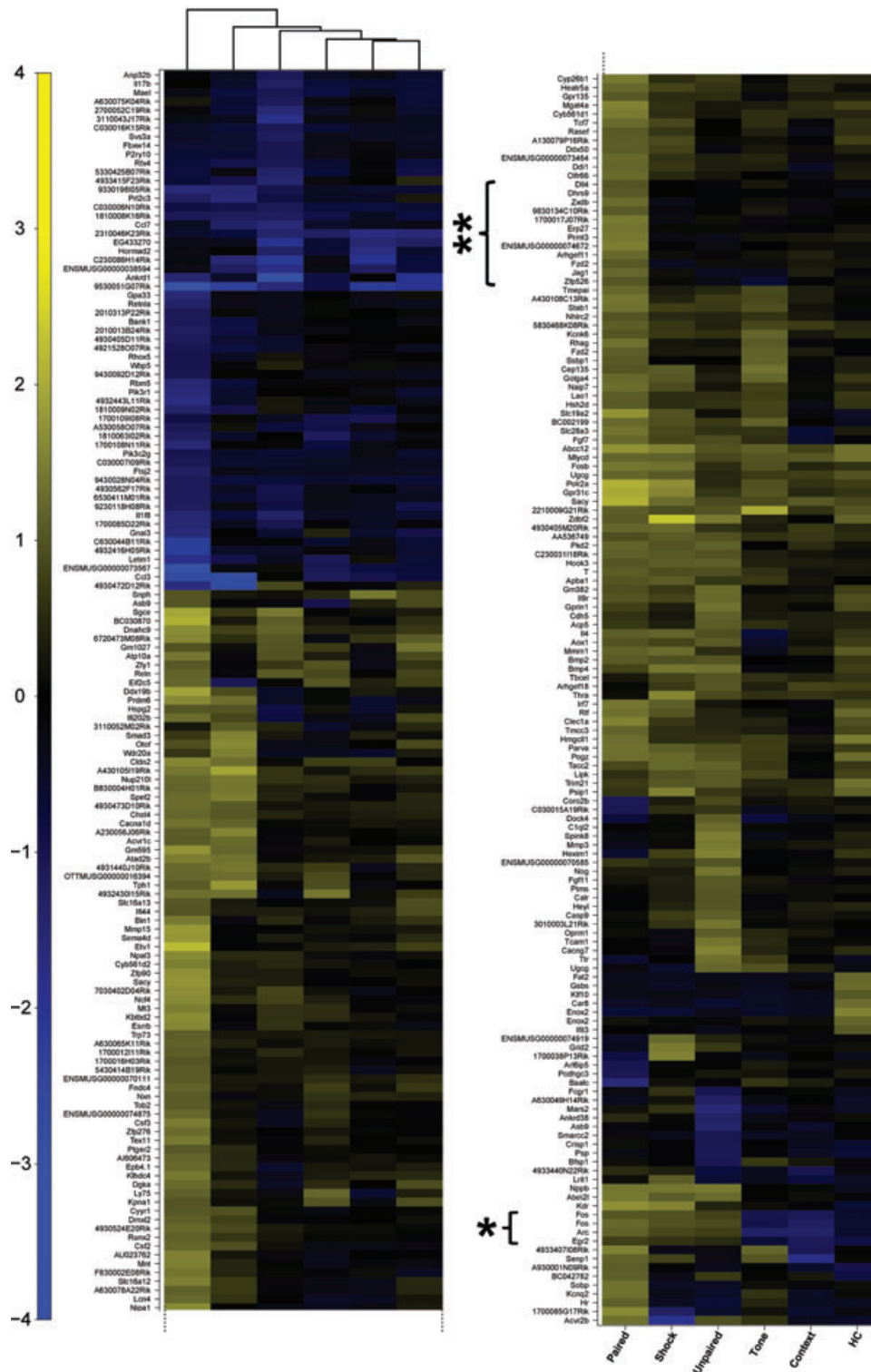


Figure 4: ‘Significance analysis of microarrays’ for reads showing at least twofold regulation at a significance level $P < 0.05$ for one of the six behavioral conditions. Color map codes for mean \log_2 fold regulation relative to the common reference. Single asterisk indicates cluster containing IEGs *c-fos*, *Arc* and *egr2*. Double asterisks indicate reads with high average expression values specifically to paired conditioning.

a measure of the variability of the data. Our experimental design involving a common reference allows calculation of the relative expression levels for all pairs of conditions. We generated volcano plots for the various conditions with respect to the HC group, which we considered to represent basal transcription levels (Fig. 5a–e). We plotted for all reads the negative log₂ (adjusted *P* values) [$-\log_2(\text{adjPval})$] against their respective mean log₂ fold relative expression levels. When comparing expression levels for the conditions paired vs. HC (Fig. 5a), we observed that a number of genes showed larger than twofold regulation with relatively low $-\log_2(\text{adjPval})$ around 3–10. In addition, there was a second group of observations that showed a similar magnitude of regulation, however with high $-\log_2(\text{adjPval})$ typically larger than 20. This was true both for up- and downregulated genes. Looking for potential reporter genes, we focused on those genes that showed upregulation by a factor larger than 2 and $-\log_2(\text{adjPval})$ higher than 20 in the paired conditioned group as compared to the HC control. We found that the IEGs *c-fos* and *Arc* met these conditions. In addition, we only found *early growth response 2* (*egr2* or *Krox20*) matching our criteria, which also has been previously described to be induced by electroconvulsive shocks in the brain (Beckmann & Wilce 1997). The gene *egr1* (*zif268*), which also has been used previously as an activity marker (Zangenehpour & Chaudhuri 2002), showed a significant upregulation by a factor of 1.97. These results confirm that the microarray analysis was sensitive enough to detect behaviorally induced changes in gene expression and that the known IEGs are showing indeed strongest regulation in the ACx. When comparing this expression profile to the other conditions shock vs. HC and unpaired vs. HC, we found a similar profile: *c-fos*, *Arc* and *Egr2* show strong induction (Fig. 5b,c). In the conditions sound vs. HC and context vs. HC, we observed hardly any strong induction of gene expression (Fig. 5d,e). We only found the gene *Ttr* (transthyretin) being upregulated in the conditions sound vs. HC and unpaired vs. HC. This may reflect a strong variability due to regulation of expression levels by factors other than behavioral experience (Buxbaum & Reixach 2009). We were particularly interested in possible genes that would show specific upregulation in the condition of paired vs. unpaired conditioning, which could be eventually used as a specific signature for associative learning to sounds. To better quantify this, we plotted again the log₂ relative expression values and corresponding $-\log_2(\text{adjPval})$ for these two conditions (Fig. 5f). We did not find any gene showing upregulation larger than twofold and a higher adjusted *P* value than 20. This indicates that the reads showing high average relative expression levels selectively for paired conditioning in the heat map (Fig. 4, double asterisks) are not particularly reliable and likely due to a single, exceptionally high measurement in the three replicates.

Taken together, our microarray analysis showed that the profiles of the IEGs *c-fos*, *Arc* and *Egr2* were highly correlated across the various behavioral conditions, consistent with our previous observations made by qPCR. However, there were no genes found that showed strong and reliable upregulation in tissue taken from paired conditioned mice as compared to unpaired conditioned mice. Probably, shocks and/or eventually related stress alone can lead to a significant

modulation, even in brain regions that are considered to be primarily involved in processing of auditory stimuli.

Discussion

In this study, we investigated the effect of auditory fear conditioning on the expression levels of IEGs in the ACx of the mouse. Our main findings are as follows: (1) As described in the literature, freezing behavior upon presentation of the previously conditioned sound is selectively found in paired conditioned mice, indicating successful association of sounds and shocks. (2) The mRNA of the IEGs *c-fos* and *Arc* is upregulated not only after paired conditioning but also after all paradigms that involve shocks. (3) A microarray analysis confirms that the known IEGs show strongest and most reliable changes upon behavioral manipulation. We could not identify a novel gene whose expression would be different between paired and unpaired conditioned mice.

Our findings are consistent with previous studies describing a strong behavioral component controlling the expression levels of IEGs (Bertaina & Destrade 1995; Guzowski *et al.* 1999, 2001; Montag-Sallaz *et al.* 1999). This shows that our fast method of detecting mRNA levels of *c-fos* and *Arc* using qPCR works with high sensitivity and reliability despite the fact that the sample likely contained a mixture of cells that showed induction of IEGs and others that did not. However, our observation that *c-fos* and *Arc* are induced after all behavioral paradigms that involved shocks indicates that their usefulness as specific markers for associative learning to sounds in the fear conditioning paradigm in the ACx could be limited to some extent. A potential concern is that the expression of *c-fos* and *Arc* in the ACx could be based on a non-specific induction that is related to stress (Senba & Ueyama 1997).

Are there alternative genes that show specific expression in paired conditioned mice only? We performed a microarray analysis to address this issue in detail. First, the microarray analysis provided similar results as compared to our previous qPCR analysis with respect to *c-fos* and *Arc*, indicating that it is also sensitive enough to detect behaviorally induced changes in gene expression in our cortex samples. Furthermore, we observed induction of other known IEGs upon behavioral training. We were particularly interested in potential genes that are expressed reliably in a differential manner between paired and unpaired conditioned mice. These are the two most stringent paradigms to test for associative learning, as only the timing between shocks and sounds is different. However, we could not find any gene that is differentially expressed.

It should be kept in mind that our qPCR-based or microarray methods do not provide cellular resolution. It is still conceivable that different subsets of neurons within the ACx could have been activated during paired and unpaired conditioning, and eventually specific genes may have been activated that surpassed the detection threshold of the microarray analysis. Methods like the cellular compartment analysis of temporal activity by fluorescence in situ hybridization (catFISH) approach that allow labeling of individual neurons at two different time points (e.g. during paired and unpaired conditioning) could be required to make this distinction (Guzowski

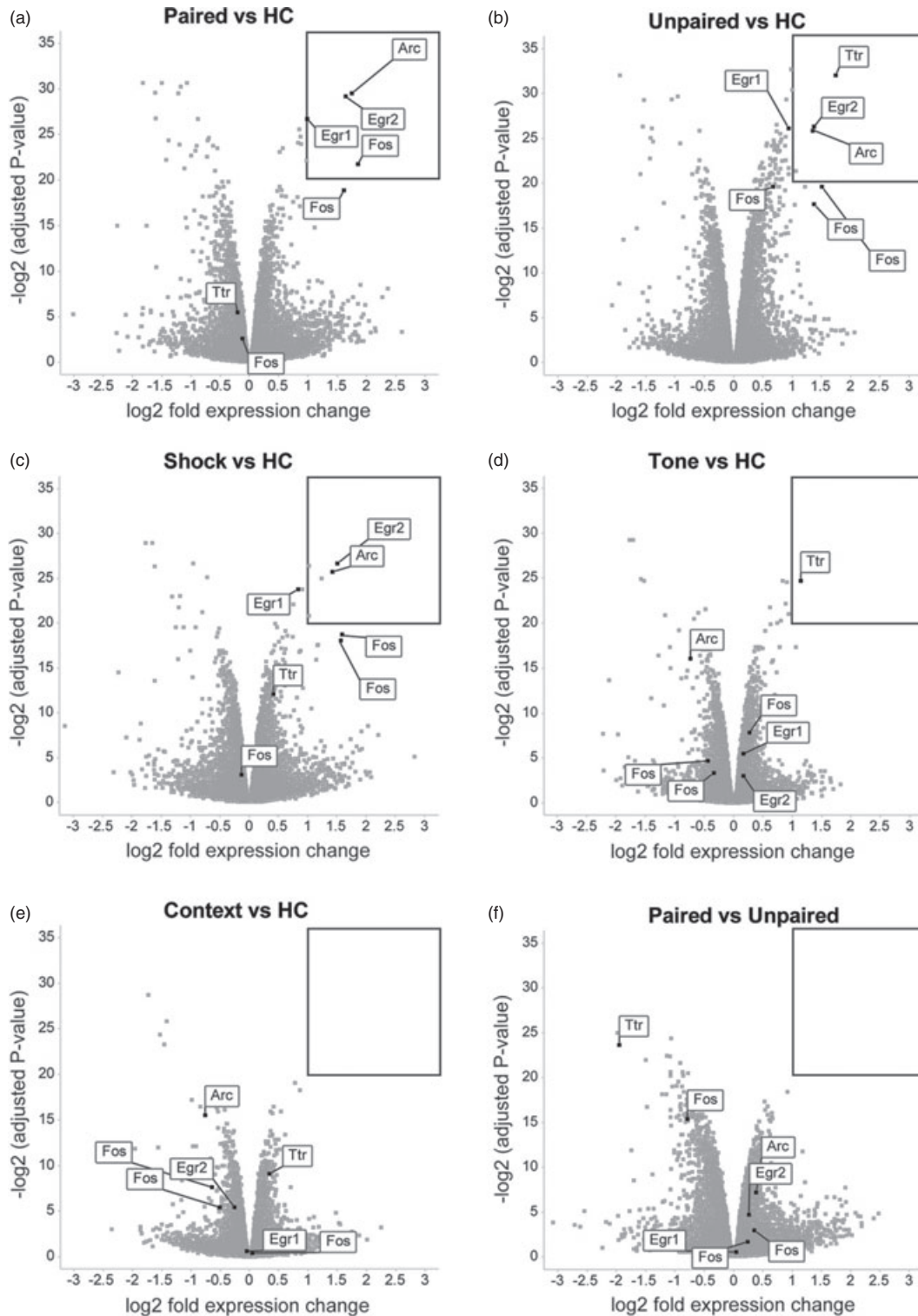


Figure 5: Volcano plots for direct comparison of relative expression levels across several behavioral treatments. The $-\log_2(\text{adjPval})$ is plotted against the mean \log_2 fold relative expression change. (a) Paired vs. HC. (b) Unpaired vs. HC. (c) Shock vs. HC. (d) Tone vs. HC. (e) Context vs. HC. (f) Paired vs. unpaired. The box delineates reads with mean \log_2 fold relative expression changes larger than 1 and $-\log_2(\text{adjPval})$ higher than 20.

et al. 1999). Furthermore, it has recently shown that the ACx plays an essential role in extinction learning (Song *et al.* 2010). It is an interesting idea to test gene expression levels following this paradigm.

What could be reasons for IEG induction in the ACx of mice receiving only shocks but not being exposed to sounds? Given the evidence that the induction of IEGs in neurons is primarily coupled to neuronal activity, our observations indicate that, surprisingly, painful stimuli can provide powerful drive to ACx neurons. There is increasing evidence that neurons in primary auditory cortices can be driven by non-auditory stimuli (Brosch *et al.* 2005; Lemus *et al.* 2010). Indeed, very recently shock-induced disinhibition of layer 2/3 pyramidal neurons of the mouse ACx has been shown to be required for fear learning (Letzkus *et al.* 2011). Changes in kinase activity regulating adaptations of synaptic weights by, e.g. AMPA receptor trafficking could mediate associative memory processes also in the ACx (Kessels & Malinow 2009). Our findings highlight that the activity levels in cortical areas mediating primarily specific sensory representations can be strongly influenced by global events originating from other modalities.

References

- Abraham, W.C., Mason, S.E., Demmer, J., Williams, J.M., Richardson, C.L., Tate, W.P., Lawlor, P.A. & Dragunow, M. (1993) Correlations between immediate early gene induction and the persistence of long-term potentiation. *Neuroscience* **56**, 717–727.
- Antunes, R. & Moita, M.A. (2010) Discriminative auditory fear learning requires both tuned and nontuned auditory pathways to the amygdala. *J Neurosci* **30**, 9782–9787.
- Barth, A.L., Gerkin, R.C. & Dean, K.L. (2004) Alteration of neuronal firing properties after in vivo experience in a FosGFP transgenic mouse. *J Neurosci* **24**, 6466–6475.
- Beckmann, A.M. & Wilce, P.A. (1997) Egr transcription factors in the nervous system. *Neurochem Int* **31**, 477–510, discussion.
- Bertaina, V. & Destrade, C. (1995) Differential time courses of c-fos mRNA expression in hippocampal subfields following acquisition and recall testing in mice. *Brain Res Cogn Brain Res* **2**, 269–275.
- Boatman, J.A. & Kim, J.J. (2006) A thalamo-cortico-amygdala pathway mediates auditory fear conditioning in the intact brain. *Eur J Neurosci* **24**, 894–900.
- Brosch, M., Selezneva, E. & Scheich, H. (2005) Nonauditory events of a behavioral procedure activate auditory cortex of highly trained monkeys. *J Neurosci* **25**, 6797–6806.
- Buxbaum, J.N. & Reixach, N. (2009) Transthyretin: the servant of many masters. *Cell Mol Life Sci* **66**, 3095–3101.
- Carpenter-Hyland, E.P., Plummer, T.K., Vazdarjanova, A. & Blake, D.T. (2010) Arc expression and neuroplasticity in primary auditory cortex during initial learning are inversely related to neural activity. *Proc Natl Acad Sci U S A* **107**, 14828–14832.
- Cullinan, W.E., Herman, J.P., Battaglia, D.F., Akil, H. & Watson, S.J. (1995) Pattern and time course of immediate early gene expression in rat brain following acute stress. *Neuroscience* **64**, 477–505.
- Dragunow, M., Abraham, W.C., Goulding, M., Mason, S.E., Robertson, H.A. & Faull, R.L. (1989) Long-term potentiation and the induction of c-fos mRNA and proteins in the dentate gyrus of unanesthetized rats. *Neurosci Lett* **101**, 274–280.
- Eferl, R. & Wagner, E.F. (2003) AP-1: a double-edged sword in tumorigenesis. *Nat Rev Cancer* **3**, 859–868.
- Fanselow, M.S. & Poulos, A.M. (2005) The neuroscience of mammalian associative learning. *Annu Rev Psychol* **56**, 207–234.
- Fleischmann, A., Hvalby, O., Jensen, V., Strelakova, T., Zacher, C., Layer, L.E., Kvello, A., Reschke, M., Spanagel, R., Sprengel, R., Wagner, E.F. & Gass, P. (2003) Impaired long-term memory and NR2A-type NMDA receptor-dependent synaptic plasticity in mice lacking c-Fos in the CNS. *J Neurosci* **23**, 9116–9122.
- Frankland, P.W., Ding, H.K., Takahashi, E., Suzuki, A., Kida, S. & Silva, A.J. (2006) Stability of recent and remote contextual fear memory. *Learn Mem* **13**, 451–457.
- Grinevich, V., Kolleker, A., Eliava, M., Takada, N., Takuma, H., Fukazawa, Y., Shigemoto, R., Kuhl, D., Waters, J., Seeburg, P.H. & Osten, P. (2009) Fluorescent Arc/Arg3.1 indicator mice: a versatile tool to study brain activity changes in vitro and in vivo. *J Neurosci Methods* **184**, 25–36.
- Guzowski, J.F., McNaughton, B.L., Barnes, C.A. & Worley, P.F. (1999) Environment-specific expression of the immediate-early gene Arc in hippocampal neuronal ensembles. *Nat Neurosci* **2**, 1120–1124.
- Guzowski, J.F., Setlow, B., Wagner, E.K. & McGaugh, J.L. (2001) Experience-dependent gene expression in the rat hippocampus after spatial learning: a comparison of the immediate-early genes Arc, c-fos, and zif268. *J Neurosci* **21**, 5089–5098.
- Hall, J., Thomas, K.L. & Everitt, B.J. (2001) Fear memory retrieval induces CREB phosphorylation and Fos expression within the amygdala. *Eur J Neurosci* **13**, 1453–1458.
- Han, J.H., Kushner, S.A., Yiu, A.P., Hsiang, H.L., Buch, T., Waisman, A., Bontempi, B., Neve, R.L., Frankland, P.W. & Joseph, S.A. (2009) Selective erasure of a fear memory. *Science* **323**, 1492–1496.
- Kamprath, K. & Wotjak, C.T. (2004) Nonassociative learning processes determine expression and extinction of conditioned fear in mice. *Learn Mem* **11**, 770–786.
- Kessels, H.W. & Malinow, R. (2009) Synaptic AMPA receptor plasticity and behavior. *Neuron* **61**, 340–350.
- Kholodar-Smith, D.B., Allen, T.A. & Brown, T.H. (2008a) Fear conditioning to discontinuous auditory cues requires perirhinal cortical function. *Behav Neurosci* **122**, 1178–1185.
- Kholodar-Smith, D.B., Boguszewski, P. & Brown, T.H. (2008b) Auditory trace fear conditioning requires perirhinal cortex. *Neurobiol Learn Mem* **90**, 537–543.
- Kopec, C.D., Kessels, H.W., Bush, D.E., Cain, C.K., LeDoux, J.E. & Malinow, R. (2007) A robust automated method to analyze rodent motion during fear conditioning. *Neuropharmacology* **52**, 228–233.
- Lavond, D.G. & Steinmetz, J.E. (2003) *Handbook of Classical Conditioning*. Kluwer Academic Publishers, Boston.
- Lemus, L., Hernandez, A., Luna, R., Zainos, A. & Romo, R. (2010) Do sensory cortices process more than one sensory modality during perceptual judgments? *Neuron* **67**, 335–348.
- Letzkus, J.J., Wolff, S.B., Meyer, E.M., Tovote, P., Courtin, J., Herry, C. & Luthi, A. (2011) A disinhibitory microcircuit for associative fear learning in the auditory cortex. *Nature* **480**, 331–335.
- Lin, D., Boyle, M.P., Dollar, P., Lee, H., Lein, E.S., Perona, P. & Anderson, D.J. (2011) Functional identification of an aggression locus in the mouse hypothalamus. *Nature* **470**, 221–226.
- Link, W., Konietzko, U., Kauselmann, G., Krug, M., Schwanke, B., Frey, U. & Kuhl, D. (1995) Somatodendritic expression of an immediate early gene is regulated by synaptic activity. *Proc Natl Acad Sci U S A* **92**, 5734–5738.
- Livak, K.J. & Schmittgen, T.D. (2001) Analysis of relative gene expression data using real-time quantitative PCR and the 2(-Delta Delta C(T)) method. *Methods* **25**, 402–408.
- Lyford, G.L., Yamagata, K., Kaufmann, W.E., Barnes, C.A., Sanders, L.K., Copeland, N.G., Gilbert, D.J., Jenkins, N.A., Lanahan, A.A. & Worley, P.F. (1995) Arc, a growth factor and activity-regulated gene, encodes a novel cytoskeleton-associated protein that is enriched in neuronal dendrites. *Neuron* **14**, 433–445.
- Mamiya, N., Fukushima, H., Suzuki, A., Matsuyama, Z., Homma, S., Frankland, P.W. & Kida, S. (2009) Brain region-specific gene expression activation required for reconsolidation and extinction of contextual fear memory. *J Neurosci* **29**, 402–413.

- Man, P.S., Wells, T. & Carter, D.A. (2007) Egr-1-d2EGFP transgenic rats identify transient populations of neurons and glial cells during postnatal brain development. *Gene Expr Patterns* **7**, 872–883.
- Maren, S. (2001) Neurobiology of Pavlovian fear conditioning. *Annu Rev Neurosci* **24**, 897–931.
- Marr, D. (1970) A theory for cerebral neocortex. *Proc R Soc Lond B Biol Sci* **176**, 161–234.
- Milanovic, S., Radulovic, J., Laban, O., Stiedl, O., Henn, F. & Spiess, J. (1998) Production of the Fos protein after contextual fear conditioning of C57BL/6N mice. *Brain Res* **784**, 37–47.
- Montag-Sallaz, M., Welzl, H., Kuhl, D., Montag, D. & Schachner, M. (1999) Novelty-induced increased expression of immediate-early genes c-fos and arg 3.1 in the mouse brain. *J Neurobiol* **38**, 234–246.
- Morgan, J.I., Cohen, D.R., Hempstead, J.L. & Curran, T. (1987) Mapping patterns of c-fos expression in the central nervous system after seizure. *Science* **237**, 192–197.
- Quirk, G.J., Armony, J.L. & LeDoux, J.E. (1997) Fear conditioning enhances different temporal components of tone-evoked spike trains in auditory cortex and lateral amygdala. *Neuron* **19**, 613–624.
- Paxinos, G. & Franklin, K.B.J. (2001) *The mouse brain in stereotaxic coordinates*, 2nd edn. Academic Press.
- Radulovic, J., Kammermeier, J. & Spiess, J. (1998) Relationship between fos production and classical fear conditioning: effects of novelty, latent inhibition, and unconditioned stimulus preexposure. *J Neurosci* **18**, 7452–7461.
- Reijmers, L.G., Perkins, B.L., Matsuo, N. & Mayford, M. (2007) Localization of a stable neural correlate of associative memory. *Science* **317**, 1230–1233.
- Romanski, L.M. & LeDoux, J.E. (1992) Equipotentiality of thalamo-amygdala and thalamo-cortico-amygdala circuits in auditory fear conditioning. *J Neurosci* **12**, 4501–4509.
- Senba, E. & Ueyama, T. (1997) Stress-induced expression of immediate early genes in the brain and peripheral organs of the rat. *Neurosci Res* **29**, 183–207.
- Sharp, F.R., Sagar, S.M., Hicks, K., Lowenstein, D. & Hisanaga, K. (1991) c-fos mRNA, Fos, and Fos-related antigen induction by hypertonic saline and stress. *J Neurosci* **11**, 2321–2331.
- Smyth, G.K. (2004) Linear models and empirical bayes methods for assessing differential expression in microarray experiments. *Stat Appl Genet Mol Biol* **3**, article 3.
- Song, E.Y., Boatman, J.A., Jung, M.W. & Kim, J.J. (2010) Auditory cortex is important in the extinction of two different tone-based conditioned fear memories in rats. *Front Behav Neurosci* **4**, 24.
- Stiebler, I., Neulist, R., Fichtel, I. & Ehret, G. (1997) The auditory cortex of the house mouse: left-right differences, tonotopic organization and quantitative analysis of frequency representation. *J Comp Physiol A* **181**, 559–571.
- Tibshirani, R. (2006) A simple method for assessing sample sizes in microarray experiments. *BMC Bioinformatics* **7**, 106.
- VanGuilder, H.D., Vrana, K.E. & Freeman, W.M. (2008) Twenty-five years of quantitative PCR for gene expression analysis. *Biotechniques* **44**, 619–626.
- Wang, K.H., Majewska, A., Schummers, J., Farley, B., Hu, C., Sur, M. & Tonegawa, S. (2006) In vivo two-photon imaging reveals a role of arc in enhancing orientation specificity in visual cortex. *Cell* **126**, 389–402.
- Waterston, R.H., Lindblad-Toh, K., Birney, E. *et al.* (2002) Initial sequencing and comparative analysis of the mouse genome. *Nature* **420**, 520–562.
- Weinberger, N.M. (2004) Specific long-term memory traces in primary auditory cortex. *Nat Rev Neurosci* **5**, 279–290.
- Zangenehpour, S. & Chaudhuri, A. (2002) Differential induction and decay curves of c-fos and zif268 revealed through dual activity maps. *Brain Res Mol Brain Res* **109**, 221–225.
- Zenz, R., Eferl, R., Scheinecker, C., Redlich, K., Smolen, J., Schonthaler, H.B., Kenner, L., Tschachler, E. & Wagner, E.F. (2008) Activator protein 1 (Fos/Jun) functions in inflammatory bone and skin disease. *Arthritis Res Ther* **10**, 201.
- Zhang, Y., Fukushima, H. & Kida, S. (2011) Induction and requirement of gene expression in the anterior cingulate cortex and medial prefrontal cortex for the consolidation of inhibitory avoidance memory. *Mol Brain* **4**, 4.

Acknowledgments

We would like to thank Anita Helm and Andreas Bichl for maintaining our mouse colony and Martin Colombini and the IMP workshop for technical assistance. Furthermore, we would like to thank Wulf Haubensak and Brice Bathellier for critical reading of the manuscript and all Rumpel group members for helpful discussions. The Institute of Molecular Pathology receives generous core funding by Boehringer Ingelheim.

Supporting Information

Additional Supporting Information may be found in the online version of this article:

Figure S1: Quantification of the extent of ACx lesions. (a) Coronal whole brain slices (100 μm thickness, every third slice shown) of two representative brains with bilateral lesions of the ACx after paraformaldehyde fixation and Nissl staining. Note that lesions do not extend deeper than cortical layers. (b) Picture of a single mouse brain taken perpendicularly to the sagittal plane. A template indicating the position of the ACx was constructed from a lateral projection of a mouse brain atlas and overlaid (Paxinos and Franklin 2001, Academic Press). Units of scale bar: 1 mm. (c) Example photograph of single brain with ACx lesion (green arrows). (d) Borders of 10 representative lesions in the right hemisphere from the mice conditioned to ‘complex sound 1’ indicated by black lines. (e) The corresponding lesion borders in the left hemisphere of the mice shown in (d). (f) Quantification of the extent of the lesions covering ACx and other cortical areas based on overlay of lesion outline and template. Data from experimental series shown in Fig. 1b,c (sound 1: lesion size: within ACx: $2.50 \pm 0.14 \text{ mm}^2$, outside ACx: $2.31 \pm 0.11 \text{ mm}^2$, $n = 21$ mice; sound 2: lesion size: within ACx: $1.80 \pm 0.22 \text{ mm}^2$, outside ACx: $2.03 \pm 0.22 \text{ mm}^2$, $n = 9$ mice; Wilcoxon rank-sum test sound 1 vs. sound 2 lesion size within ACx: $P < 0.011$, Wilcoxon rank-sum test sound 1 vs. sound 2 lesion size outside ACx: $P > 0.349$). The size of the ACx is $\sim 3.4 \text{ mm}^2$ according to the template. The small but significant difference in the extent of the lesions within the ACx is unlikely to explain the profound behavioral effect, as this is still clearly observed in subgroups of mice selected to have matched lesion sizes (sound 1: freezing levels: silence: $3\% \pm 3\%$, CS: $13\% \pm 11\%$; lesion size within ACx: $2.41 \pm 0.16 \text{ mm}^2$, lesion size outside ACx: $2.21 \pm 0.22 \text{ mm}^2$, $n = 4$ mice; sound 2: freezing levels: silence: $9\% \pm 8\%$, CS: $53\% \pm 6\%$; lesion size within ACx: $2.40 \pm 0.18 \text{ mm}^2$, lesion size outside ACx: $2.19 \pm 0.23 \text{ mm}^2$, $n = 4$ mice; Wilcoxon rank-sum test sound 1 vs. sound 2 during silence: $P > 0.171$, Wilcoxon rank-sum test sham vs. lesion during CS: $P < 0.029$).

As a service to our authors and readers, this journal provides supporting information supplied by the authors. Such materials are peer-reviewed and may be re-organized for online delivery, but are not copy-edited or typeset. Technical support issues arising from supporting information (other than missing files) should be addressed to the authors.

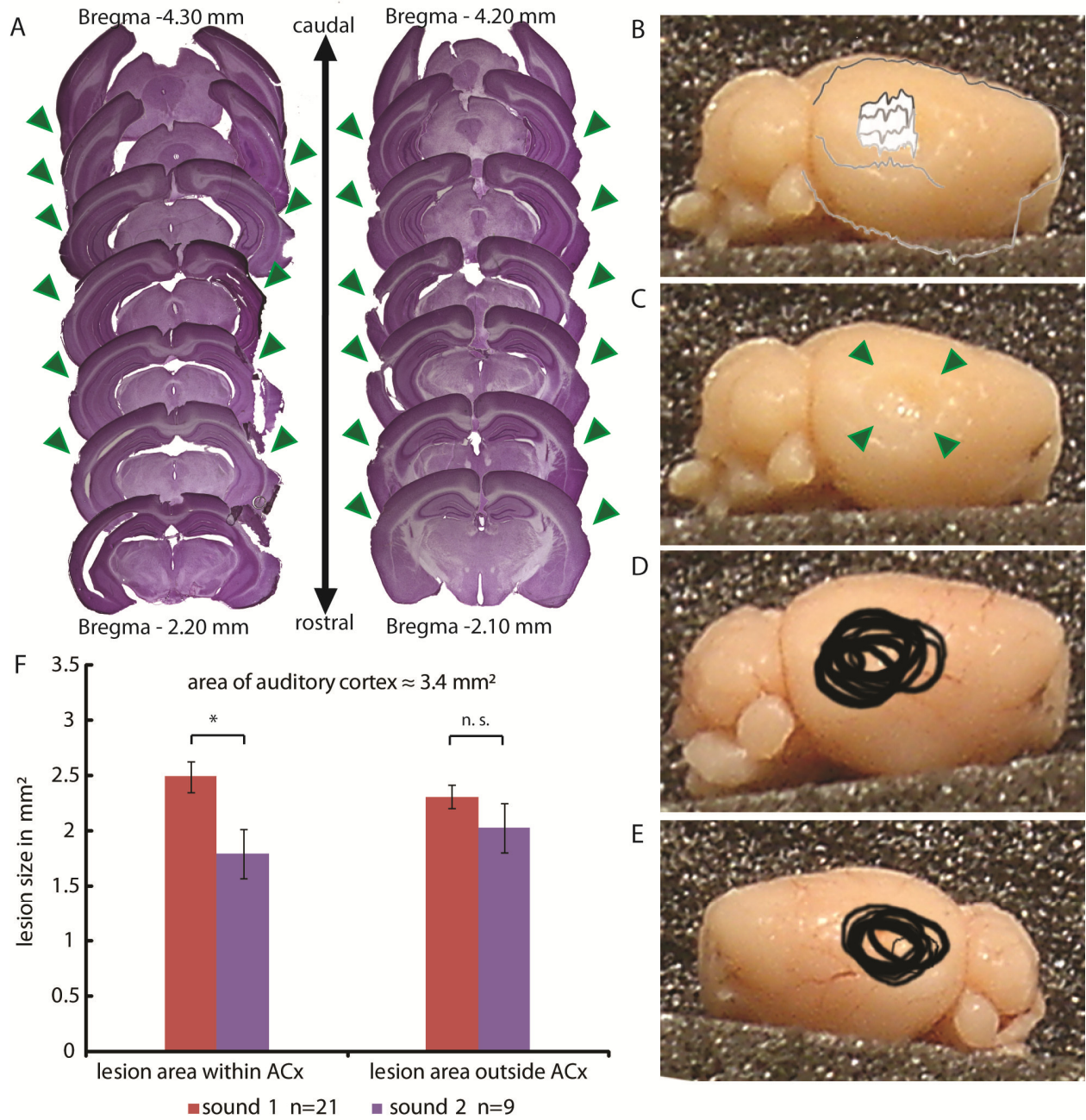


Figure S1

6. Manuscript II: Correlation of neuronal activity *in vivo* with gene expression levels in a transgenic mouse model allowing single cell resolution photolabeling.

Manuel Peter¹, Brice Bathellier¹, Bruno Fontinha¹ and Simon Rumpel¹

1) Institute of Molecular Pathology (IMP), Dr. Bohr-Gasse 7, 1030 Vienna, Austria

Author contributions:

Manuel Peter: designed the experiments, characterized the photoactivatable proteins, generated and characterized the mouse lines, performed and analyzed the *c-fos* immunohistochemistry after *in vivo* imaging and prepared the manuscript

Brice Bathelier: performed the *in vivo* calcium imaging experiments and analyzed the imaging data

Bruno Fontinha: performed electrophysiology experiments

Simon Rumpel: designed the experiments and prepared the manuscript

Description of the manuscript

In this study we characterized different photoactivatable proteins and tested their usability to label single neurons *in vivo*. We generated and characterized transgenic mice expressing photoactivatable GFP. This mouse lines allow us to conditionally photolabel single neurons *in vivo* and labeled neurons can be re-identified *in vivo* and *in vitro*. We further demonstrate that photolabeling can be combined with *in vivo* functional calcium imaging and use these mouse lines to correlate *in vivo* activity levels of individual neurons with a histological analysis of the immediate early gene *c-fos*. This manuscript has been submitted for publication (January 2012).

6.1 Abstract

One of the biggest tasks in neuroscience is to explain activity patterns of individual neurons during behavior by their cellular characteristics and their connectivity within the neuronal network. To greatly facilitate linking *in vivo* experiments with a more detailed molecular or physiological analysis *in vitro*, we have generated and characterized genetically modified mice expressing photoactivatable GFP (PA-GFP) that allow conditional photolabeling of individual neurons. Repeated photolabeling at the soma reveals basic morphological features due to diffusion of activated PA-GFP into the dendrites. Neurons photolabeled *in vivo* can be re-identified in acute brain slices and targeted for electrophysiological recordings. Here, we take advantage of PA-GFP expressing mice to correlate spontaneous *in vivo* firing rates of individual neurons with their expression levels of the immediate early gene *c-fos*. Fos expression levels were highly variable in active and non-active cells and were on average similar, suggesting that additional factors beyond activity control the *c-fos* locus under basal conditions. Generally, the mouse models described in this study enable the combination of various analytical approaches to characterize living cells, also beyond the neurosciences.

6.2 Introduction

Recent advances in electrophysiological recording techniques or optical calcium imaging techniques *in vivo* have yielded much information about firing patterns in populations of neurons in response to particular sensory stimuli or in the context of behavioral tasks (Ohki et al., 2005; Pastalkova et al., 2008). However, it is still difficult to explain or even to predict the emergence of the various activity patterns that can be observed in a given neuronal population. One major step towards this goal is to gain additional information like cell-intrinsic properties such as gene expression profiles and the specific connectivity of the neuron under observation. Encouragingly, in the last years a number of approaches have been established in mammalian model organisms to overcome some of these limitations including the identification of the cell type (Pinault, 1996; Klausberger et al., 2005; Haubensak et al., 2010; Kerlin et al., 2010; Runyan et al., 2010), the projection type (Herry et al., 2008; Lima et al., 2009) or the connectivity of the recorded neuron (Marshel et al., 2010; Bock et al., 2011; Briggman et al., 2011; Ko et al., 2011).

Here, we generated and characterized three mouse lines expressing photoactivatable GFP (PA-GFP, (Patterson and Lippincott-Schwartz, 2002)) that can be optimally used for optical recording of neuronal activity and that allow the selection and photolabeling of individual neurons for subsequent analysis of their morphology, expression patterns, cell type or connectivity (Ruta et al., 2010; Lien and Scanziani, 2011). These mouse lines can overcome some of the shortcomings of the previously mentioned approaches and have their particular advantages if the neurons of interest are sparse and preferably maintained alive for further analysis. Furthermore, we used the mice to correlate *in vivo* activity levels of individual neurons with the expression levels of the immediate early gene *c-fos* with single cell resolution. So called immediate early genes (IEGs, e.g. *Arc*, *c-fos*) are characterized by generally low expression levels under basal conditions, however, show strong and transient expression triggered by events that lead to pronounced neuronal activity like tetanic stimulation, kainate injections or Channelrhodopsin-mediated stimulation (Dragunow et al., 1989; Lyford et al., 1995; Lin et al., 2011). Interestingly, expression of IEGs could be also observed in

subsets of neurons in particular brain regions after behavioral manipulation (Guzowski et al., 1999). For these reasons IEGs are widely used as reporters of previous neuronal activation and to delineate neurons involved in particular behaviors (Gall et al., 1998; Barth et al., 2004). However, up to date there is only little direct experimental evidence that an identified, single neuron *in vivo* indeed shows increased activity and correlated increased IEG expression. Recently, Yassin et al. used a reporter mouse expressing GFP under control of the *c-fos* promoter to characterize neurons that show high GFP levels even under basal conditions. They find that these neurons are indeed characterized by higher spontaneous firing rates and stronger excitatory inputs, supporting the idea that *c-fos* expression levels are correlated with activity levels even under basal conditions (Yassin et al., 2010). Here, we used PA-GFP expressing mice to take a complementary approach to test this hypothesis by first photolabeling neurons based on their spontaneous firing rates *in vivo* and then test for their Fos expression levels.

6.3 Results

6.3.1 Selection of a photactivatable fluorescent protein for *in vivo* expression

As a first step towards the generation of a mouse model that would allow phototagging of individual neurons in the living brain, we characterized several PA-FPs. The optimal PA-FP would show low cytotoxicity, low basal fluorescence, high fluorescence after activation and, importantly, is effectively activatable using two-photon excitation. We expressed six paFPs in cultured HEK293 cells (PA-GFP (Patterson and Lippincott-Schwartz, 2002), PS-CFP11 (Chudakov et al., 2007), PAmCherry (Subach et al., 2009), Kaede (Ando et al., 2002), KikGR (Tsutsui et al., 2005), Dendra2 (Gurskaya et al., 2006)) and characterized their one and two-photon activation properties. We found that only a subset of the characterized PA-FPs was efficiently activatable using two-photon excitation (Table 1). Among those, PA-GFP showed the strongest change in

Manuscript II

fluorescence following activation (Fig1). We therefore selected PA-GFP for the following experiments.

Table 1: Functional characterization of various photoactivatable/photoswitchable proteins

paFP	single photon activation	2-photon activation	activation wl (nm)	imaging wl (nm)	fluorescence increase (x fold)
PA-GFP	nf / green	+	740	950	86
PS-CFP2	cyan / green	+	740	940	43
PAmCherry	nf / red	+	800 - 880	950	2
Dendra2	green / red	-			
Kaede	green / red	-			
KikGR	green / red	-			

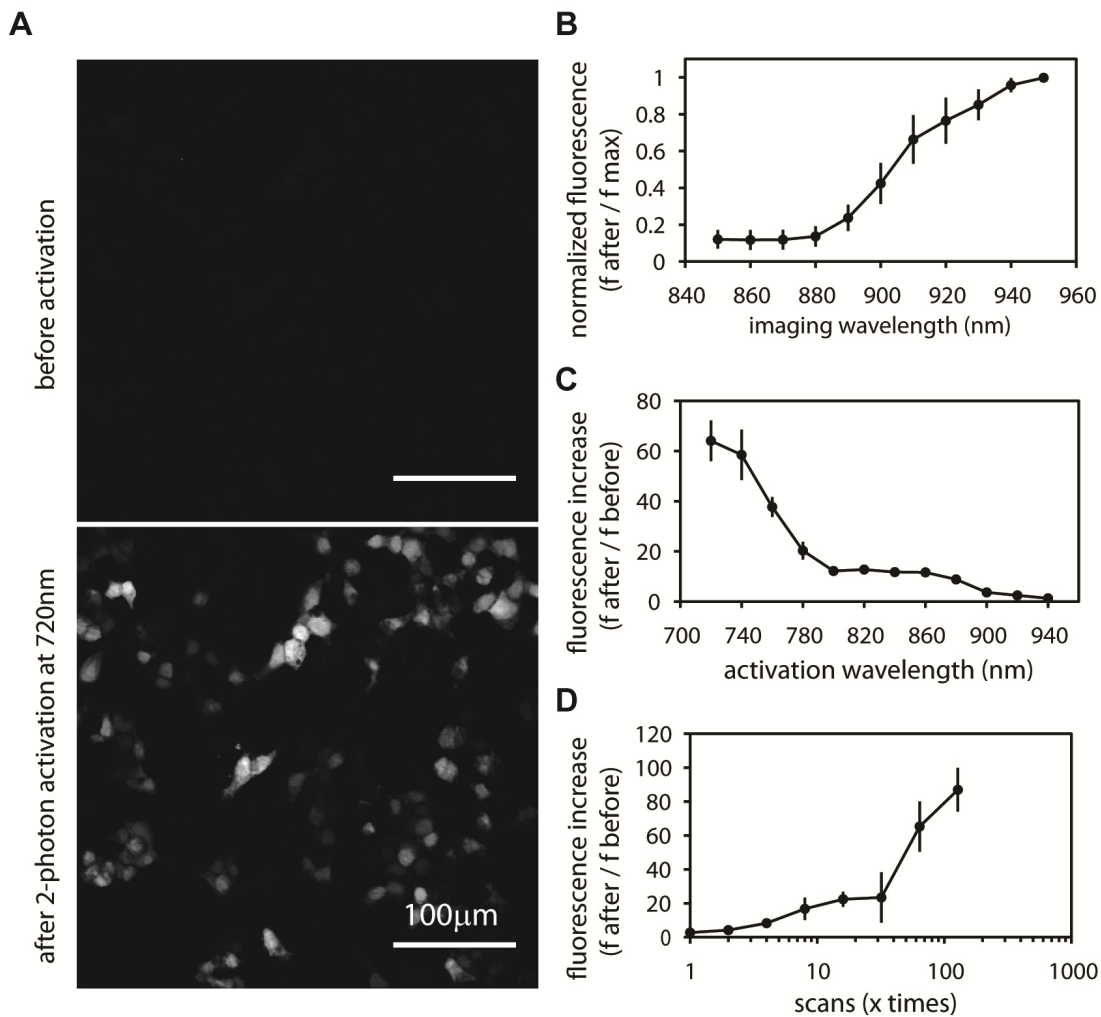


Figure 1: *In vitro* characterization of PA-GFP in Hek293 cells. A: Images show a Hek293 cell culture expressing PA-GFP from the CMV promoter. Upper image shows Hek293 cells before photoactivation

Manuscript II

and lower image shows the same cells after photoactivation at 750nm. B: Two-photon emission spectrum of photoactivated PA-GFP. Hek293 cells were photoactivated at 750nm and the fluorescence was imaged at different wavelengths ranging from 850 to 950nm. The fluorescence was normalized to 950nm. C: Two-photon activation spectrum of PA-GFP. Hek293 cells were activated at wavelengths ranging from 730nm to 940nm and fluorescence was measured at 950nm. D: Fluorescence increase after consecutive photoactivation of PA-GFP. Hek293 cells were activated consecutively at 730nm and the fluorescence increase was measured at 950nm.

Neurons are so tightly packed within the neuropil that individual dendrites and axons cannot be resolved with conventional light microscopy. Due to this limitation, photoactivation of PA-GFP would be predominantly targeted to the soma, which is big enough to be unanimously identifiable *in vivo*. We reasoned that photolabeling of neurons is facilitated if PA-GFP was enriched at the soma. Therefore, we compared the efficiency of photolabeling in primary neuronal cultures expressing PA-GFP and PA-GFP fused to a nuclear localization signal (PA-GFP::NLS). The NLS used in this construct had been identified from the SV40 large T antigen, consists of seven amino acids and promotes the accumulation of fusion proteins in the nucleus (Kalderon et al., 1984). We co-expressed the constitutively red fluorescent protein tdTomato (Shaner et al., 2004) using a 2A strategy to identify transfected neurons before photolabeling and to normalize variations in expression levels (de Felipe et al., 2006). We monitored the fluorescence intensity of PA-GFP at neuronal somata one minute before photolabeling, 5 min after and 30 min after photolabeling at the soma (Fig. 2a). We found that neurons expressing PA-GFP::NLS showed significantly higher green/red fluorescence ratios at the soma after photolabeling as PA-GFP expressing neurons (-1min: PA-GFP::NLS 0.54 ± 0.05 , PA-GFP 0.43 ± 0.02 , $p=0.09$; +5min: PA-GFP::NLS 6.18 ± 0.35 , PA-GFP 4.23 ± 0.33 , $p<0.001$; +30 min: PA-GFP::NLS 5.23 ± 0.37 , PA-GFP 3.12 ± 0.21 , $p<0.001$; Wilcoxon rank sum test; $n=7$ neurons for PA-GFP::NLS and PA-GFP each; Fig. 2b). For both constructs we observed a reduction in the green/red ratio in the measurements from 5 minutes to 30 minutes after photolabeling. This is likely due to diffusion of activated PA-GFP from the soma into the neurites, as their morphology became visible also in the green channel after photolabeling. This loss was less pronounced in neurons expressing PA-GFP::NLS (PA-GFP::NLS $84.3\% \pm 1.7\%$, PA-GFP $74.5\% \pm 3.0\%$, $p<0.026$;

Manuscript II

Wilcoxon rank sum test, Fig. 2c), indicating that the NLS causes an enrichment, but not complete trapping of PA-GFP in the nucleus. Together, these findings indicate that the NLS can improve photolabeling efficiency and we considered a PA-GFP::NLS fusion protein for the generation of transgenic mice.

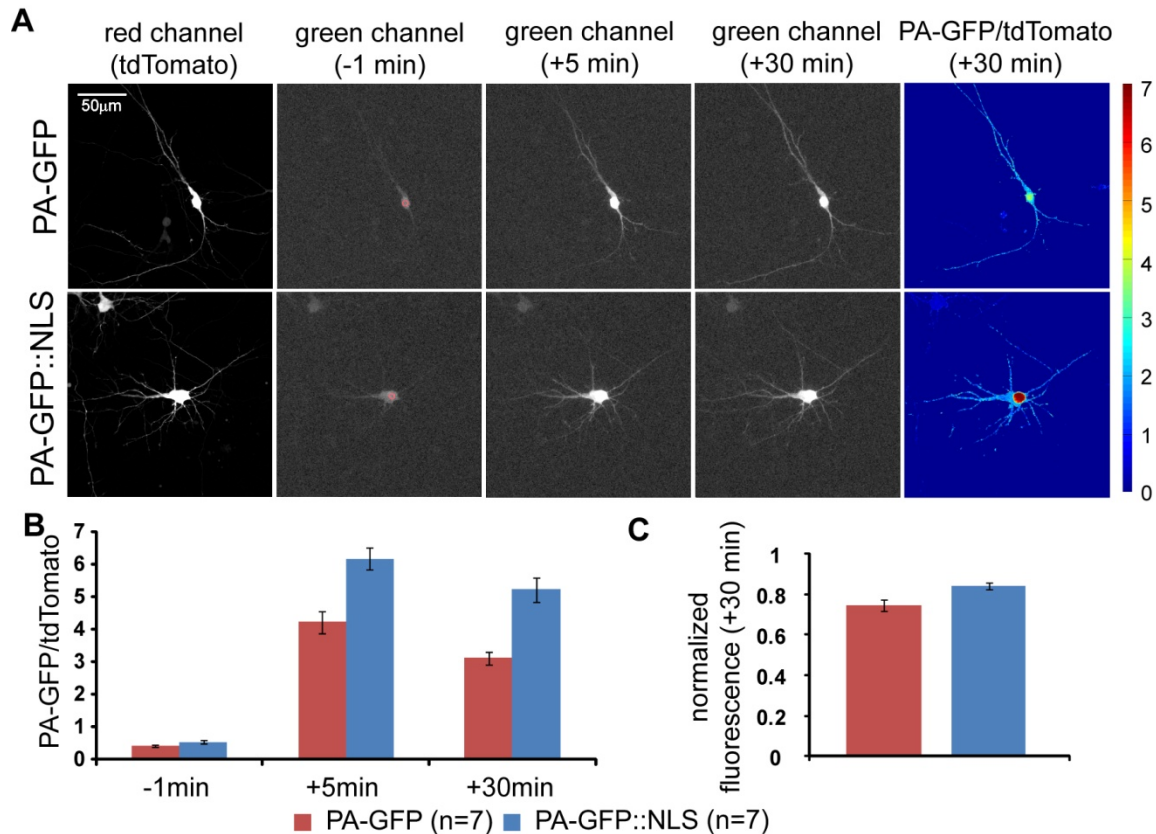


Figure 2: The nuclear localization signal enriches PA-GFP at the soma. A: PA-GFP or PA-GFP::NLS were co-expressed with tdTomato in primary neuronal cultures. PA-GFP was photoactivated at the soma (red circle). Images were taken before (-1min), directly after (+5min) and 30min (+30min) following photolabeling. Representative images in the red and green fluorescence channel for PA-GFP and for PA-GFP::NLS expressing neurons are shown for several time points. Same gamma correction was applied to all monochrome images to visualize also relatively low fluorescence intensities of the dendrites. Pseudocolor images display ratio of intensities in green and red channels. B: The mean fluorescence ratio at the soma of green and red channels before, directly after and 30min after photolabeling indicates higher labeling efficacy in neurons expressing PA-GFP::NLS. C: Decay of photolabel intensity at the soma quantified as normalized PA-GFP fluorescence at the soma 30min after photolabeling.

6.3.2 Generation of genetically modified reporter mice expressing PA-GFP

We used two strategies to generate genetically modified mice. We used conventional transgenics, which relies on the random insertion of an expression construct in the genome (Fig. 3a). The advantage of this system is that transgenic mice can be obtained in relatively short periods of time and can reach very high expression levels due to insertion of multiple copies. However, individual transgenic founder lines typically show strong variability in their expression patterns despite the usage of the Thy1.2 promoter, which in the brain drives expression predominantly in neurons (Caroni, 1997; Feng et al., 2000). As a complement, we also generated knock-in mice in which PA-GFP::NLS is expressed under control of the constitutive CAGGS promoter from the targeted ROSA26 locus (line R26 PA-GFP::NLS; Fig. 3b). Generally, this strategy leads to a broad expression in most cell types (Niwa et al., 1991; Novak et al., 2000). However, as the targeting construct contains a stop-cassette that can be excised upon Cre-mediated recombination, crossing these reporter mice with Cre-driver lines can restrict expression of PA-GFP::NLS to genetically defined cell types.

Manuscript II

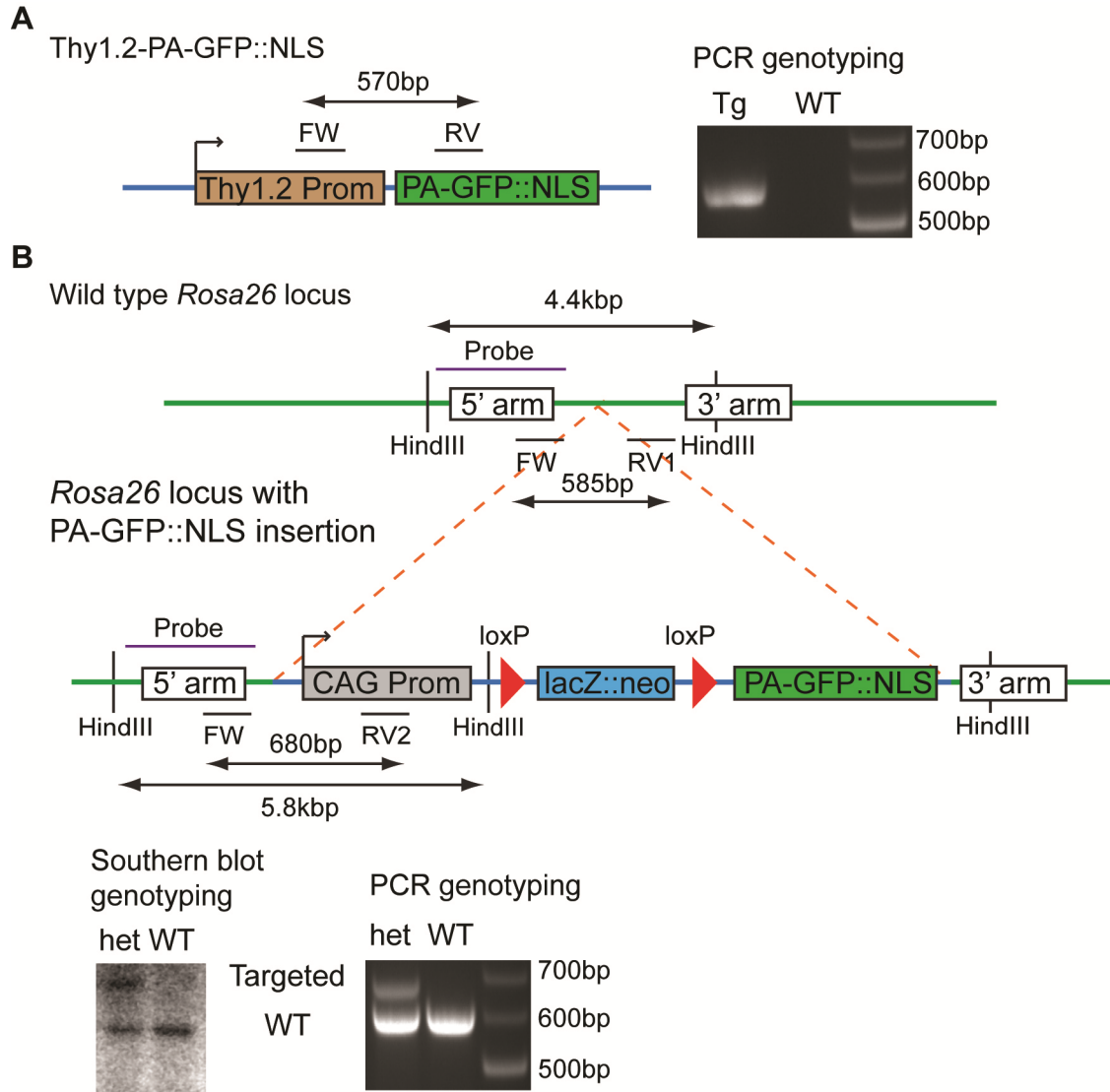


Figure 3: Genetic strategies for the generation of PA-GFP::NLS expressing mice. A: Schematic of the construct used for the generation of transgenic mice expressing PA-GFP::NLS under the control of the Thy1.2 promoter (left). 'FW', 'RV' indicate location of binding sites of forward and reverse primers used for genotyping yielding a 570bp PCR product. Representative image of a gel electrophoresis of products obtained from a genotyping PCR from a transgenic mouse (Tg) and a wild type (WT) mouse (right). B: Schematic diagram of the PA-GFP::NLS knock in strategy into the *Rosa26* locus. After Cre-mediated recombination of loxP sites a stop cassette (*lacZ::neo*) is excised and leads to expression of PA-GFP::NLS under the control of the ubiquitous CAGGS (CAG) promoter. 'FW', 'RV1' and 'RV2' indicate location of binding sites of primers used for genotyping yielding a 585bp or 680bp PCR product for the wild type or knock in allele respectively. 'Probe' indicates binding site for probe used for southern blot analysis after *HindIII* digestion of genomic DNA, resulting in the labeling of a 4.4kb or 5.8kb band in the southern blot. Representative southern blot shown for a wild type (WT) and heterozygous (het) mouse

Manuscript II

(bottom left). Representative image of a gel electrophoresis of products obtained from a genotyping PCR from a heterozygous mouse (het) and a wild type (WT) mouse (bottom right).

After generation of the transgenic lines we first characterized the expression patterns of PA-GFP::*NLS* in coronal brain sections using immunohistochemical detection of PA-GFP::*NLS*. We screened in total six Thy1.2 founder lines in which four showed significant expression in the brain. We focused on two of them: In mice of line Thy1.2#5 PA-GFP was strongly expressed in cortical layer 5 and fewer, but very strongly expressing neurons in layers 2/3 (n=3 sections from 3 mice), representative section shown in Fig. 4a). Mice of line Thy1.2#6 showed more evenly distributed expression across cortical layers, whereas the labeling intensity of individual neurons tended to be more weakly as compared to line 5 (n=3 sections from 3 mice, Fig 4a).

To further analyze the expression pattern of PA-GFP::*NLS* in the transgenic mice, we performed immunohistochemical detection of GFP, the neuronal marker protein NeuN and as a third marker either CamKII for detection of excitatory neurons or GABA for detection of inhibitory neurons (Fig. 4b). Coronal sections of the auditory cortex from three mice from lines Thy1.2#5 and Thy1.2#6 were stained and we quantified the fraction of NeuN and CamKII double positive neurons that were in addition GFP positive for the six cortical layers of both lines (Fig. 4c). We found that in line Thy1.2#5 CamKII-positive neurons were predominantly expressing PA-GFP in layers 5 and 6, whereas GABA-positive neurons were mostly found in layers 1-3 and 6. In line Thy1.2#6 labeling of CamKII-positive and GABA-positive neurons expressing PA-GFP were more evenly distributed across cortical layers.

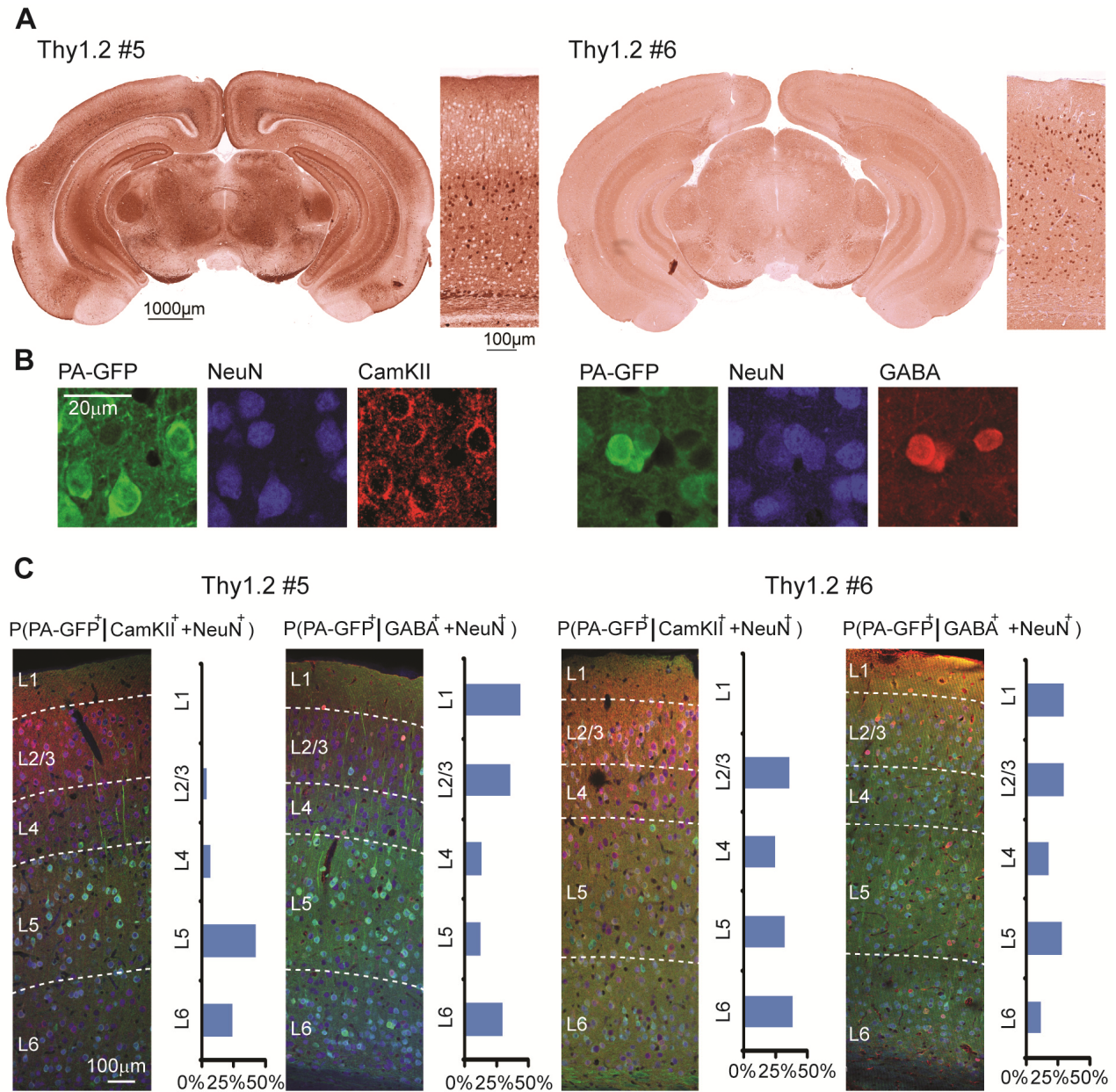


Figure 4: Expression patterns of PA-GFP::NLS in the transgenic mouse lines. A: Coronal brain sections of the Thy1.2#5 (left) and the Thy1.2#6 (right) lines immunohistochemically stained for PA-GFP. Higher-magnification details show neocortical layers. B: Examples of sections stained for PA-GFP/NeuN/CamKII (left) and PA-GFP/NeuN/GABA (right). C: Quantification of cell type-specific expression of PA-GFP::NLS in the Thy1.2#5 (left) and the Thy1.2#6 (right) line. Neocortical layers are indicated by dashed lines on representative triple-stained coronal sections. Bar graphs represent fraction of NeuN and CamKII or NeuN and GABA double positive neurons that also express PA-GFP for all 6 cortical layers.

Manuscript II

To characterize the expression in R26 PA-GFP::NLS mice we analyzed mice that had been crossed to EMX1-Cre and Nestin-Cre driver mice. Both driver lines show predominant expression of Cre in neurons and should therefore lead to broad PA-GFP::NLS expression in the brain (Tronche et al., 1999; Gorski et al., 2002). To assess possible background expression of PA-GFP::NLS despite the stop-cassette, we also analyzed the brains of R26 PA-GFP::NLS mice that do not express Cre. We found strong and broad expression of PA-GFP in brain sections from R26 PA-GFP::NLS x EMX1-Cre mice (n=3 mice) whereas virtually no PA-GFP expression was detected in Cre-negative littermates (n=3 mice, Fig.5a).

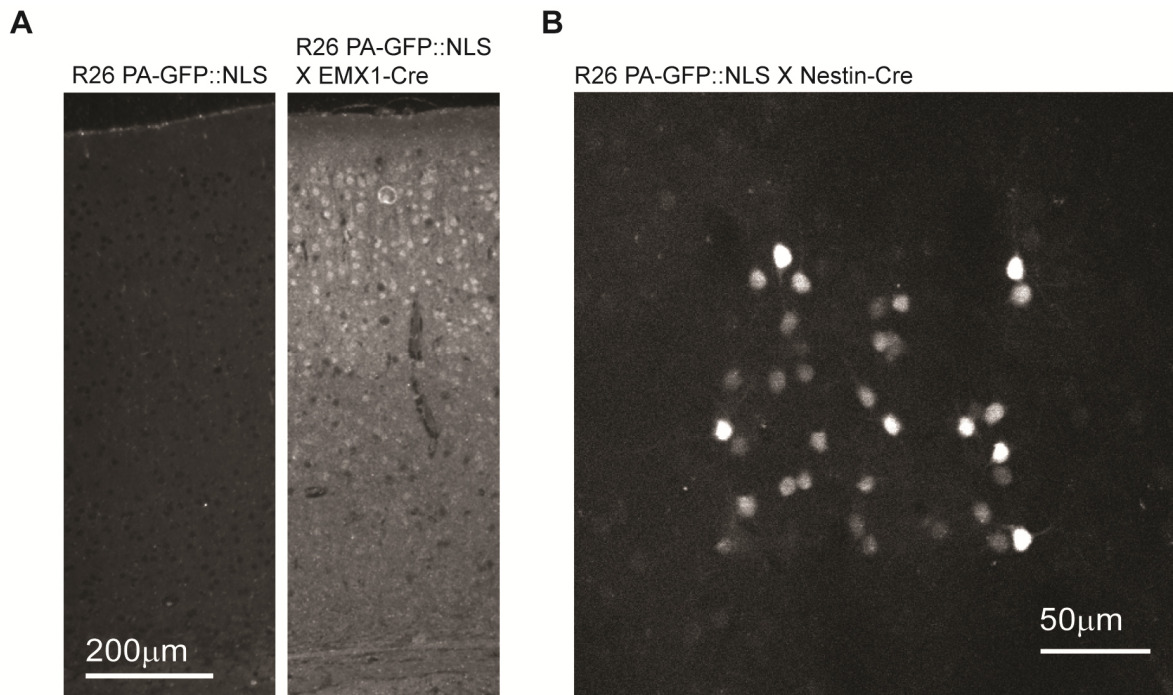


Figure 5: PA-GFP expression in the R26 PA-GFP::NLS mouse. A: Coronal sections of the neocortex obtained from the R26 PA-GFP::NLS knock-in mouse line that were immunohistochemically stained for PA-GFP. Without expression of Cre-recombinase PA-GFP::NLS expression is essentially blocked by the stop-cassette (left). In mice crossed with an EMX1-Cre mouse line, which leads to the removal of the Stop cassette, strong expression of PA-GFP::NLS can be detected (right). B: *In vivo* imaging in the auditory cortex of the R26 PA-GFP::NLS mouse line crossed with a Nestin-Cre mouse line. Neurons were photolabeled in a square shaped ROI.

6.3.3 Functional characterization of mice expressing PA-GFP::NLS

After confirmation of expression of PA-GFP::NLS in the cortex using histological methods, we were interested in testing the efficiency of photolabeling neurons in the living brain. Towards this end we implanted a small cranial glass window over the auditory cortex which provided us with chronic optical access to the brain (Loewenstein et al., 2011). Using two-photon laser scanning microscopy in anaesthetized mice, we were able to identify PA-GFP::NLS expressing cells based on basal fluorescence at very high intensity settings at 900-950nm excitation wavelength. In all three lines we were able to readily photolabel neurons at a depth of typically 100-300 μ m below the dura after brief excitation at 720-750nm at the soma (Thy1.2#6: Fig.6a-c; Thy1.2#5: Fig.7a; R26 PA-GFP::NLS: Fig.5b). The two-photon approach provided us with sufficient resolution to label single, nearby neurons (Fig. 6a) without labeling neurons above or below the focal plane (Fig. 6b,c). This would not have been achievable using conventional one-photon excitation.

How long does the photolabel persist? We again implanted mice with cranial windows and photolabeled individual neurons in cortical layers 2/3. We re-visited the neurons at various time intervals up to two days and acquired images with identical power and detection settings (line Thy1.2#5, n=3 mice, 30 neurons, each imaged at 4-9 time points after photolabeling). We found that the fluorescence intensity at the soma decays significantly over the time course of hours to days (Fig.6d). The decay of fluorescence over time $F(t)$ could be approximated well by the following double exponential function:

$$F(t) = a_1 * \exp(-t/\tau_1) + a_2 * \exp(-t/\tau_2) + C$$

The fitted parameters were: $a_1=0.27$; $\tau_1=1.2$ hrs; $a_2=0.66$; $\tau_2=9.3$ hrs and $C=0.06$. The shorter time constant could primarily reflect diffusion processes of activated PA-GFP::NLS from the soma, whereas the longer time constant in the order of several hours could reflect processes related to the turnover of the fluorescent protein itself (Corish and Tyler-Smith, 1999). Despite this loss of fluorescence, strongly labeled somata could be readily re-identified for intervals for more than a day after *in vivo* labeling. Interestingly, we found that 8 out of 13 neurons that had been photolabeled

Manuscript II

previously could be re-labeled to fluorescence intensities between 45-85% of the intensity observed after the previous photoactivation (Fig.6e). Taken together, these experiments demonstrated that the genetically modified mice allow photolabeling of individual neurons with good signal/noise ratio for more than a day.

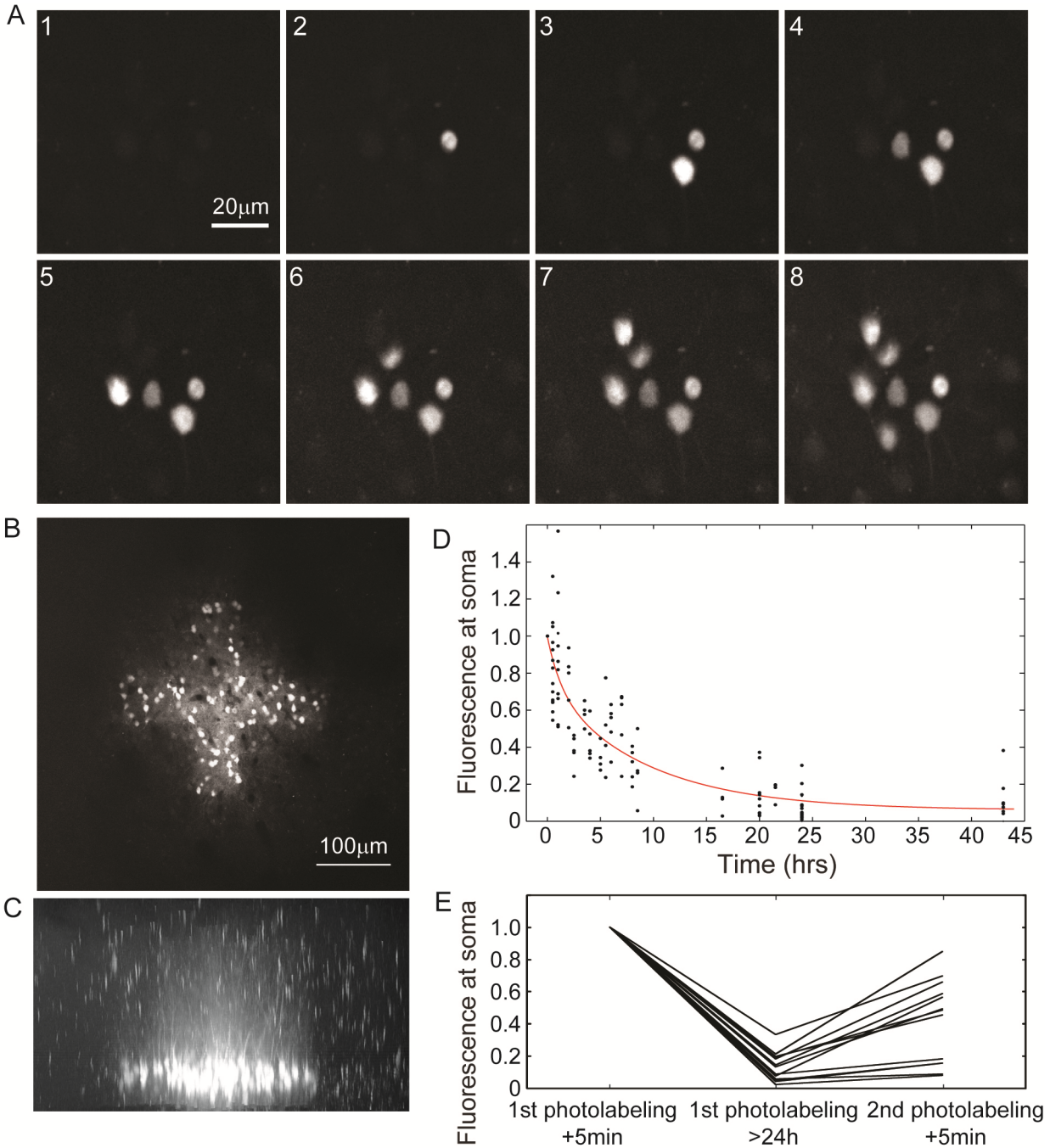


Figure 6: Photolabeling of neurons *in vivo*. A: Two-photon images of individual neurons consecutively photolabeled *in vivo*. Nearby neurons can be labeled with high precision. B: Bulk labeling of neurons in a

Manuscript II

cross shaped ROI. C: Side view of an image stack showing the same neurons displayed in (B). Note, only neurons in the plane of activation were photolabeled. D: Intensity of the photolabel at the soma at various time points after photolabeling. Points represent individual measurements (n=4-9 measurements from 30 neurons). Red line indicates double exponential fit to the fluorescence decay. Individual photolabeled neurons for more than a day. E: Re-labeling of previously photolabeled neurons. Lines represent normalized fluorescence intensity at the soma of individual neurons directly after initial photolabeling, after more than 24 hours and directly after second photolabeling.

Following photolabeling of cultured neurons expressing PA-GFP::NLS at the soma we observed an increase in fluorescence of the neurites that was likely due to diffusion of activated GFP. To test to what extent this effect would also occur *in vivo* and could potentially provide morphological information we performed a series of photolabeling experiments in which we strongly and repeatedly activated the soma of individual neurons for 3 times during the period of 45 minutes (line Thy1.2#5, n=7 neurons from 4 mice). After photolabeling we acquired image stacks of the labeled neurons and we found that this protocol leads to an intense labeling of neuronal dendrites. The label was strong enough that it could be used for anatomical tracing of neurites. We predominantly found morphologies consistent with layer 2/3 pyramidal neurons (Fig.7a,b) and only few neurons with more star-shaped arborizations that could represent putative interneurons (Fig. 7c). In our hands, it was not possible to readily identify axons, likely due to lower label intensity as compared to dendrites and decreasing quality of imaging conditions towards deeper layers.

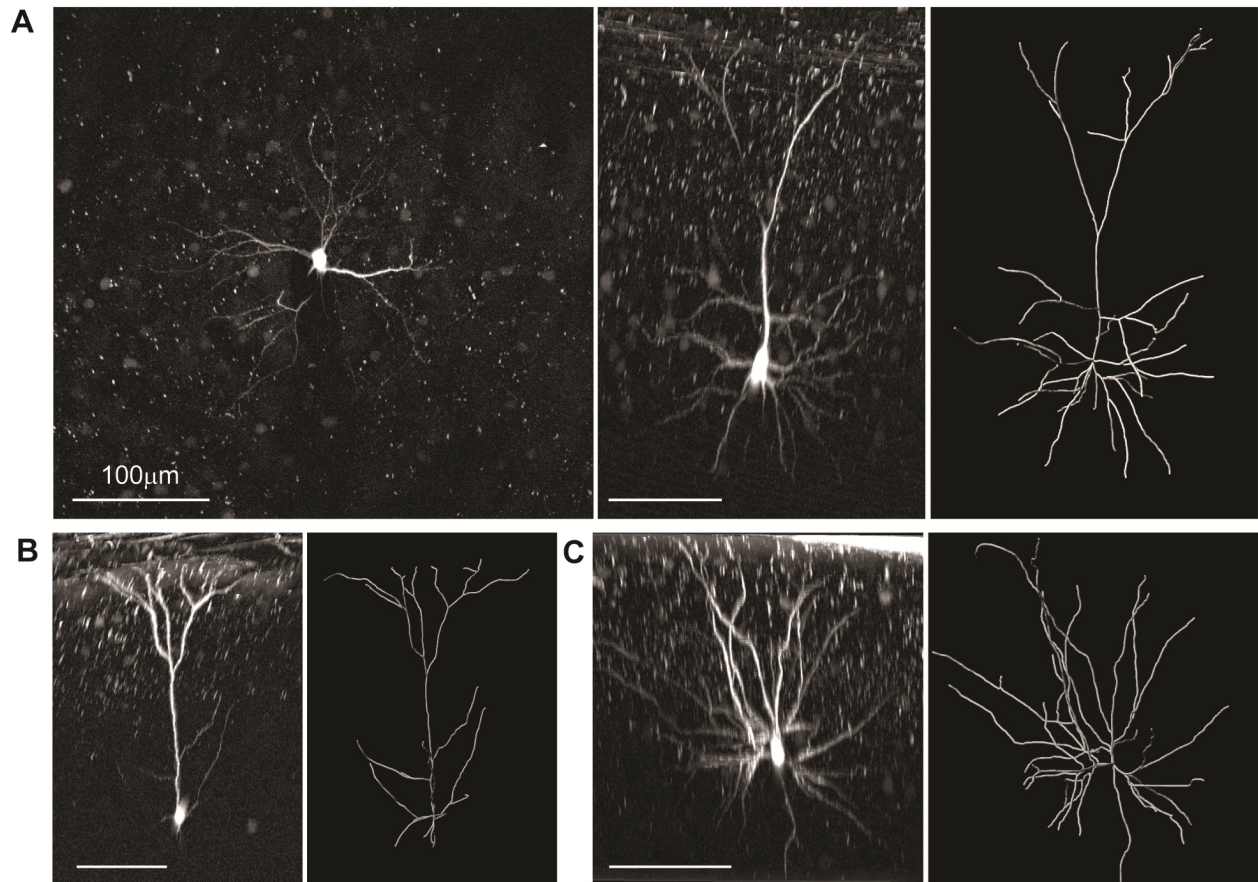


Figure 7: Photolabeling reveals dendritic morphology. A: Maximum intensity projection of an image stack taken *in vivo* of a previously photolabeled neuron (left). Side projection of the stack (middle) and *in silico* reconstruction of the neuron (right). B: Side projection of another putative pyramidal cell (left) and reconstruction (right). C: Side projection of an image stack taken *in vivo* of a putative interneuron (left) and reconstruction (right). All scale bars indicate 100μm.

Photolabeling could also be efficiently performed in acute brain slices prepared from mice expressing PA-GFP::NLS, which could be advantageous for targeted dendritic patching of selected neurons *in vitro* (Fig. 8). Together, these findings show that PA-GFP::NLS expressing mice can provide morphological information of selected neurons that can be used for cell type identification.

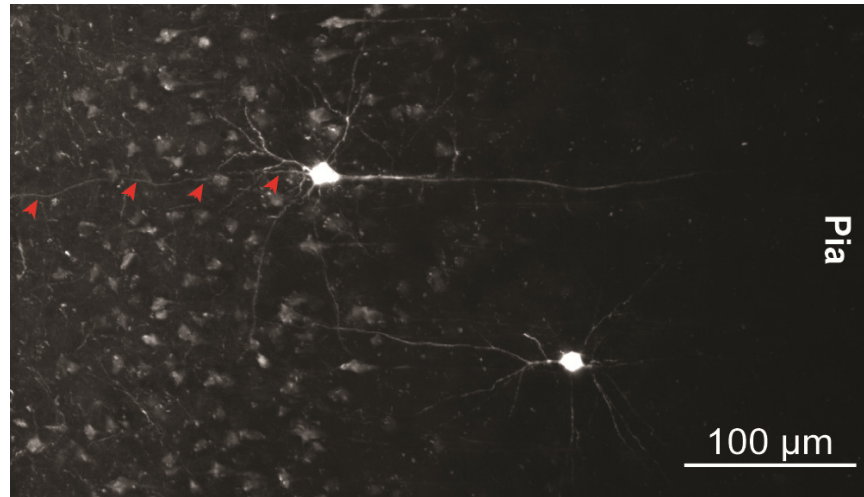


Figure 8: Photolabeling of neurons in acute brain slices. Maximum intensity projection of a two-photon image stack taken from two neurons that previously have been photolabeled *in vitro*. Details of the neuronal morphology can be visualized by the diffusion of PA-GFP from the soma, the site of photoactivation, into neurites. Red arrows show the axon of a photolabeled neuron.

The acute brain slice preparation provides very good experimental control and success rates for the physiological analysis of dendritic and synaptic function. We were therefore interested to test in how far *in vivo* photolabeled neurons could be re-identified in acute brain slices. We found that the photolabel persisted the preparation procedure and allowed the identification of individual neurons using epifluorescence microscopy in acute brain slices (Fig.9a). We succeeded in targeting patch-clamp whole-cell recordings to neurons that had been photolabeled and we characterized their electrophysiological properties in the current-clamp mode (Fig.9b). We found that these cells had average resting potentials of -62 ± 7 mV and average input resistances of 266 ± 90 M Ω , respectively (n=5). Furthermore, the neurons displayed discharge patterns that are consistent with layer 2/3 pyramidal neurons. Our findings demonstrate that *in vivo* photolabeling can be combined with subsequent slice electrophysiology and allows the targeted patching of neurons selected *in vivo*.

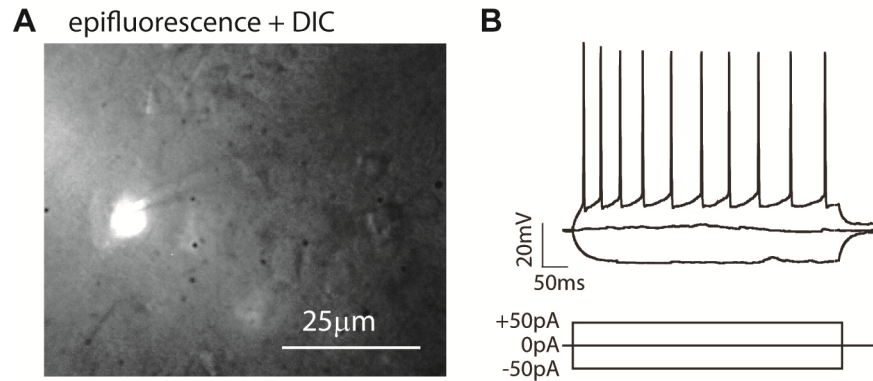


Figure 9: Identification of *in vivo* photolabeled neurons in the brain slice preparation: A: Composite fluorescence and DIC image of a brain slice containing a neuron previously photolabeled *in vivo* targeted with a patch pipette. B: Patch-clamp current-clamp recording of the membrane potential of the neuron shown in A in response to hyper- and depolarizing current injections

Furthermore, we were interested in how far the *in vivo* photolabeled neurons could be re-identified in fixed tissue. To test this, we photolabeled neurons as described above and subsequently sacrificed the mice and fixated the brains. We observed that the fixation procedure leads to a significant loss in PA-GFP fluorescence, nevertheless, individual neurons could be readily re-identified in image stacks taken from 70 μ m slices of the fixed brains (Fig.10). This finding demonstrated that PA-GFP::NLS expressing mice can greatly facilitate the linkage of *in vivo* experiments on single, identified neurons and subsequent immunohistochemical analysis of their expression profile.

Manuscript II

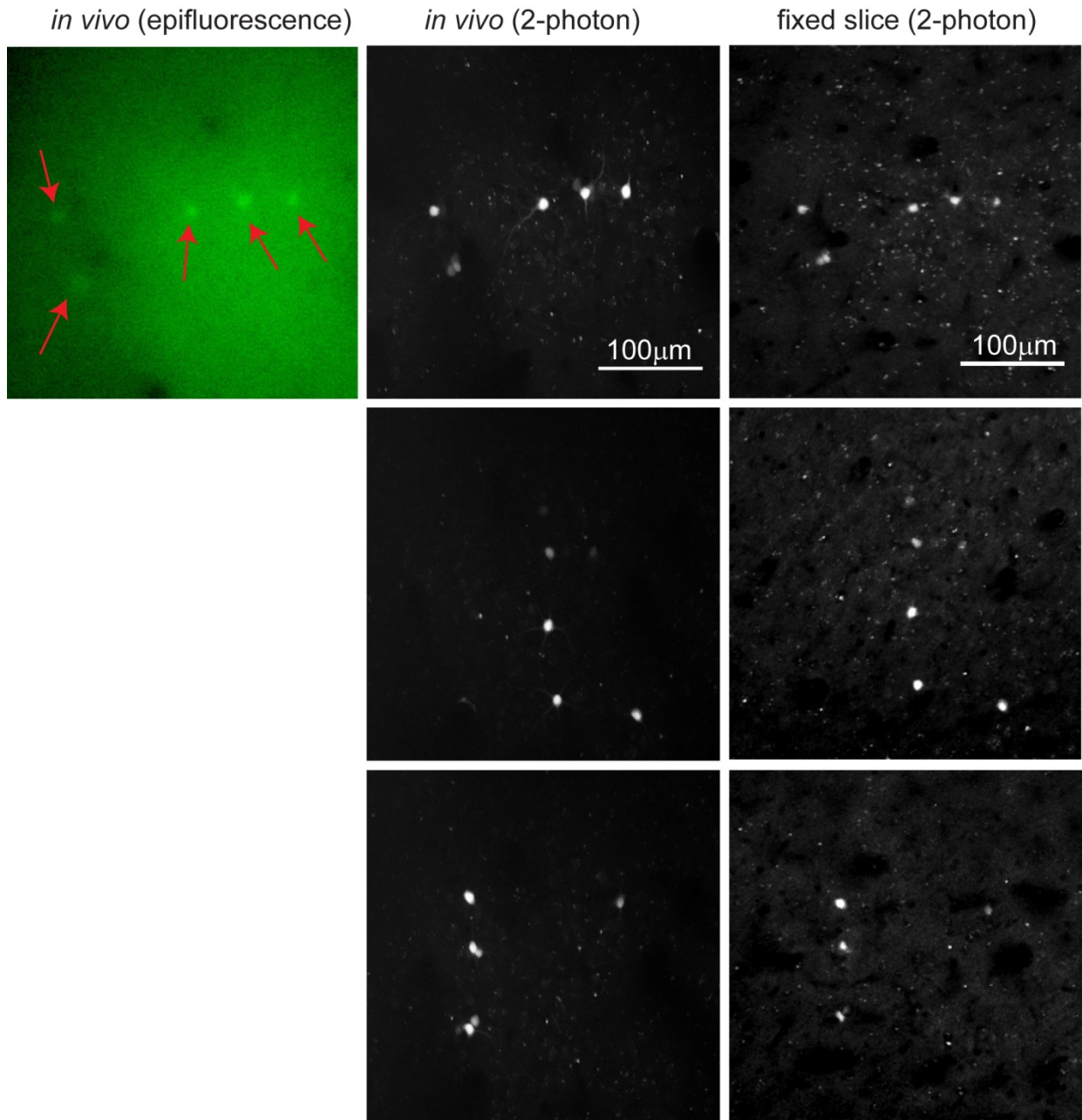


Figure 10: Re-identification of neurons in fixed brain slices that previously have been photolabeled *in vivo*. The rows correspond to three examples. The first column shows an epifluorescence image taken *in vivo*. Individual neurons indicated by red arrows. The middle column shows two-photon *in vivo* images of neurons that have been photolabeled in an arbitrary pattern. The right column shows two-photon images of the same neurons in a brain slice after fixation.

6.3.4 Single cell correlation of *in vivo* activity and endogenous Fos expression

So called immediate early genes (IEGs, e.g. *Arc*, *c-fos*) are characterized by generally low expression levels under basal conditions, however, show strong and transient expression triggered by events that lead to strong neuronal activity like tetanic stimulation, kainate injections or Channelrhodopsin-mediated stimulation (Dragunow et al., 1989; Lyford et al., 1995; Lin et al., 2011). Interestingly, expression of IEGs could be also observed in subsets of neurons in particular brain regions after behavioral manipulation (Guzowski et al., 1999). These are major reasons why IEGs are widely used as reporters of previous neuronal activation and to delineate neurons involved in particular behaviors (Gall et al., 1998; Barth et al., 2004). However, up to date there is only little direct experimental evidence that an identified, single neuron *in vivo* indeed shows increased activity and correlated increased IEG expression. Recently, Yassin et al. used a reporter mouse expressing GFP under control of the *c-fos* promoter to characterize neurons that show high GFP levels even under basal conditions. They find that these neurons are indeed characterized by higher spontaneous firing rates and stronger excitatory inputs, supporting the idea that *c-fos* expression levels are correlated with activity levels (Yassin et al., 2010).

Spontaneous activity levels of neurons in the auditory cortex *in vivo* vary over an order of magnitude and their distribution is dominated by cells with low firing and only a minor fraction of cells showing strong firing rates (Hromadka et al., 2008). Are all neurons with high *in vivo* activity levels distinguished by strong *c-fos* expression or does this rule apply only to a subpopulation of them? To answer this question it is important to identify highly active cells first and then analyze the respective expression levels, in particular as they represent only a small fraction of the whole population. We therefore combined *in vivo* calcium imaging to characterize the firing rates in a population of neurons, with *in vivo* photolabeling of neurons with either very high or very low activity levels and subsequent immunohistochemical detection of Fos in photolabeled neurons.

When photolabeling neurons based on a measurement of activity levels of several minutes, the important question arises how stable spontaneous firing rates are

Manuscript II

in vivo. To address this point we bulk-loaded layer 2/3 neurons in the auditory cortex of wild-type mice with the green calcium indicator OGB1-AM, implanted a small cranial window and imaged the same neuronal populations (18 populations, 43-100 neurons each) for a period of approximately 10 minutes at two time points 1.5 hrs apart. We found that spontaneous activity levels in the mouse auditory cortex were highly correlated over time (Corr. coef. = 0.78, Fig.11a). We concluded that the analysis of the spontaneous firing rate at a given time point can serve as a good indicator for the activity level over the last hours (Fig.11b), which is in the temporal range of induced Fos expression (Zangenehpour and Chaudhuri, 2002).

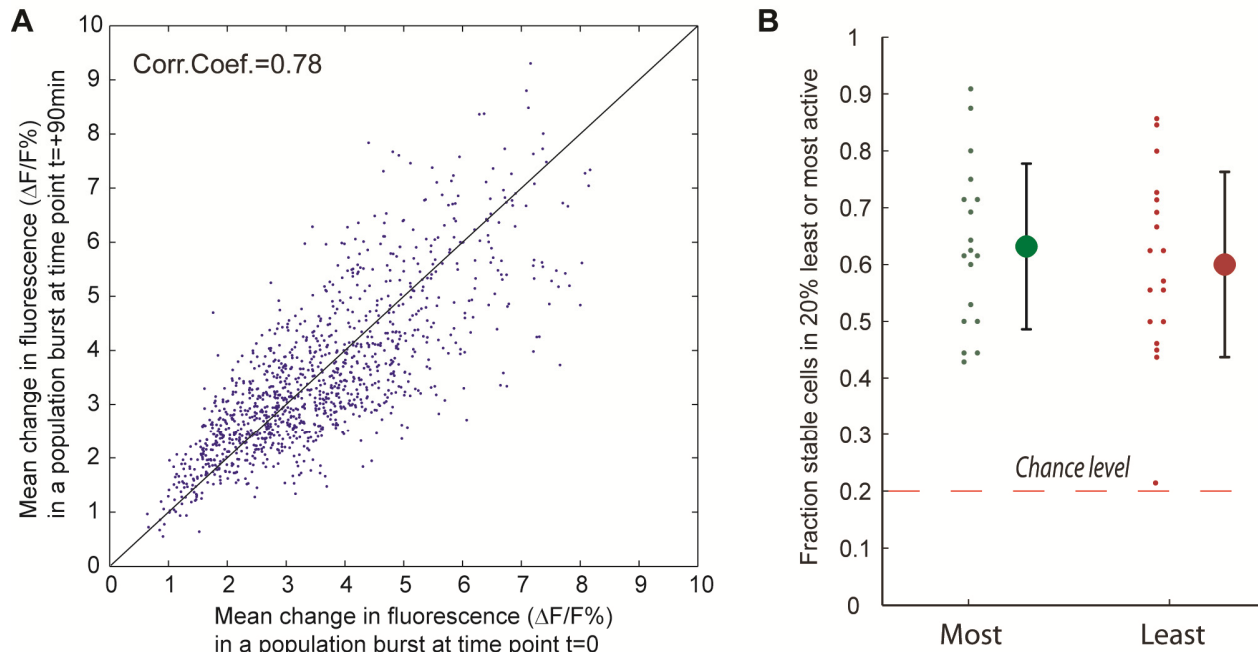


Figure 11: Stability of spontaneous activity levels *in vivo*. A: Populations of neurons in the auditory cortex *in vivo* were bulk loaded with the calcium sensitive dye OGB1 and the levels of spontaneous activity were measured for approximately 10 minutes at two time points ($t=0\text{min}$, $t=+90\text{min}$). To quantify spontaneous activity, we measured the average change in fluorescence ($\Delta F/F\%$) during a spontaneously occurring population burst for each neuron. In the scatter plot data for individual neurons is shown (18 populations, 43-100 neurons each). The activity levels between both time points over one hour apart are strongly correlated. B: Quantification of the fraction of neurons that have been in the 20% most or 20% least active neurons in a given imaged population at time point $t=0\text{min}$, that also fall in the same quantile at time point $t=90\text{min}$. Individual dots represent data per imaged neuronal population. Error bars represent SD.

Manuscript II

To combine calcium imaging with photolabeling in transgenic mice (Thy1.2#6, 9 mice) we used the red calcium indicator Rhod2-AM that allows spectral unmixing of the GFP signal. We again bulk-loaded layer 2/3 neurons with the indicator and recorded the spontaneous activity levels in a population of ~40 neurons over 2 minutes (Fig. 13a, b). Following an online analysis we chose to photolabel 20% of the neurons with either the highest or lowest activity levels in a given population (~75% success rate). Subsequently, we fixated the brains and performed immunohistochemical detection of Fos-levels in the photolabeled neurons (Fig. 13c). With our staining conditions approximately 40% of the neurons showed detectable levels of Fos under basal conditions (Fig. 12a).

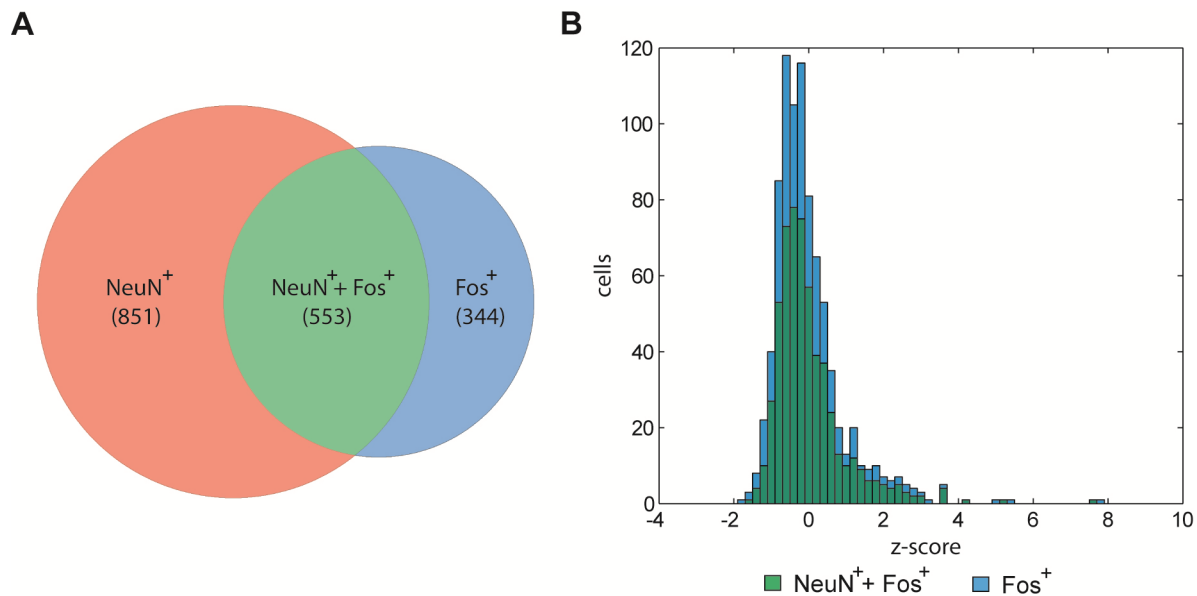


Figure 12: Analysis of Fos expression levels in immunohistochemically identified neurons: A: Brain slices were stained for the neuronal marker NeuN and for Fos. The Venn diagram shows the amount of NeuN (NeuN⁺) and Fos (Fos⁺) and double-positive cells (NeuN⁺+Fos⁺). Approximately 40% of all neurons show detectable Fos levels. B: Histogram of the distribution of the z-scores of Fos positive and double positive neurons. The distribution of Fos-levels obtained from all cells in an image plane (Fos⁺) is comparable to the distribution of Fos-levels in neurons only (NeuN⁺+Fos⁺). This shows that the Fos-levels measured from all cells in an image plane serve well as an estimate of the distribution of Fos-levels in neurons and can be used to construct z-scores for neurons.

Manuscript II

The distribution of labeling intensities for neurons was comparable to the distribution of intensities obtained from all stained cells (Fig. 12b). When comparing Fos-label intensities from neurons that were selected and photolabeled *in vivo* for particularly high or low spontaneous firing rates, we found in both groups considerable variability in expression levels (Fig. 13d-f). We observed that the neurons with the highest Fos levels were found in the group of neurons with the highest firing rates, however, on the population level no significant differences were observed. On the methodological side, the association of single neuron *in vivo* firing rates and Fos-detection *in vitro* was greatly facilitated by the direct labeling of the somata, which made indirect alignment of images based on landmarks obsolete.

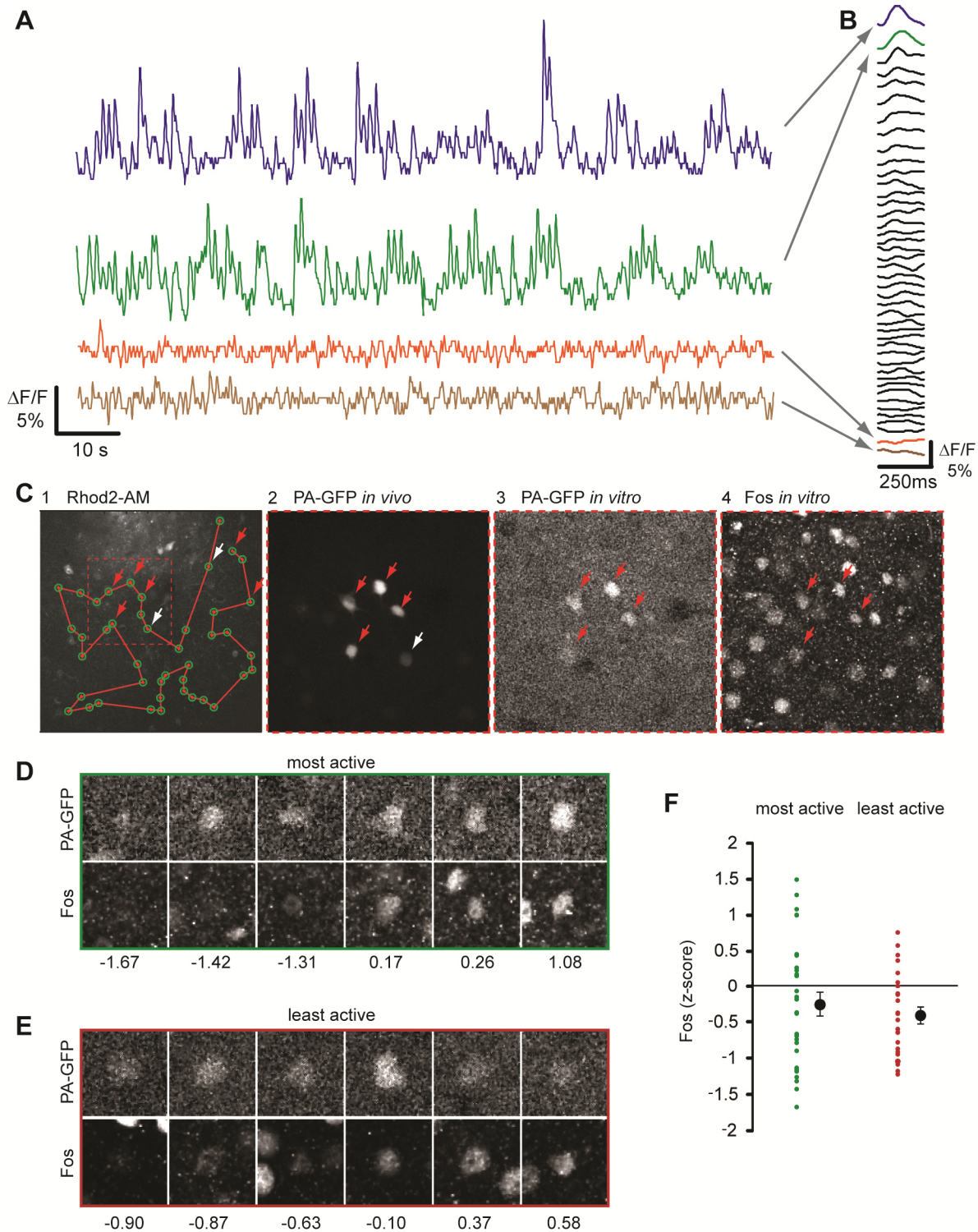


Figure 13: Correlation of single cell *in vivo* activity levels with Fos expression. A: Example traces of fluorescence measurements of auditory cortex neurons bulk labeled *in vivo* with the calcium indicator Rhod2. B: The fluorescence transients during spontaneously occurring population bursts were averaged for each neuron in the population and sorted by their amplitude. Arrows indicate corresponding averages

Manuscript II

for the traces shown in (A). C: Experimental workflow. 1: Calcium imaging of a neuronal population. The green circles mark simultaneously recorded neurons and the red line depicts the scan line used for fast imaging of activity. Arrows show neurons which were photolabeled following an online analysis of their activity levels. Red arrows indicate neurons re-identified *in vitro*, white arrows indicate neurons which could not be re-identified. 2: Image taken *in vivo* of neurons photolabeled after calcium imaging. 3: Same neurons shown in (2) re-identified after preparation of fixed brain slices. 4: Immunohistochemical detection of Fos in the same brain slice shown in (3). D: Examples of the PA-GFP signal and corresponding Fos label in fixed brain slices previously selected *in vivo* for high spontaneous activity levels. E: Examples of the PA-GFP signal and corresponding Fos label in fixed brain slices previously selected *in vivo* for low spontaneous activity levels. Numbers in panels D, E indicate the corresponding z-scores of Fos expression levels. F: Individual and average z-scores of neurons of the neurons being either in the top or bottom 20% of spontaneously active neurons. Error bars represent SEM.

6.4 Discussion

In this study we generated and demonstrated the utility of genetically modified mice expressing PA-GFP::NLS for various experimental approaches in which the photolabeling of neurons allows the combination of several levels of analysis on individual, identified cells. We believe that a major application of the mice in the future could be the combination of *in vivo* calcium imaging with either histological staining or *in vitro* electrophysiology. Also, the combination of calcium imaging with intense photolabeling to reveal the dendritic morphology could be helpful to gain a better understanding of the various cell types that are forming a functional assembly in a given neuronal population. This cannot be achieved by imaging in a transgenic mouse in which only a single or few cell types are labeled. Thus, mice allowing efficient photolabeling of functionally identified neurons can become an important complement to the expanding set of driver mouse lines expressing Cre recombinase (Gong et al., 2003; Madisen et al., 2010; Portales-Casamar et al., 2010). Furthermore, to understand how the transcriptional profile of a given cell translates into a specific cell type and physiological function PA-GFP::NLS expressing mice can be used to combine functional characterization *in vivo* and subsequent transcriptional profiling. Laser capture dissection or isolation of living cells from brain tissue has been demonstrated earlier (Emmert-Buck et al., 1996; Sugino et al., 2006).

Manuscript II

Further variants of PA-FP expressing mice are conceivable for the future. Whereas most experimental designs are practical with a life-time of the label of one to two days, a tighter localization of the PA-FP to the nucleus could improve both label intensity and life-time. Fusion of fluorescent proteins to one of the major components of chromatin, Histone 2B, is a proven strategy (Hadjantonakis and Papaioannou, 2004; Lien and Scanziani, 2011). In addition, the ongoing development of red PA-FPs (Subach et al., 2009; Subach et al., 2010) or red calcium indicators (Zhao et al., 2011) will likely expand the spectrum of fluorophores with sufficient sensitivity and signal/noise ratios for *in vivo* applications and will also offer higher flexibility in experimental approaches.

In this study, we took advantage of PA-GFP::NLS expressing mice to correlate *in vivo* activity levels of individual neurons with the expression levels of the immediate early gene *c-fos*. This is important as IEG expression is widely used post hoc as a bona fide marker for neuronal activity and IEG promoters have been used to generate reporter mice (Fleischmann et al., 2003; Barth et al., 2004; Wang et al., 2006). We found that neurons that have been selected for particularly high activity levels under basal conditions have highly variable and on average similar Fos expression levels as neurons selected for low activity levels. Our observation indicates that not all neurons with high *in vivo* activity levels are distinguished by strong Fos expression. This suggests that additional factors besides neuronal activity control the level of Fos expression in individual neurons under basal conditions. In the context of previous work our findings imply that only a fraction of highly active neurons is embedded in a strongly interconnected sub-network characterized by high Fos-levels (Yassin et al., 2010).

We focused on the characterization of PA-GFP::NLS expressing mice in the context of the brain and demonstrate their applicability for several experimental approaches to elucidate neuronal function. The R26 PA-GFP::NLS mice in particular are expected to allow broad and strong expression in most tissues of the body. We expect therefore that this mouse model can be readily used also in other biological fields in which labeling of individual cells could turn out to be instrumental.

6.5 Experimental Procedures

6.5.1 Cell culture

Hek293 cells: PA-GFP, PS-CFP1I, PamCherry, Dendra2, Kaede and KikGR fused to a NLS were cloned in the pCMV-MCS vector (Stratagene) using standard molecular cloning techniques. Hek293 cells were grown to 80% confluency and transfected with Lipofectamin 2000 (Invitrogen 11668-019) and the plasmid DNA containing the PA-FP following the manufacturers protocol. 24h later the cells were fixed for 5min with 4% Paraformaldehyde.

Cortical neurons: Cortical neurons were isolated from E17 C57bl6 mouse embryos. Cortices were removed and digested with 0.25% Trypsin (GIBCO 15050-065) for 3min at 37°C to get single cells. The neurons were resuspended in BME medium (GIBCO 41010-026) supplemented with 1% Penicillin-Streptomycin (GIBCO 15140-122), 1% L-Glutamin 200mM (GIBCO 25030-024), 1% Insulin-Transferrin-Selenium-A Supplement (GIBCO 51300-044), 0.6% Glucose solution (40%) and 10% FBS (GIBCO 10500-064) and seeded at a density of 10000 cells on Poly-L-Lysine Coated Coverslips (BD 354085). Neurons were incubated for 1h at 37 °C, 5% CO₂ and then the medium was changed to Neurobasal medium (GIBCO 21103) supplemented with 5% B27 supplement (GIBCO 17504-044), 0.5% GlutaMAX (GIBCO 35050) and 1% Penicillin-Streptomycin (GIBCO 15140-122). Neurons were incubated at 37 °C and 5% CO₂ for 7 days and then transfected with Lipofectamin 2000 following the manufacturers protocol. 72h after transfection neurons were used for the photoactivation experiments.

6.5.2 In vitro Imaging

Hek293 photoactivation experiments were done using an Ultima *in vivo* multiphoton microscopy system (Prairie Technologies) with a 20 X 0,95 numerical aperture objective lens (Olympus) and a Ti: Sapphire multiphoton laser (Coherent). To define the best imaging wavelength for an activated PA-FP, cells were first photolabeled and then imaged at wavelength ranging from 850nm-950nm. To test if the PA-FP can be switched using 2-photon illumination ROIs were activated at different wavelength ranging from 720nm-940nm and imaged afterwards to see if a significant fluorescence

Manuscript II

increase was induced. To the fluorescence increase induced by photoactivation ROIs were scanned multiple times (1-128 times), an image was taken at the optimal imaging wavelength and the fluorescence increase was quantified using ImageJ.

Photoactivation experiments in primary cortical cultures were performed on an upright Zeiss LSM 780 confocal laser scanning microscope (Zeiss). Photoactivation at the soma was done using a 405nm diode. Green (PA-GFP) and red (tdTomato) fluorescence signals were captured simultaneously by using the 488- and 561-nm laser lines. Images were quantified using a custom written script in Matlab (Mathworks).

6.5.3 Histology

PA-GFP staining: 8-12 week old mice were sacrificed, the brain removed and fixed in 4% PFA overnight. On the next day the brains were dehydrated in a graded alcohol series, embedded in paraffin and cut to 2 μ m slices. PA-GFP staining was performed on a Discovery XT (Ventana Medical Systems) machine. The rabbit polyclonal anti GFP antibody (Abcam ab290) was used at a concentration of 1:1000. PA-GFP was visualized using a secondary biotynilated goat anti rabbit antibody (Dako, E 0432) with DAB as a substrate. The slices were scanned on a Mirax Scan (Carl Zeiss MicroImaging GmbH, Germany) slide scanner. For the R26 PA-GFP::NLS mice the slices were incubated for 2h at RT with the secondary antibody Dye-Light 549 goat anti rabbit IgG (Thermo Scientific 35507) dilution 1:1000 in PBS containing 5% normal goat serum and 0.1% Triton-X 100.

GABA/CamKII/NeuN staining: Brains were cut on a vibratome to 70 μ m thick slices and incubated for 2h at RT in PBS containing 10% normal goat serum (Jackson Immuno research 005-000-121) and 1% Triton-X 100 (Sigma-Aldrich T8787). Subsequently, brain slices were washed with PBS and incubated with the primary antibody for GABA dilution 1:1000 (Sigma A2052) or CamKII dilution 1:75 (Abcam ab52476) in PBS containing 5% normal goat serum and 0.1% Triton-X 100 at 4°C overnight. On the next day the incubation was continued for 1h at RT. Afterwards the slices were washed 3 X 10min with PBS and incubated with the secondary antibody Dye-Light 549 goat anti rabbit IgG (Thermo Scientific 35507) dilution 1:1000 in PBS

Manuscript II

containing 5% normal goat serum and 0.1% Triton-X 100 at RT for 2h. To counter stain for NeuN positive cells a primary NeuN antibody (Millipore MAB377) was conjugated with the Zenon Labelling kit (Molecular Probes Z-25013) following the manufacturers protocol and added at a dilution of 1:100 to the secondary antibody mixture. After 2h the slices were washed 3 X 10min with PBS, post fixed for 15min with 4% PFA, again washed 2 X 10min with PBS and mounted on cover slips. The slides were imaged on a confocal laser scanning microscope (Zeiss).

Fos staining: Directly after the *in vivo* calcium imaging session mice were transcardially perfused with 20ml PBS containing 10U/ml Heparin (Sigma H3393) and 20ml 4% PFA. The brains were removed and post-fixed for 45min in 4%PFA. Next, brains were embedded in low melting Agarose (Sigma A9793) and cut parallel to the imaging plane in to 70 μ m slices on a vibratome (VT-1000, Leica). Slices were incubated for 2h at RT in PBS containing 10% normal goat serum (Jackson Immuno research 005-000-121) and 1% Triton-X 100 (Sigma-Aldrich T8787). Afterwards brain slices were washed with PBS and incubated with the primary Fos antibody at a dilution of 1:1000 (Santa Cruz Biotechnology sc-52) in PBS containing 5% normal goat serum and 0.1% Triton-X 100 at 4oC overnight. On the next day the incubation was continued for 1h at RT. Subsequently, the slices were washed 3 X 10min with PBS and incubated with the secondary Alexa Fluor 647 goat anti rabbit IgG Antibody (Molecular Probes A-21244) dilution 1:1000 in PBS containing 5% normal goat serum and 0.1% Triton-X 100 at RT for 2h. Then the slices were washed 3 X 10min with PBS and mounted on cover slips. The slides were imaged on a confocal laser scanning microscope (Zeiss).

6.5.4 Generation of genetically modified mice

Thy1.2-PA-GFP::NLS lines: The Thy1.2 vector as described by (Caroni, 1997) was generously provided by Pico Caroni (Friedrich Miescher Institute for Biomedical Research, Basel). The PA-GFP::NLS fusion was cloned into the *Xho*I site of the Thy1.2 plasmid and the expression construct was recovered by *Pvu*II and *Eco*RI digestion. To generate transgenic mice the expression construct was injected in fertilized oocytes using standard techniques. The embryos were obtained from crosses between (C57BL6/J and CBA) F1 hybrids. Transgenic founders were identified using PCR with

Manuscript II

the following primers: Thy1fw (CTACCAGCTGGCTGACCTGTAG) which binds to the Thy1 sequence and PAGFPRV (CTTGTCGGCCATGATATAGACGTTG) which binds to the PA-GFP sequence. Positive founders were back-crossed to C57BL6/J mice and the expression pattern of the transgene was analyzed using immunohistochemistry as described above.

R26 PA-GFP::NLS mice: The pROSA26-1 targeting plasmid (Soriano, 1999) was used to generate the PA-GFP::NLS knock in mice. First the PA-GFP::NLS and the WPRE sequence were cloned into the PCCALL2 plasmid (Novak 2000) which contains the CAGGS promoter to generate PCCALL2-PA-GFP::NLS. The construct was cut using *Ascl* and *AsisI* and the resulting fragment was cloned into a modified pROSA26-1 plasmid to generate the final targeting construct. The construct contains the 5' and 3' homology arms, the CAGGS promoter, a betaGeo cassette flanked by loxP sites, the PA-GFP::NLS transgene and a WPRE sequence. The construct was linearized using *Acc65I* and electroporated into A9 129/B6 F1 hybrid ES cells, which were established from blastocysts isolated from C57BL6/J females mated to 129 males (Ohhata et al., 2011) using standard techniques. Neomycin resistant clones were screened by southern blot analysis with a probe which binds to the 5' arm. Positive ES cell clones were injected into C57BL6/J blastocysts. Highly chimeric mice were bred with C57BL6/J mice. Successful targeting of the R26 locus was verified by PCR and southern blotting.

6.5.5 Slice preparation

On a given day, one mouse was sacrificed by quick cervical dislocation, decapitated and the brain rapidly removed from the skull. The brain was then immersed (approximately for 1 minute) in ice-cold oxygenated (95% O₂ / 5% CO₂) dissection solution containing (in mM) 110 choline chloride, 25 NaHCO₃, 1.25 NaH₂PO₄, 2.5 KCl, 0.5 CaCl₂, 7 MgCl₂, 11.6 ascorbic acid, 3.1 pyruvic acid and 25 D-glucose (final pH ≈ 7.4). Two coronal cuts were made to remove a small anterior portion of the brain and the cerebellum, respectively. The brain was then fixed, anterior surface down, to the specimen plate using cyanoacrylate glue (Roti coll 1) and submerged quickly afterwards in the buffer tray filled with ice-cold oxygenated (95% O₂ / 5% CO₂) dissection solution

as previously. Acute coronal whole-brain slices (300 μm -thick) were made using a vibratome (Leica VT1200S, Germany) at a speed of 0.12 mm/second. Slices were then transferred to a resting chamber filled with standard artificial cerebrospinal fluid (ACSF) composed of (in mM) 118 NaCl, 2.5 KCl, 26.5 NaHCO₃, 1 NaH₂PO₄, 1 NaCl₂, 2 CaCl₂ and 20 D-glucose, aerated with 95% O₂/ 5% CO₂, for 30 minutes at a temperature of 33°C, and subsequently maintained at room temperature throughout the experiments.

6.5.6 Electrophysiology

One individual slice was transferred to a submerged slice recording chamber where it was gently immobilized by a silver grid with attached nylon mesh. The grid was placed parallel to the slice to prevent damaged of the dendritic trees that run parallel towards the pia. Before the beginning of the recordings, all slices were inspected for fluorescence (Olympus BX51WI upright microscope equipped with a 100-W power range mercury short-arc lamp (USHIO, Tokyo, Japan) and with infrared (IR) video microscopy and differential contrast optics) to determine the precise location of the previously labeled PA-GFP expressing neurons. GFP fluorescence was visualised with a mirror unit (U-MWIB3, Olympus) equipped with a blue excitation bandpass filter (460 – 495 nm) via a water immersion objective (40x/0,8NA, Olympus). Whole-cell patch-clamp recordings in current-clamp mode were acquired from the somata of the identified fluorescence neurons with Multiclamp 700B amplifiers (Axon Instruments, Molecular Devices, Foster City, CA). Patch pipettes were pulled from borosilicate glass (2.0mm outer and 1.16mm inner diameter glass, Warner Instruments) on a Flaming/Brown micropipette puller (Sutter Instrument, Novato, CA), yielding a final resistance of 3 – 5 M Ω . The pipette intracellular solution contained (in mM) 130 K-gluconate, 5 KCl, 2.5 MgCl₂, 10 HEPES, 0.6 EGTA, 4 Na₂ATP, 0.4 Na₃GTP and 10 Na₂-phosphocreatine (pH = 7.25 adjusted with KOH; 290 mOsm). To characterize the pattern of neuronal action potential firing, a series of 500 ms current pulses were applied in 20 pA steps, from -40 to 340 pA. Electrophysiological data was low-pass filtered using the 10 and 3kHz four-pole Bessel filter, sampled at 10kHz (Digidata 1440A, Axon Instruments) and collected using pClamp10 software (Molecular Devices, Inc., USA). Offline analysis of intrinsic

neuronal properties was made using the data analysis software Clampfit 10.2 (Molecular Devices, Inc., USA). All the recordings were made at room temperature.

6.5.7 *In vivo* imaging

Surgery: Thy1.2-PA-GFP::NLS or R26 PA-GFP::NLS mice in the age of 8 – 12 weeks were used for the imaging experiments. All experiments were performed in accordance with the Austrian laboratory animal law guidelines for animal research and had been approved by the Viennese Magistratsabteilung 58 (Approval #: M58 / 02182 / 2007 /11; M58 / 02063 / 2008 /8). To obtain optical access to the auditory cortex a small imaging window was implanted over the auditory cortex as described elsewhere (Loewenstein et al., 2011).

***In vivo* imaging:** *In vivo* calcium imaging and photoactivation was done using an Ultima *in vivo* multiphoton microscopy system (Prairie Technologies) with a 20x objective lens (XLUMPlan FI, n.a.=0.95, Olympus) and a Ti: Sapphire multiphoton laser (Coherent). Mice were anesthetized with Isoflurane and photoactivation was performed at 750nm and imaging of the photolabeled neurons at 950nm.

Time course: Positions of single neurons were identified based on their weak basal fluorescence. Next, a ROI was placed over the soma of the neurons and the neurons were photolabeled. Photolabeled neurons were revisited and imaged at different time points. For analysis, images were background subtracted and the fluorescence of the individual neurons was normalized to the fluorescence level directly measured after photolabeling.

Reactivation: Single neurons were photolabeled and revisited after 24h. After measuring their fluorescence they were photolabeled and again revisited after 24 hours. For analysis, images were background subtracted and the fluorescence was normalized to the fluorescence level measured directly after photolabeling.

Filling of neurons: Single neurons were consecutively photolabeled 3 times at an interval of 15minutes. Subsequently, image stacks were taken from the photolabeled neurons and the dendritic morphology was reconstructed using IMARIS software (Bitplane, Switzerland).

Manuscript II

In vivo Ca imaging: A wide craniotomy (~ 1x2 mm) was performed above the right auditory cortex under isoflurane anesthesia (1.5 to 2%). Dye preparation and injection were done according to standard procedure (Garaschuk et al., 2006). The calcium sensitive dyes Rhod2-AM or Oregon Green BAPTA 1 (OGB1) were dissolved in DMSO and 20% Pluronic acid to a concentration of 2.5 mM or 10 mM respectively. This stock solution was diluted 1/10 into the pipette solution (150 mM NaCl, 2.5 mM KCl and 10 mM HEPES) to be pressure ejected (0.7 bar: 10 pulses of 10 sec) in the brain through a thin glass pipette (~ 5 M Ω tip resistance) using a Femtojet (Eppendorf). Injections were performed at several loci to increase the coverage of the auditory cortex. The craniotomy was then closed with a thin cover glass and sealed with dental cement (Ortho-Jet, Lang Dental). A metal post was also implanted on the head for fixation of the animal in the imaging apparatus and kept under light isoflurane anesthesia (1%).

Fields of stained neurons were imaged using a two-photon microscope (Ultima IV, Prairie Technologies) equipped with a 20x objective (XLUMPlan FI, n.a.=0.95, Olympus). Rhod2-AM and OGB1 were excited at 900 nm and 950 nm respectively using a pulsed laser (Chameleon Ultra, Coherent). In all experiments, the field of view was set to be 200x200 μ m. Neurons were detected on an initial image of the field of view using a semi-automated method implemented in a custom-built Matlab (The Mathworks) software. The image (512x512 pixel) was band passed filtered (Gaussian: high cut 6.5 pixels, low cut 30 pixels) and local maxima of intensity were detected as putative neurons. Then detection errors and astrocytes were removed by the user based on their morphology. The line scan trajectory was computed to cover all user-confirmed neurons with a minimal displacement (approximate solution of the travelling salesman problem obtained by a genetic algorithm). A ~ 2 μ m-wide cross corresponding to an added travel length of ~10 μ m was drawn on each neuron to increase the dwell time of the line scan on neurons with respect to neuropile. This allowed us to increase the signal to noise ratio of neuronal recordings. The fluorescence from any given neuron was the average signal from all segments of the line scan that were within 3.5 μ m from

Manuscript II

its center. Line scans rate was between 33 to 25 lines/seconds, depending on the number of recorded neurons.

All recordings consisted of 8 blocks of 15 seconds separated by a minimum of two seconds. The normalized change in calcium fluorescence $\Delta F/F$ was computed in each block. The selection of most or least active neurons was based on the following analysis. To gain temporal precision, the real time course of the neuronal firing rate was evaluated by deconvolution (Yaksi and Friedrich, 2006) of a single exponential kernel with a single time constant $\tau = 1.3$ sec corresponding to the typical decay time of calcium transient for both Rhod-2 and OGB1. The mean population activity was computed as the deconvolved calcium signals averaged across all simultaneously recorded neurons. Bursts of population activity were detected as peaks of the mean population activity that were 3 standard deviations above the mean. A 250 ms time bin centered on the peak of each burst was defined and the relative change of $\Delta F/F$ during this time bin was computed for each neuron as a surrogate of its spiking activity. The mean activity of each neuron was computed as the mean $\Delta F/F$ change across all detected bursts. This measure was used to rank the neurons and select the 20 % most or least active neurons for photoactivation.

Analysis of Fos expression levels: PA-GFP labeled neurons were identified in the fixed slices and a z-stack containing the neurons was taken. Additionally, the labeled neurons were registered to a stack that was taken *in vivo* after the labeling and the scan line was superimposed. This procedure confirmed the high fidelity of the photolabeling procedure. On the image plane containing the photolabeled neurons the fluorescence of all Fos positive cells was measured: for each cell a standardized, round ROI was manually positioned on the soma and the mean fluorescence calculated using ImageJ. The values for a given image plane (47-231 cells) were standardized using their z-score to compensate for possible differences in global staining intensity. If a given photolabeled neuron did not give a detectable Fos signal, the ROI for this cell was positioned using the PA-GFP signal.

6.6 Acknowledgements

We thank Pico Caroni (FMI Basel) for the Thy1.2 plasmid and Ulli Elling (IMBA Wien) for the modified Rosa26 targeting plasmids. We thank Eva Wiedemann for excellent technical assistance and Anita Helm and Andreas Bichl for maintaining our mouse colony. Furthermore, we would like to thank Wulf Haubensak for critical reading of the manuscript and all Rumpel group members for helpful discussions. This work was supported by the Austrian Science Fund (FWF): P21930-B09 (M.P.), HFSP long-term fellowship (B.B.), GABBA PhD program (B.F.) and the Boehringer Ingelheim GmbH.

7. General discussion

In this thesis we tested if immediate early genes which are widely used as post hoc markers for active neurons could be utilized to label neurons based on their activity. We used auditory cued fear conditioning which is a well described behavior paradigm for associative learning (Maren, 2001) and monitored the expression of the two most widely used immediate early genes *c-fos* and *Arc* in the auditory cortex of mice after the acquisition of this fear memory. We found that freezing behavior is selective to the paired condition and that AFC to certain complex sounds is dependent on the ACx. Furthermore, that IEG expression is strongly upregulated in the ACx after behavior manipulation but this upregulation is not specific to the paired condition and could be observed in all behavior paradigms containing a shock. These results indicate that IEG driven expression of a reporter gene will most likely not differentially label neurons that are engaged in a specific task from neurons which were activated by other modalities or spontaneous activity. Therefore, we tested an alternative approach that relies on photoactivatable proteins. We generated mice that express PA-GFP and found that these mice can be used to conditionally label individual neurons *in vivo* for many hours which greatly facilitates their re-identification. Photolabeling can be combined with functional calcium imaging which allows a further analysis of *in vivo* characterized neurons. We demonstrated this by correlating spontaneous activity in the auditory cortex under basal conditions with an immunohistochemical detection of the IEG *c-fos* on a single cell level.

7.1.1 The auditory cortex is necessary for auditory cued fear conditioning to complex sounds.

The contribution of primary cortical areas to the processing of fear memories is still a matter of debate because auditory information can reach the lateral amygdala, via a direct thalamo-amygdala or an indirect thalamo-cortical-amygdala pathway. It was shown that if simple pure tones are used for fear conditioning either one of these pathways is sufficient for the acquisition of the fear memory (Romanski and LeDoux,

General discussion

1992) and mice are able to learn this paradigm without the ACx (Song et al., 2010). One general notion is that the direct pathway is important for the rapid acquiring of fear memories and that the cortical pathway is used for the discrimination of more complex sounds (Fanselow and Poulos, 2005). Recent studies showed that lesioning the ACx after AFC leads to memory deficits because it attenuates the fear response to the sound (Boatman and Kim, 2006). Furthermore, pretraining lesions affect the learning of a discrimination task if complex sounds are used instead of pure tones (Ohl et al., 1999). We reasoned that complex sounds should resemble more faithfully the sounds mice encounter in their natural environment. Similar to previous reports (Song et al., 2010; Johansen et al., 2011) we found strong and robust freezing responses in mice after presentation of a previously conditioned sound. Is this memory formation depended on the auditory cortex? Pre-training lesions of the ACx lead to an attenuation of the fear response in half of the tested sounds. This is in accordance to a recent study where silencing the ACx during AFC to a complex sound also lead to significant decrease of freezing during the memory test (Letzkus et al., 2011). As expected, sham operated animals showed normal freezing to the CS. ACx lesions could have a general non-specific effect which is not related to memory formation. However, lesioned mice could be retrained to pure tones which is consistent with earlier findings (Romanski and LeDoux, 1992) arguing against this hypothesis. Our results show that the ACx plays an important role during the acquisition of the fear memory but it could also be important for memory storage or memory retrieval. Future experiments where the ACx is inhibited by muscimol during the memory test session would be necessary to answer this question. Surprisingly, we found that fear conditioning was only ACx depended in half of the tested complex sounds and learning of these other sounds could be mediated via the direct thalamo-amygdala pathway. This result raises the question what makes a sound a complex sound and what are the differences between them. We only tested a limited set of sounds (10) and could not find obvious spectro-temporal differences between them. Tests with a broader set of different sounds would be necessary to answer this question.

General discussion

7.1.2 Immediate early genes show strong upregulation after AFC

Fear conditioning to a complex sound was specific to the paired conditioning because only in this paradigm we detected a significant increase in freezing during the memory test. How are these behavioral results reflected on the level of gene expression? We found strong induction of *c-fos* and *Arc* after paired auditory cued fear conditioning. This was expected because other groups also reported strong IEG inductions after various behavioral treatments (Bertaina and Destrade, 1995; Milanovic et al., 1998; Guzowski et al., 2001; Huff et al., 2006; Shires and Aggleton, 2008; Mamiya et al., 2009; Carpenter-Hyland et al., 2010; Rapanelli et al., 2010; Zhang et al., 2011) including AFC (Radulovic et al., 1998). We also found a dissociation of IEG expression and freezing behavior because IEG expression in the ACx was strongly induced in the unpaired and the shock group which did not elicit freezing during the memory test. Because we observed that known IEGs report activity rather than learning of a specific association we decided to screen for potential learning specific genes. We reasoned that comparing the paired with the unpaired group should allow us to disassociate the learning event from other unspecific events because both groups receive the same amount of tone and shock presentation however only in the paired group a specific memory is formed. Again we found strong induction of *c-fos* and *Arc* only in paradigms containing shocks similar to our qPCR results. Additionally another hit of our screen was *zif-268* which is also known to be upregulated after behavior manipulation indicating that our microarray analysis is sensitive enough to detect behavioral induced changes in IEG expression. We did not find differentially expressed genes when we compared the paired and the unpaired group. This however should not mean that there are no genes which could be differentially expressed. It is still feasible that different subsets of neurons were activated specific to the learning event and these neurons therefore have a different expression profile. However, we do not detect this because the levels could be below the detection threshold of our microarray analysis. Methods like catFISH (Guzowski et al., 1999) that allow the detection of IEG expression of a cell at two different time points would be necessary to further make this distinction.

With both our methods we detected a marked increase of IEG expression only when mice received footshocks during the conditioning session. This raises the

General discussion

possibility that not only neuronal activity, but also other unrelated factors like stress (Cullinan et al., 1995; Ons et al., 2010) could induce IEG expression in the cortex. If IEG expression faithfully represents neuronal activity another intriguing hypothesis could be possible. Only paradigms that included shocks increased IEG expression which could indicate that also cross modal inputs like a painful stimulus could lead to neuronal activity in the ACx. Usually primary cortical areas only respond to their specific modality however studies in monkeys showed that ACx neurons can specifically fire to visual and somatosensory stimuli (Brosch et al., 2005; Lemus et al., 2010). Further it was shown that the pairing of visual stimuli with auditory stimuli can increase the acuity of responses in the ACx (Kayser et al., 2010). The most compelling evidence, however, comes from a study that shows that footshocks can activate neuronal responses in ACx neurons. The authors showed that footshocks alone lead to a disinhibition of L2/3 pyramidal cells in the ACx. This resulted in higher neuronal activity if the tone was paired with a footshock compared to the tone alone. This shock induced disinhibition and the convergence of tone and shock in the ACx could be essential for fear learning (Letzkus et al., 2011). The shock induced activity could therefore also account for the increase of IEG expression we observe in behavior paradigms that contain footshocks. It is also feasible that painful stimuli lead to a large unspecific brain activation which could result in a broad IEG expression. Therefore it would be necessary to also look at other primary cortical areas like the visual cortex after AFC. What could be the biological significance of this large, unspecific activation? In principle it is possible that it is a general arousal signal for the animal to be prepared for a specific situation. Taken together our results show that activity in primary cortical areas can be influenced by global events which originate from other modalities which could limit the use of IEGs to specifically label neurons.

7.1.3 Neuronal activity under basal conditions does not correlate with *c-fos* expression.

We previously found that IEG expression in the ACx could also be activated by painful stimuli. We next asked if basal neuronal activity *in vivo* correlates with *c-fos*

General discussion

expression at the single cell level. We used the PA-GFP mouse to combined functional *in vivo* calcium imaging with a histological detection of the IEG *c-fos*. Despite the fact that IEGs are extensively used as markers for active neurons, there is still little experimental evidence that single cells that have a higher neuronal activity indeed also have higher levels of *c-fos* expression. Until now only one study correlated Fos expression with neural activity. In this study a transgenic mouse was used that expresses GFP under the control of the *c-fos* promoter. If higher active neurons indeed show higher Fos levels this should be reflected on the GFP expression and therefore active neurons can be identified based on the GFP fluorescence. Yassin et al. used this mouse to identify active and non active neurons under basal conditions and recorded from these neurons. Indeed, they found on average that GFP positive neurons also show higher spontaneous firing rates, a bigger excitatory drive and also have a higher connection probability (Yassin et al., 2010). However, in this study the number of patched cells was low and only very few GFP positive neurons showed an increased firing rate compared to GFP negative neurons. Further, the selection of neurons was based on the GFP expression and activity levels were characterized afterward. This could lead to a selection bias because only highly labeled neurons were selected. Also, Fos expression was not assayed directly and it is possible that the GFP expression in the transgenic mouse is different from the Fos expression from the endogenous locus. Therefore, we used a complementary approach by using the PA-GFP mouse to correlate spontaneous activity levels with Fos expression levels. In contrast to the previous study we observed that neurons which were either selected for high spontaneous activity or low spontaneous activity under basal conditions had highly variable Fos expression levels and we further could not find significant differences in the population means of the two groups. However, the few highest Fos expressing neurons were also found in the highly active group. Eventually these neurons could be analogous to the few highly labeled neurons also in the previous study. This would imply that only a small fraction of highly active neurons which also show high levels of Fos expression are embedded in strongly interconnected subnetworks and further that additional unknown factors other than neuronal activity can also increase Fos expression in the ACx. Therefore, an interesting future experiment would be to label

General discussion

highly and weakly active neurons and combine this with a connectivity analysis afterwards. This would allow testing if higher active neurons indeed have a higher connectivity rate.

7.1.4 Applications of the PA-GFP::*NLS* mice

We think that the main applications of these mouse lines are experiments that require *in vivo* labeling and an unambiguous re-identification of the same cells *in vivo* and *in vitro*. One of the major applications of this mouse will be the combination of functional *in vivo* calcium imaging with electrophysiological recordings or histological stainings. We found that *in vivo* calcium imaging can be combined with photolabeling of single cells which could be a more specific alternative to cell labeling with IEGs. Further, repeated photolabeling at the soma reveals the basic dendritic morphology of the neuron. This could be helpful to gain a better understanding of the different cell types that form a functional neuronal assembly. These mouse lines could also be used to better understand the connectivity in neuronal assemblies. It has been shown that functional calcium imaging can be combined with *in vivo* electrophysiology (Rothschild et al., 2010) however this method can be difficult to implement and the throughput is low. One solution is to combine slice electrophysiology and computer guided reconstruction of neurons (Hofer et al., 2011; Ko et al., 2011). With this method many neurons are patched and then these neurons are registered back to the previously *in vivo* characterized neurons. This can lower the throughput because there is a chance that the patched cell was not of interest. We found that photolabeling can be combined with *in vivo* calcium imaging and labeled neurons can be readily identified in the slice preparation. Therefore photolabeling could be an alternative to the previously described method because it would greatly facilitate the re-identification of *in vivo* characterized neurons. Indeed, it has been shown previously in the visual cortex that it is possible to combine a functional characterization with photolabeling and slice electrophysiology (Lien and Scanziani, 2011). The PA-GFP::*NLS* mice could also facilitate experiments that allow us to better understand how the expression pattern of a given cell determines its function in a neuronal circuit. Therefore, *in vivo* calcium imaging and photolabeling

General discussion

could be combined with a detailed histological analysis or also with microdissection of neuronal tissue to assess the expression profile of single neurons (Citri et al., 2012) or populations of neurons (Sugino et al., 2006). Photolabeling is not restricted to the *in vivo* preparation. We were able to photolabel neurons *in vitro* in the slice preparation which also revealed dendritic and axonal projections and could therefore be used to guide the patching of dendrites. Further, it could be a fast alternative approach to biocytine filling because no immunohistological detection is necessary to visualize the neuron. However, we were not able to detect dendritic spines which are usually visible when biocytine is used (Campbell et al., 2005).

Using the PA-GFP::NLS mice to photolabel neurons also has some limitations. We could reliably revisit cells up to 20 hours after photolabeling. This limits the time for an experiment to about one day and some experiments which require a longer or a permanent label are not possible. We found that the biggest factor of this fluorescence loss is the diffusion of photoactivated PA-GFP out of the soma. Therefore, a tighter localization of PA-GFP to the nucleus would be advantageous. Fusing PA-GFP to the histone protein H2B (Hadjantonakis and Papaioannou, 2004) should result in a much longer labeling lifetime because PA-GFP gets incorporated into the chromatin and cannot diffuse into the dendrites. Recently, it has been reported that overexpression of a H2B::PA-GFP fusion from a viral vector allowed to revisit the neurons up to 7 days after photolabeling (Lien and Scanziani, 2011). The viral approach could also lead to higher expression levels because multiple copies of the transgene are expressed in the same cell. Still, it would be feasible to generate mice that express a H2B::PA-GFP fusion because this would eliminate the need of injecting a virus and would further eliminate differences in the expression. One disadvantage of this approach, however, is that axonal and dendritic labeling would not be possible anymore.

So far only one color is available for photolabeling. Having multiple colors would make the photolabeling approach more flexible and if the activation spectra of two proteins are far enough apart would even allow to label different cell populations with different colors. Until now two mice that express the green to red photoswitchable protein Kaede (Tomura et al., 2008) or KikGr (Nowotschin and Hadjantonakis, 2009)

General discussion

have been reported. However, Kaede and KikGr are can be difficult to photoswitch using two-photon excitation (own observation) and (Hatta et al., 2006; Watanabe et al., 2007; Brown et al., 2010). Further these proteins occupy two color channels which could make it more difficult to combine them with a calcium dye. At the moment the most widely used calcium dyes and genetically encoded calcium indicators are green and have therefore similar spectral characteristics as PA-GFP. We tried to temporally separate the PA-GFP fluorescence signal from the green calcium dye OGB1-AM however this was not possible because we still detected a strong green OGB1-AM fluorescence after two days. In our study we used the red calcium dye Rhod2 because it can be imaged at a wavelength where PA-GFP is not efficiently photoactivated. This allowed us to spectrally unmix these two signals but we also found that this dye is more difficult to use for bulk loading neurons compared to OGB1-AM. However, there is a constant development of new red photoactivatable proteins like PAmCherry (Subach et al., 2009) or PSTagRFP (Subach et al., 2010) that could potentially be combined with green calcium indicators. Further a genetically encoded red calcium indicator (Zhao et al., 2011) has been reported recently and could be used in the PA-GFP mouse.

In the Thy1.2-PA-GFP::NLS mouse lines we found that not all of the cells express PA-GFP. We characterized and selected two mouse lines which have a broad expression in the cortex however we were not able to photolabel all the neurons *in vivo*. In the ideal mouse all neurons of a specific class should express PA-GFP. This could be achieved by generating more transgenic lines because all founders have a different expression pattern due to the context dependency of the expression cassette. However one has to screen many lines and it is not guaranteed to obtain a line for every neuronal class. Therefore, we generated conditional Rosa26 knock-in mice that express PA-GFP::NLS from a strong ubiquitous promoter. This strategy allowed us maximize PA-GFP expression in all tissues. The PA-GFP::NLS expression pattern in this line is dependent on the efficiency of the Cre recombinase and we found strong expression after crossing these mice with Cre driver lines. The amount of neuronal classes that can express the transgene is limited by the availability of Cre driver lines. Nevertheless Cre driver lines to target excitatory neurons like the CamKII-Cre (Tsien et al., 1996b) line or for inhibitory interneurons like the GAD2-Cre (Taniguchi et al., 2011) line are available

General discussion

and can be crossed with the R26 PAGFP::NLS mice. Alternatively injections with viruses expressing Cre under a certain neuronal specific promoter are possible. In the R26 PAGFP::NLS line one has to keep in mind that the expression strength of the PAGFP could be lower compared to the Thy1.2 transgenic lines because only a single copy of the transgene is present in each cell.

In this study we demonstrated that the mouse lines we generated can be used to link *in vivo* activity of neurons with a subsequent histological or electrophysiological analysis. We think that these mice could be useful tools to better understand the functional principles of neuronal networks and the emergence of neuronal activity patterns in the cortex. Applications of these mouse lines are not restricted to the neuroscience field. Especially the knock-in mouse, that allows PA-GFP expression in most tissues of the body, should be useful and possible applications could arise in the fields of developmental biology, immunology, hematology or cancer research in which populations of cells have to be labeled at a specific time point and their spread has to be followed using microscopy or potentially FACS.

References

8. References

- Abraham WC, Mason SE, Demmer J, Williams JM, Richardson CL, Tate WP, Lawlor PA, Dragunow M (1993) Correlations between immediate early gene induction and the persistence of long-term potentiation. *Neuroscience* 56:717-727.
- Ando R, Hama H, Yamamoto-Hino M, Mizuno H, Miyawaki A (2002) An optical marker based on the UV-induced green-to-red photoconversion of a fluorescent protein. *Proc Natl Acad Sci U S A* 99:12651-12656.
- Antunes R, Moita MA (2010) Discriminative auditory fear learning requires both tuned and nontuned auditory pathways to the amygdala. *J Neurosci* 30:9782-9787.
- Anwyl R (2009) Metabotropic glutamate receptor-dependent long-term potentiation. *Neuropharmacology* 56:735-740.
- Bakin JS, Weinberger NM (1990) Classical conditioning induces CS-specific receptive field plasticity in the auditory cortex of the guinea pig. *Brain Res* 536:271-286.
- Barth AL, Gerkin RC, Dean KL (2004) Alteration of neuronal firing properties after in vivo experience in a FosGFP transgenic mouse. *J Neurosci* 24:6466-6475.
- Bean BP (2007) The action potential in mammalian central neurons. *Nat Rev Neurosci* 8:451-465.
- Bertaina V, Destrade C (1995) Differential time courses of c-fos mRNA expression in hippocampal subfields following acquisition and recall testing in mice. *Brain Res Cogn Brain Res* 2:269-275.
- Bliss TV, Lomo T (1973) Long-lasting potentiation of synaptic transmission in the dentate area of the anaesthetized rabbit following stimulation of the perforant path. *J Physiol* 232:331-356.
- Boatman JA, Kim JJ (2006) A thalamo-cortico-amygdala pathway mediates auditory fear conditioning in the intact brain. *Eur J Neurosci* 24:894-900.
- Bock DD, Lee WC, Kerlin AM, Andermann ML, Hood G, Wetzel AW, Yurgenson S, Soucy ER, Kim HS, Reid RC (2011) Network anatomy and in vivo physiology of visual cortical neurons. *Nature* 471:177-182.
- Boyden ES, Zhang F, Bamberg E, Nagel G, Deisseroth K (2005) Millisecond-timescale, genetically targeted optical control of neural activity. *Nat Neurosci* 8:1263-1268.
- Branda CS, Dymecki SM (2004) Talking about a revolution: The impact of site-specific recombinases on genetic analyses in mice. *Dev Cell* 6:7-28.
- Briggman KL, Helmstaedter M, Denk W (2011) Wiring specificity in the direction-selectivity circuit of the retina. *Nature* 471:183-188.
- Brosch M, Selezneva E, Scheich H (2005) Nonauditory events of a behavioral procedure activate auditory cortex of highly trained monkeys. *J Neurosci* 25:6797-6806.
- Brown SC, Bolte S, Gaudin M, Pereira C, Marion J, Soler MN, Satiat-Jeunemaitre B (2010) Exploring plant endomembrane dynamics using the photoconvertible protein Kaede. *Plant J* 63:696-711.
- Campbell RE, Han SK, Herbison AE (2005) Biocytin filling of adult gonadotropin-releasing hormone neurons in situ reveals extensive, spiny, dendritic processes. *Endocrinology* 146:1163-1169.

References

- Caroni P (1997) Overexpression of growth-associated proteins in the neurons of adult transgenic mice. *J Neurosci Methods* 71:3-9.
- Carpenter-Hyland EP, Plummer TK, Vazdarjanova A, Blake DT (2010) Arc expression and neuroplasticity in primary auditory cortex during initial learning are inversely related to neural activity. *Proc Natl Acad Sci U S A* 107:14828-14832.
- Chudakov DM, Lukyanov S, Lukyanov KA (2007) Tracking intracellular protein movements using photoswitchable fluorescent proteins PS-CFP2 and Dendra2. *Nat Protoc* 2:2024-2032.
- Citri A, Pang ZP, Sudhof TC, Wernig M, Malenka RC (2012) Comprehensive qPCR profiling of gene expression in single neuronal cells. *Nat Protoc* 7:118-127.
- Coan EJ, Collingridge GL (1987) Characterization of an N-methyl-D-aspartate receptor component of synaptic transmission in rat hippocampal slices. *Neuroscience* 22:1-8.
- Corish P, Tyler-Smith C (1999) Attenuation of green fluorescent protein half-life in mammalian cells. *Protein Eng* 12:1035-1040.
- Cullinan WE, Herman JP, Battaglia DF, Akil H, Watson SJ (1995) Pattern and time course of immediate early gene expression in rat brain following acute stress. *Neuroscience* 64:477-505.
- de Felipe P, Luke GA, Hughes LE, Gani D, Halpin C, Ryan MD (2006) E unum pluribus: multiple proteins from a self-processing polyprotein. *Trends Biotechnol* 24:68-75.
- Dragunow M, Abraham WC, Goulding M, Mason SE, Robertson HA, Faull RL (1989) Long-term potentiation and the induction of c-fos mRNA and proteins in the dentate gyrus of unanesthetized rats. *Neurosci Lett* 101:274-280.
- Eferl R, Wagner EF (2003) AP-1: a double-edged sword in tumorigenesis. *Nat Rev Cancer* 3:859-868.
- Eguchi M, Yamaguchi S (2009) In vivo and in vitro visualization of gene expression dynamics over extensive areas of the brain. *Neuroimage* 44:1274-1283.
- Emmert-Buck MR, Bonner RF, Smith PD, Chuaqui RF, Zhuang Z, Goldstein SR, Weiss RA, Liotta LA (1996) Laser capture microdissection. *Science* 274:998-1001.
- Fanselow MS, Poulos AM (2005) The neuroscience of mammalian associative learning. *Annu Rev Psychol* 56:207-234.
- Feng G, Mellor RH, Bernstein M, Keller-Peck C, Nguyen QT, Wallace M, Nerbonne JM, Lichtman JW, Sanes JR (2000) Imaging neuronal subsets in transgenic mice expressing multiple spectral variants of GFP. *Neuron* 28:41-51.
- Fleischmann A, Hvalby O, Jensen V, Strekalova T, Zacher C, Layer LE, Kvello A, Reschke M, Spanagel R, Sprengel R, Wagner EF, Gass P (2003) Impaired long-term memory and NR2A-type NMDA receptor-dependent synaptic plasticity in mice lacking c-Fos in the CNS. *J Neurosci* 23:9116-9122.
- Fries P, Nikolic D, Singer W (2007) The gamma cycle. *Trends Neurosci* 30:309-316.
- Fritz J, Shamma S, Elhilali M, Klein D (2003) Rapid task-related plasticity of spectrotemporal receptive fields in primary auditory cortex. *Nat Neurosci* 6:1216-1223.
- Gall CM, Hess US, Lynch G (1998) Mapping brain networks engaged by, and changed by, learning. *Neurobiol Learn Mem* 70:14-36.
- Garaschuk O, Milos RI, Konnerth A (2006) Targeted bulk-loading of fluorescent indicators for two-photon brain imaging in vivo. *Nat Protoc* 1:380-386.

References

- Gong S, Doughty M, Harbaugh CR, Cummins A, Hatten ME, Heintz N, Gerfen CR (2007) Targeting Cre recombinase to specific neuron populations with bacterial artificial chromosome constructs. *J Neurosci* 27:9817-9823.
- Gong S, Zheng C, Doughty ML, Losos K, Didkovsky N, Schambra UB, Nowak NJ, Joyner A, Leblanc G, Hatten ME, Heintz N (2003) A gene expression atlas of the central nervous system based on bacterial artificial chromosomes. *Nature* 425:917-925.
- Gorski JA, Talley T, Qiu M, Puelles L, Rubenstein JL, Jones KR (2002) Cortical excitatory neurons and glia, but not GABAergic neurons, are produced in the *Emx1*-expressing lineage. *J Neurosci* 22:6309-6314.
- Grinevich V, Kollekter A, Eliava M, Takada N, Takuma H, Fukazawa Y, Shigemoto R, Kuhl D, Waters J, Seeburg PH, Osten P (2009) Fluorescent Arc/Arg3.1 indicator mice: a versatile tool to study brain activity changes in vitro and in vivo. *J Neurosci Methods* 184:25-36.
- Gurskaya NG, Verkhusha VV, Shcheglov AS, Staroverov DB, Chepurnykh TV, Fradkov AF, Lukyanov S, Lukyanov KA (2006) Engineering of a monomeric green-to-red photoactivatable fluorescent protein induced by blue light. *Nat Biotechnol* 24:461-465.
- Guzowski JF, McNaughton BL, Barnes CA, Worley PF (1999) Environment-specific expression of the immediate-early gene *Arc* in hippocampal neuronal ensembles. *Nat Neurosci* 2:1120-1124.
- Guzowski JF, Setlow B, Wagner EK, McGaugh JL (2001) Experience-dependent gene expression in the rat hippocampus after spatial learning: a comparison of the immediate-early genes *Arc*, *c-fos*, and *zif268*. *J Neurosci* 21:5089-5098.
- Guzowski JF, Lyford GL, Stevenson GD, Houston FP, McGaugh JL, Worley PF, Barnes CA (2000) Inhibition of activity-dependent *arc* protein expression in the rat hippocampus impairs the maintenance of long-term potentiation and the consolidation of long-term memory. *J Neurosci* 20:3993-4001.
- Habuchi S, Ando R, Dedecker P, Verheijen W, Mizuno H, Miyawaki A, Hofkens J (2005) Reversible single-molecule photoswitching in the GFP-like fluorescent protein Dronpa. *Proc Natl Acad Sci U S A* 102:9511-9516.
- Hadjantonakis AK, Papaioannou VE (2004) Dynamic in vivo imaging and cell tracking using a histone fluorescent protein fusion in mice. *BMC Biotechnol* 4:33.
- Hall J, Thomas KL, Everitt BJ (2001) Fear memory retrieval induces CREB phosphorylation and Fos expression within the amygdala. *Eur J Neurosci* 13:1453-1458.
- Hatta K, Tsujii H, Omura T (2006) Cell tracking using a photoconvertible fluorescent protein. *Nat Protoc* 1:960-967.
- Haubensak W, Kunwar PS, Cai H, Ciocchi S, Wall NR, Ponnusamy R, Biag J, Dong HW, Deisseroth K, Callaway EM, Fanselow MS, Luthi A, Anderson DJ (2010) Genetic dissection of an amygdala microcircuit that gates conditioned fear. *Nature* 468:270-276.
- Hebb DO (1949) *The organization of behavior; a neuropsychological theory*. New York,: Wiley.
- Heil P (2004) First-spike latency of auditory neurons revisited. *Curr Opin Neurobiol* 14:461-467.

References

- Henderson JN, Gepshtein R, Heenan JR, Kallio K, Huppert D, Remington SJ (2009) Structure and mechanism of the photoactivatable green fluorescent protein. *J Am Chem Soc* 131:4176-4177.
- Herry C, Ciocchi S, Senn V, Demmou L, Muller C, Luthi A (2008) Switching on and off fear by distinct neuronal circuits. *Nature* 454:600-606.
- Hofer SB, Ko H, Pichler B, Vogelstein J, Ros H, Zeng H, Lein E, Lesica NA, Mrsic-Flogel TD (2011) Differential connectivity and response dynamics of excitatory and inhibitory neurons in visual cortex. *Nat Neurosci* 14:1045-1052.
- Hromadka T, Deweese MR, Zador AM (2008) Sparse representation of sounds in the unanesthetized auditory cortex. *PLoS Biol* 6:e16.
- Hubel DH, Wiesel TN (1968) Receptive fields and functional architecture of monkey striate cortex. *J Physiol* 195:215-243.
- Huff NC, Frank M, Wright-Hardesty K, Sprunger D, Matus-Amat P, Higgins E, Rudy JW (2006) Amygdala regulation of immediate-early gene expression in the hippocampus induced by contextual fear conditioning. *J Neurosci* 26:1616-1623.
- Inoue N, Nakao H, Migishima R, Hino T, Matsui M, Hayashi F, Nakao K, Manabe T, Aiba A, Inokuchi K (2009) Requirement of the immediate early gene *vesl-1S/homer-1a* for fear memory formation. *Mol Brain* 2:7.
- Johansen JP, Cain CK, Ostroff LE, LeDoux JE (2011) Molecular mechanisms of fear learning and memory. *Cell* 147:509-524.
- Johnson RS, Spiegelman BM, Papaioannou V (1992) Pleiotropic effects of a null mutation in the *c-fos* proto-oncogene. *Cell* 71:577-586.
- Jones MW, Errington ML, French PJ, Fine A, Bliss TV, Garel S, Charnay P, Bozon B, Laroche S, Davis S (2001) A requirement for the immediate early gene *Zif268* in the expression of late LTP and long-term memories. *Nat Neurosci* 4:289-296.
- Kalderon D, Roberts BL, Richardson WD, Smith AE (1984) A short amino acid sequence able to specify nuclear location. *Cell* 39:499-509.
- Karin M, Liu Z, Zandi E (1997) AP-1 function and regulation. *Curr Opin Cell Biol* 9:240-246.
- Kawashima T, Okuno H, Nonaka M, Adachi-Morishima A, Kyo N, Okamura M, Takemoto-Kimura S, Worley PF, Bito H (2009) Synaptic activity-responsive element in the *Arc/Arg3.1* promoter essential for synapse-to-nucleus signaling in activated neurons. *Proc Natl Acad Sci U S A* 106:316-321.
- Kayser C, Logothetis NK, Panzeri S (2010) Visual enhancement of the information representation in auditory cortex. *Curr Biol* 20:19-24.
- Kerlin AM, Andermann ML, Berezovskii VK, Reid RC (2010) Broadly tuned response properties of diverse inhibitory neuron subtypes in mouse visual cortex. *Neuron* 67:858-871.
- Kilgard MP, Merzenich MM (1998) Cortical map reorganization enabled by nucleus basalis activity. *Science* 279:1714-1718.
- Klausberger T, Marton LF, O'Neill J, Huck JH, Dalezios Y, Fuentealba P, Suen WY, Papp E, Kaneko T, Watanabe M, Csicsvari J, Somogyi P (2005) Complementary roles of cholecystinin- and parvalbumin-expressing GABAergic neurons in hippocampal network oscillations. *J Neurosci* 25:9782-9793.

References

- Ko H, Hofer SB, Pichler B, Buchanan KA, Sjöström PJ, Mrsic-Flogel TD (2011) Functional specificity of local synaptic connections in neocortical networks. *Nature* 473:87-91.
- Kuhlman SJ, Huang ZJ (2008) High-resolution labeling and functional manipulation of specific neuron types in mouse brain by Cre-activated viral gene expression. *PLoS One* 3:e2005.
- LeDoux J (2007) The amygdala. *Curr Biol* 17:R868-874.
- LeDoux JE (2000) Emotion circuits in the brain. *Annu Rev Neurosci* 23:155-184.
- LeDoux JE, Cicchetti P, Xagoraris A, Romanski LM (1990) The lateral amygdaloid nucleus: sensory interface of the amygdala in fear conditioning. *J Neurosci* 10:1062-1069.
- Lemus L, Hernandez A, Luna R, Zainos A, Romo R (2010) Do sensory cortices process more than one sensory modality during perceptual judgments? *Neuron* 67:335-348.
- Letzkus JJ, Wolff SB, Meyer EM, Tovote P, Courtin J, Herry C, Luthi A (2011) A disinhibitory microcircuit for associative fear learning in the auditory cortex. *Nature* 480:331-335.
- Lien AD, Scanziani M (2011) In vivo Labeling of Constellations of Functionally Identified Neurons for Targeted in vitro Recordings. *Front Neural Circuits* 5:16.
- Lima SQ, Hromádka T, Znamenskiy P, Zador AM (2009) PINP: a new method of tagging neuronal populations for identification during in vivo electrophysiological recording. *PLoS One* 4:e6099.
- Lin D, Boyle MP, Dollar P, Lee H, Lein ES, Perona P, Anderson DJ (2011) Functional identification of an aggression locus in the mouse hypothalamus. *Nature* 470:221-226.
- Link W, Konietzko U, Kauselmann G, Krug M, Schwanke B, Frey U, Kuhl D (1995) Somatodendritic expression of an immediate early gene is regulated by synaptic activity. *Proc Natl Acad Sci U S A* 92:5734-5738.
- Lippincott-Schwartz J, Patterson GH (2009) Photoactivatable fluorescent proteins for diffraction-limited and super-resolution imaging. *Trends Cell Biol* 19:555-565.
- Loewenstein Y, Kuras A, Rumpel S (2011) Multiplicative dynamics underlie the emergence of the log-normal distribution of spine sizes in the neocortex in vivo. *J Neurosci* 31:9481-9488.
- Luo H, Nakatsu F, Furuno A, Kato H, Yamamoto A, Ohno H (2006) Visualization of the post-Golgi trafficking of multiphoton photoactivated transferrin receptors. *Cell Struct Funct* 31:63-75.
- Luo L, Callaway EM, Svoboda K (2008) Genetic dissection of neural circuits. *Neuron* 57:634-660.
- Lyford GL, Yamagata K, Kaufmann WE, Barnes CA, Sanders LK, Copeland NG, Gilbert DJ, Jenkins NA, Lanahan AA, Worley PF (1995) Arc, a growth factor and activity-regulated gene, encodes a novel cytoskeleton-associated protein that is enriched in neuronal dendrites. *Neuron* 14:433-445.
- Lynch MA (2004) Long-term potentiation and memory. *Physiol Rev* 84:87-136.
- Madisen L, Zwingman TA, Sunkin SM, Oh SW, Zariwala HA, Gu H, Ng LL, Palmiter RD, Hawrylycz MJ, Jones AR, Lein ES, Zeng H (2010) A robust and high-throughput

References

- Cre reporting and characterization system for the whole mouse brain. *Nat Neurosci* 13:133-140.
- Malenka RC, Nicoll RA (1999) Long-term potentiation--a decade of progress? *Science* 285:1870-1874.
- Malenka RC, Kauer JA, Zucker RS, Nicoll RA (1988) Postsynaptic calcium is sufficient for potentiation of hippocampal synaptic transmission. *Science* 242:81-84.
- Mamiya N, Fukushima H, Suzuki A, Matsuyama Z, Homma S, Frankland PW, Kida S (2009) Brain region-specific gene expression activation required for reconsolidation and extinction of contextual fear memory. *J Neurosci* 29:402-413.
- Man PS, Wells T, Carter DA (2007) Egr-1-d2EGFP transgenic rats identify transient populations of neurons and glial cells during postnatal brain development. *Gene Expr Patterns* 7:872-883.
- Maren S (2001) Neurobiology of Pavlovian fear conditioning. *Annu Rev Neurosci* 24:897-931.
- Markram H, Toledo-Rodriguez M, Wang Y, Gupta A, Silberberg G, Wu C (2004) Interneurons of the neocortical inhibitory system. *Nat Rev Neurosci* 5:793-807.
- Marr D (1970) A theory for cerebral neocortex. *Proc R Soc Lond B Biol Sci* 176:161-234.
- Marshel JH, Mori T, Nielsen KJ, Callaway EM (2010) Targeting single neuronal networks for gene expression and cell labeling in vivo. *Neuron* 67:562-574.
- Milanovic S, Radulovic J, Laban O, Stiedl O, Henn F, Spiess J (1998) Production of the Fos protein after contextual fear conditioning of C57BL/6N mice. *Brain Res* 784:37-47.
- Molina AJ, Shirihai OS (2009) Monitoring mitochondrial dynamics with photoactivatable [corrected] green fluorescent protein. *Methods Enzymol* 457:289-304.
- Morgan JI, Cohen DR, Hempstead JL, Curran T (1987) Mapping patterns of c-fos expression in the central nervous system after seizure. *Science* 237:192-197.
- Mountcastle VB (1997) The columnar organization of the neocortex. *Brain* 120 (Pt 4):701-722.
- Niwa H, Yamamura K, Miyazaki J (1991) Efficient selection for high-expression transfectants with a novel eukaryotic vector. *Gene* 108:193-199.
- Novak A, Guo C, Yang W, Nagy A, Lobe CG (2000) Z/EG, a double reporter mouse line that expresses enhanced green fluorescent protein upon Cre-mediated excision. *Genesis* 28:147-155.
- Nowotschin S, Hadjantonakis AK (2009) Use of KikGR a photoconvertible green-to-red fluorescent protein for cell labeling and lineage analysis in ES cells and mouse embryos. *BMC Dev Biol* 9:49.
- Ohhata T, Senner CE, Hemberger M, Wutz A (2011) Lineage-specific function of the noncoding Tsix RNA for Xist repression and Xi reactivation in mice. *Genes Dev* 25:1702-1715.
- Ohki K, Chung S, Ch'ng YH, Kara P, Reid RC (2005) Functional imaging with cellular resolution reveals precise micro-architecture in visual cortex. *Nature* 433:597-603.
- Ohl FW, Wetzel W, Wagner T, Rech A, Scheich H (1999) Bilateral ablation of auditory cortex in Mongolian gerbil affects discrimination of frequency modulated tones but not of pure tones. *Learn Mem* 6:347-362.

References

- Okuno H (2011) Regulation and function of immediate-early genes in the brain: beyond neuronal activity markers. *Neurosci Res* 69:175-186.
- Ons S, Rotllant D, Marin-Blasco IJ, Armario A (2010) Immediate-early gene response to repeated immobilization: Fos protein and arc mRNA levels appear to be less sensitive than c-fos mRNA to adaptation. *Eur J Neurosci* 31:2043-2052.
- Orban PC, Chui D, Marth JD (1992) Tissue- and site-specific DNA recombination in transgenic mice. *Proc Natl Acad Sci U S A* 89:6861-6865.
- Pastalkova E, Itskov V, Amarasingham A, Buzsaki G (2008) Internally generated cell assembly sequences in the rat hippocampus. *Science* 321:1322-1327.
- Patterson GH, Lippincott-Schwartz J (2002) A photoactivatable GFP for selective photolabeling of proteins and cells. *Science* 297:1873-1877.
- Peng S, Zhang Y, Zhang J, Wang H, Ren B (2011) Glutamate receptors and signal transduction in learning and memory. *Mol Biol Rep* 38:453-460.
- Pinault D (1996) A novel single-cell staining procedure performed in vivo under electrophysiological control: morpho-functional features of juxtacellularly labeled thalamic cells and other central neurons with biocytin or Neurobiotin. *J Neurosci Methods* 65:113-136.
- Plath N et al. (2006) Arc/Arg3.1 is essential for the consolidation of synaptic plasticity and memories. *Neuron* 52:437-444.
- Portales-Casamar E et al. (2010) A regulatory toolbox of MiniPromoters to drive selective expression in the brain. *Proc Natl Acad Sci U S A* 107:16589-16594.
- Quirk GJ, Repa C, LeDoux JE (1995) Fear conditioning enhances short-latency auditory responses of lateral amygdala neurons: parallel recordings in the freely behaving rat. *Neuron* 15:1029-1039.
- Quirk GJ, Armony JL, LeDoux JE (1997) Fear conditioning enhances different temporal components of tone-evoked spike trains in auditory cortex and lateral amygdala. *Neuron* 19:613-624.
- Radulovic J, Kammermeier J, Spiess J (1998) Relationship between fos production and classical fear conditioning: effects of novelty, latent inhibition, and unconditioned stimulus preexposure. *J Neurosci* 18:7452-7461.
- Rapanelli M, Lew SE, Frick LR, Zanutto BS (2010) Plasticity in the rat prefrontal cortex: linking gene expression and an operant learning with a computational theory. *PLoS One* 5:e8656.
- Reijmers LG, Perkins BL, Matsuo N, Mayford M (2007) Localization of a stable neural correlate of associative memory. *Science* 317:1230-1233.
- Rial Verde EM, Lee-Osbourne J, Worley PF, Malinow R, Cline HT (2006) Increased expression of the immediate-early gene arc/arg3.1 reduces AMPA receptor-mediated synaptic transmission. *Neuron* 52:461-474.
- Rogan MT, Staubli UV, LeDoux JE (1997) Fear conditioning induces associative long-term potentiation in the amygdala. *Nature* 390:604-607.
- Romanski LM, LeDoux JE (1992) Equipotentiality of thalamo-amygdala and thalamo-cortico-amygdala circuits in auditory fear conditioning. *J Neurosci* 12:4501-4509.
- Rothschild G, Nelken I, Mizrahi A (2010) Functional organization and population dynamics in the mouse primary auditory cortex. *Nat Neurosci* 13:353-360.
- Rumpel S, LeDoux J, Zador A, Malinow R (2005) Postsynaptic receptor trafficking underlying a form of associative learning. *Science* 308:83-88.

References

- Runyan CA, Schummers J, Van Wart A, Kuhlman SJ, Wilson NR, Huang ZJ, Sur M (2010) Response features of parvalbumin-expressing interneurons suggest precise roles for subtypes of inhibition in visual cortex. *Neuron* 67:847-857.
- Ruta V, Datta SR, Vasconcelos ML, Freeland J, Looger LL, Axel R (2010) A dimorphic pheromone circuit in *Drosophila* from sensory input to descending output. *Nature* 468:686-690.
- Sakata S, Harris KD (2009) Laminar structure of spontaneous and sensory-evoked population activity in auditory cortex. *Neuron* 64:404-418.
- Sato T, Takahoko M, Okamoto H (2006) HuC:Kaede, a useful tool to label neural morphologies in networks in vivo. *Genesis* 44:136-142.
- Sauer B (1987) Functional expression of the cre-lox site-specific recombination system in the yeast *Saccharomyces cerevisiae*. *Mol Cell Biol* 7:2087-2096.
- Shaner NC, Campbell RE, Steinbach PA, Giepmans BN, Palmer AE, Tsien RY (2004) Improved monomeric red, orange and yellow fluorescent proteins derived from *Discosoma* sp. red fluorescent protein. *Nat Biotechnol* 22:1567-1572.
- Sheng M, McFadden G, Greenberg ME (1990) Membrane depolarization and calcium induce c-fos transcription via phosphorylation of transcription factor CREB. *Neuron* 4:571-582.
- Shepherd JD, Rumbaugh G, Wu J, Chowdhury S, Plath N, Kuhl D, Huganir RL, Worley PF (2006) Arc/Arg3.1 mediates homeostatic synaptic scaling of AMPA receptors. *Neuron* 52:475-484.
- Shires KL, Aggleton JP (2008) Mapping immediate-early gene activity in the rat after place learning in a water-maze: the importance of matched control conditions. *Eur J Neurosci* 28:982-996.
- Silberberg G, Gupta A, Markram H (2002) Stereotypy in neocortical microcircuits. *Trends Neurosci* 25:227-230.
- Silberberg G, Grillner S, LeBeau FE, Maex R, Markram H (2005) Synaptic pathways in neural microcircuits. *Trends Neurosci* 28:541-551.
- Smeyne RJ, Schilling K, Robertson L, Luk D, Oberdick J, Curran T, Morgan JI (1992) fos-lacZ transgenic mice: mapping sites of gene induction in the central nervous system. *Neuron* 8:13-23.
- Song EY, Boatman JA, Jung MW, Kim JJ (2010) Auditory Cortex is Important in the Extinction of Two Different Tone-Based Conditioned Fear Memories in Rats. *Front Behav Neurosci* 4:24.
- Soriano P (1999) Generalized lacZ expression with the ROSA26 Cre reporter strain. *Nat Genet* 21:70-71.
- Steward O, Wallace CS, Lyford GL, Worley PF (1998) Synaptic activation causes the mRNA for the IEG Arc to localize selectively near activated postsynaptic sites on dendrites. *Neuron* 21:741-751.
- Stiel AC, Trowitzsch S, Weber G, Andresen M, Eggeling C, Hell SW, Jakobs S, Wahl MC (2007) 1.8 A bright-state structure of the reversibly switchable fluorescent protein Dronpa guides the generation of fast switching variants. *Biochem J* 402:35-42.
- Subach FV, Patterson GH, Renz M, Lippincott-Schwartz J, Verkhusha VV (2010) Bright monomeric photoactivatable red fluorescent protein for two-color super-resolution sptPALM of live cells. *J Am Chem Soc* 132:6481-6491.

References

- Subach FV, Patterson GH, Manley S, Gillette JM, Lippincott-Schwartz J, Verkhusha VV (2009) Photoactivatable mCherry for high-resolution two-color fluorescence microscopy. *Nature methods* 6:153-159.
- Sugino K, Hempel CM, Miller MN, Hattox AM, Shapiro P, Wu C, Huang ZJ, Nelson SB (2006) Molecular taxonomy of major neuronal classes in the adult mouse forebrain. *Nat Neurosci* 9:99-107.
- Tamamaki N, Yanagawa Y, Tomioka R, Miyazaki J, Obata K, Kaneko T (2003) Green fluorescent protein expression and colocalization with calretinin, parvalbumin, and somatostatin in the GAD67-GFP knock-in mouse. *J Comp Neurol* 467:60-79.
- Tang YP, Shimizu E, Dube GR, Rampon C, Kerchner GA, Zhuo M, Liu G, Tsien JZ (1999) Genetic enhancement of learning and memory in mice. *Nature* 401:63-69.
- Taniguchi H, He M, Wu P, Kim S, Paik R, Sugino K, Kvitsiani D, Fu Y, Lu J, Lin Y, Miyoshi G, Shima Y, Fishell G, Nelson SB, Huang ZJ (2011) A resource of Cre driver lines for genetic targeting of GABAergic neurons in cerebral cortex. *Neuron* 71:995-1013.
- Tian L, Hires SA, Mao T, Huber D, Chiappe ME, Chalasani SH, Petreanu L, Akerboom J, McKinney SA, Schreiter ER, Bargmann CI, Jayaraman V, Svoboda K, Looger LL (2009) Imaging neural activity in worms, flies and mice with improved GCaMP calcium indicators. *Nature methods* 6:875-881.
- Tomura M, Yoshida N, Tanaka J, Karasawa S, Miwa Y, Miyawaki A, Kanagawa O (2008) Monitoring cellular movement in vivo with photoconvertible fluorescence protein "Kaede" transgenic mice. *Proc Natl Acad Sci U S A* 105:10871-10876.
- Tronche F, Kellendonk C, Kretz O, Gass P, Anlag K, Orban PC, Bock R, Klein R, Schutz G (1999) Disruption of the glucocorticoid receptor gene in the nervous system results in reduced anxiety. *Nat Genet* 23:99-103.
- Tsien JZ, Huerta PT, Tonegawa S (1996a) The essential role of hippocampal CA1 NMDA receptor-dependent synaptic plasticity in spatial memory. *Cell* 87:1327-1338.
- Tsien JZ, Chen DF, Gerber D, Tom C, Mercer EH, Anderson DJ, Mayford M, Kandel ER, Tonegawa S (1996b) Subregion- and cell type-restricted gene knockout in mouse brain. *Cell* 87:1317-1326.
- Tsutsui H, Karasawa S, Shimizu H, Nukina N, Miyawaki A (2005) Semi-rational engineering of a coral fluorescent protein into an efficient highlighter. *EMBO reports* 6:233-238.
- van Thor JJ, Gensch T, Hellingwerf KJ, Johnson LN (2002) Phototransformation of green fluorescent protein with UV and visible light leads to decarboxylation of glutamate 222. *Nat Struct Biol* 9:37-41.
- Wang KH, Majewska A, Schummers J, Farley B, Hu C, Sur M, Tonegawa S (2006) In vivo two-photon imaging reveals a role of arc in enhancing orientation specificity in visual cortex. *Cell* 126:389-402.
- Wang X, Lu T, Snider RK, Liang L (2005) Sustained firing in auditory cortex evoked by preferred stimuli. *Nature* 435:341-346.
- Watanabe W, Shimada T, Matsunaga S, Kurihara D, Fukui K, Shin-Ichi Arimura S, Tsutsumi N, Isobe K, Itoh K (2007) Single-organelle tracking by two-photon conversion. *Opt Express* 15:2490-2498.

References

- Weinberger NM (2004) Specific long-term memory traces in primary auditory cortex. *Nat Rev Neurosci* 5:279-290.
- White LE, Coppola DM, Fitzpatrick D (2001) The contribution of sensory experience to the maturation of orientation selectivity in ferret visual cortex. *Nature* 411:1049-1052.
- Yaksi E, Friedrich RW (2006) Reconstruction of firing rate changes across neuronal populations by temporally deconvolved Ca²⁺ imaging. *Nature methods* 3:377-383.
- Yassin L, Benedetti BL, Jouhanneau JS, Wen JA, Poulet JF, Barth AL (2010) An embedded subnetwork of highly active neurons in the neocortex. *Neuron* 68:1043-1050.
- Yoshimura Y, Callaway EM (2005) Fine-scale specificity of cortical networks depends on inhibitory cell type and connectivity. *Nat Neurosci* 8:1552-1559.
- Zangenehpour S, Chaudhuri A (2002) Differential induction and decay curves of c-fos and zif268 revealed through dual activity maps. *Brain Res Mol Brain Res* 109:221-225.
- Zenz R, Eferl R, Scheinecker C, Redlich K, Smolen J, Schonhaler HB, Kenner L, Tschachler E, Wagner EF (2008) Activator protein 1 (Fos/Jun) functions in inflammatory bone and skin disease. *Arthritis Res Ther* 10:201.
- Zhang F, Wang LP, Brauner M, Liewald JF, Kay K, Watzke N, Wood PG, Bamberg E, Nagel G, Gottschalk A, Deisseroth K (2007) Multimodal fast optical interrogation of neural circuitry. *Nature* 446:633-639.
- Zhang J, Zhang D, McQuade JS, Behbehani M, Tsien JZ, Xu M (2002) c-fos regulates neuronal excitability and survival. *Nat Genet* 30:416-420.
- Zhang Y, Fukushima H, Kida S (2011) Induction and requirement of gene expression in the anterior cingulate cortex and medial prefrontal cortex for the consolidation of inhibitory avoidance memory. *Mol Brain* 4:4.
- Zhao Y, Araki S, Wu J, Teramoto T, Chang YF, Nakano M, Abdelfattah AS, Fujiwara M, Ishihara T, Nagai T, Campbell RE (2011) An expanded palette of genetically encoded Ca²⁺ indicators. *Science* 333:1888-1891.

Acknowledgements

9. Acknowledgements

First of all I want to thank Simon Rumpel for his constant support and guidance during my PhD and also for the opportunity to work on this projects.

I am grateful to all the past and present Rumpel lab members Bruno, Brice, Juliane, Evi, Kaja, Konsti, Jiss, Dominik, Lyubov, Tanja and Abhiyan for all their help, fruitful discussions and fun in the lab.

I also want to acknowledge the Haubensack lab for creating a really nice working atmosphere and Wulf for reading my manuscripts and interesting discussions.

I also want to thank all my friends especially Agnieszka, Emanuel and Crisu for their support and all the fun we had inside and outside of the lab.

Curriculum vitae

10. Curriculum vitae

Personal information

Name: Manuel Peter
Nationality: Austrian
Date of Birth: 6th June 1981
Place of Birth: Feldbach, Austria

Education

- 1987 – 1991: Elementary school: *Volksschule Sacre Coeur Graz, Austria*
- 1991 – 1999: Secondary school: *Bundesrealgymnasium Oeverseegeasse Graz, Austria*
- 2000 – 2005: *Karl-Franzens University Graz, Austria*
Bachelor studies: Molecular Biology
Graduated as Bakkalaureus der Biologie on the 12th July 2005
- 2005 – 2007: *Karl-Franzens University Graz, Austria*
Master studies: Molecular Microbiology
- 2006 – 2007: Master thesis at the *University of Technology Graz, Austria* at the Institute of Molecular Biotechnology
Thesis: “Evolution of fluorescent reporter proteins for the gene expression analysis in *Pichia pastoris*”
Supervisor: Dr. Anton Glieder
Graduated as Magister rerum naturalium on the 21th Dezember 21 2007 at the Karl-Franzens University Graz
- 2008 - present: *Research Institute of Molecular Pathology Vienna, Austria*
PhD student under the supervision of Dr. Simon Rumpel

Publications

Peter M, Scheuch H, Burkard T, Tinter J, Wernle T, Rumpel S (2012) Induction of immediate early genes in the mouse auditory cortex after auditory cued fear conditioning to complex sounds. *Genes Brain Behav.*

Curriculum vitae

Poster presentations

Peter M. and Rumpel S.: Characterization of a *c-fos* reporter mouse for *in vivo* imaging. (8th Göttingen Meeting of the German Neuroscience Society, 2009)

Peter M. and Rumpel S.: A marker mouse for labeling individual neurons *in vivo*. (7th FENS Forum of European Neuroscience, 2010)

Peter M. and Rumpel S.: Conditional photolabeling of individual neurons in a transgenic mouse *in vivo*. (EMBO/EMBL Symposium, Structure & Function of Neuronal Circuits, 2010)

Peter M. and Rumpel S.: Photolabeling of individual neurons in a transgenic mouse *in vivo*. (40th Neuroscience Meeting of the Society for Neuroscience, 2010)

Peter M., Bathellier B., Fontinha B. M. and Rumpel S.: Photolabeling of individual neurons in a transgenic mouse *in vivo*. (Gordon Research Conference on Excitatory Synapses & Brain Function, 2011)

Peter M., Bathellier B., Fontinha B. M. and Rumpel S.: Conditional photolabeling of individual neurons in a transgenic mouse *in vivo*. (41st Neuroscience Meeting of the Society for Neuroscience, 2011)